Max-Planck-Institut
für Meteorologie

MAX-PLANCK-GESELLSCHAFT

International Max Planck Research School
on Earth System Modelling

Relative contribution of the mid-latitude circumglobal wave train to the South Asian summer monsoon

Sajjad Saeed

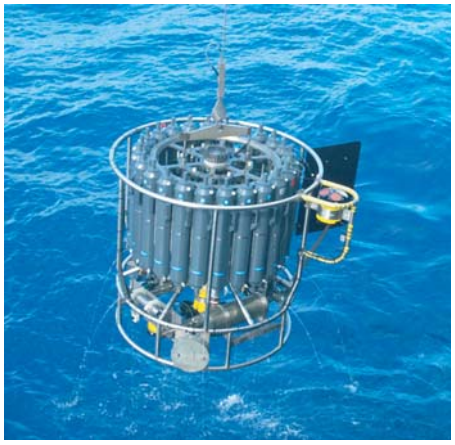

Berichte zur Erdsystemforschung 106/2011

Reports on Earth System Science

Hinweis

Die Berichte zur Erdsystemforschung werden vom Max-Planck-Institut für Meteorologie in Hamburg in unregelmäßiger Abfolge herausgegeben.

Sie enthalten wissenschaftliche und technische Beiträge, inklusive Dissertationen.

Die Beiträge geben nicht notwendigerweise die Auffassung des Instituts wieder.

Die "Berichte zur Erdsystemforschung" führen die vorherigen Reihen "Reports" und "Examensarbeiten" weiter.

Notice

The Reports on Earth System Science are published by the Max Planck Institute for Meteorology in Hamburg. They appear in irregular intervals.

They contain scientific and technical contributions, including Ph. D. theses.

The Reports do not necessarily reflect the opinion of the Institute.

The "Reports on Earth System Science" continue the former "Reports" and "Examensarbeiten" of the Max Planck Institute.

Anschrift / Address

Max-Planck-Institut für Meteorologie
Bundesstrasse 53
20146 Hamburg
Deutschland

Tel.: +49-(0)40-4 11 73-0
Fax: +49-(0)40-4 11 73-298
Web: www.mpimet.mpg.de

Layout:

Bettina Diallo, PR & Grafik

Titelfotos:
vorne:
Christian Klepp - Jochem Marotzke - Christian Klepp
hinten:
Clotilde Dubois - Christian Klepp - Katsumasa Tanaka

Berichte zur Erdsystemforschung 106/2011

Relative contribution of the mid-latitude circumglobal wave train to the South Asian summer monsoon

Sajjad Saeed

aus Rawalakot (A.K), Pakistan

Hamburg 2011

Reports on Earth System Science 106/2011

ISSN 1614-1199

Sajjad Saeed
Max-Planck-Institut für Meteorologie
Bundesstrasse 53
20146 Hamburg
Germany

Als Dissertation angenommen
vom Department Geowissenschaften der Universität Hamburg

auf Grund der Gutachten von
Prof. Dr. Martin Claussen
und
Dr. Wolfgang A. Müller

Hamburg, den 29. November 2011
Prof. Dr. Jürgen Oßenbrügge
Leiter des Departments für Geowissenschaften

ISSN 1614-1199

Relative contribution of the mid-latitude circumglobal wave train to the South Asian summer monsoon

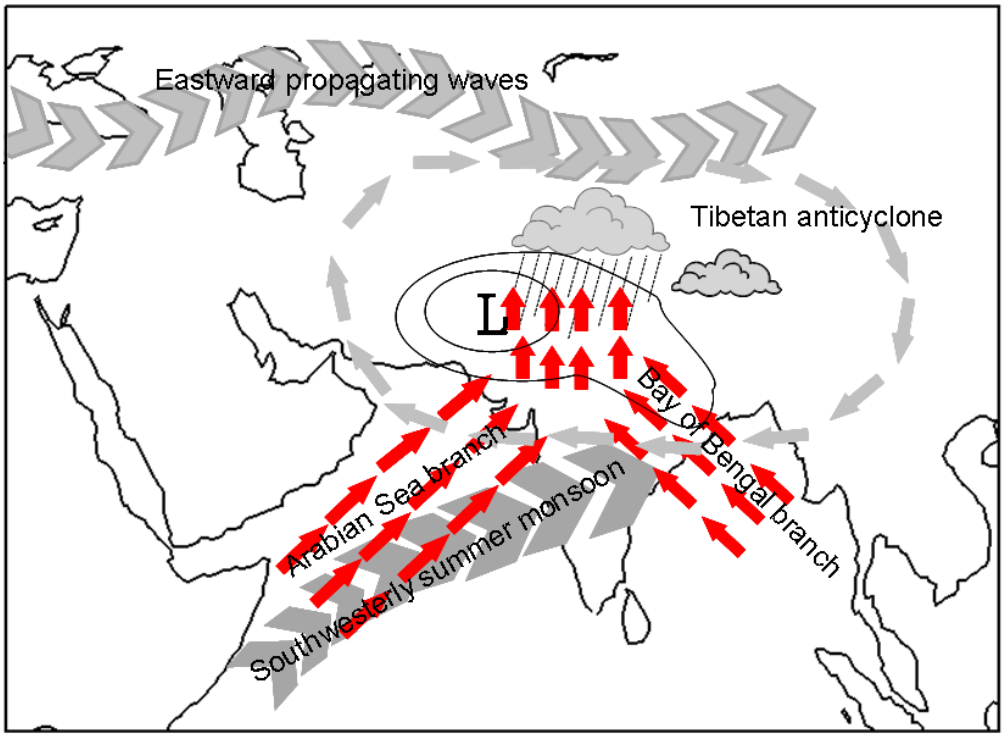

Sajjad Saeed

Hamburg 2011

Contents

Abstract

Although there are increasing evidences of interaction between the mid-latitude circulation and intraseasonal variations of the South Asian summer monsoon, however, it is not fully clear that how the mid-latitude circulation may influence the summer monsoon over South Asia region. In this thesis ERA40 reanalysis data and ECHAM5 climate model simulations are used to examine the mid-latitude monsoon interaction. Special emphasis is given to the large scale mid-latitude circumglobal wave train (CGT) and its relationship to the South Asian summer monsoon. It is found that an eastward propagation of mid-latitude CGT can influence the surface heat low and associated monsoon precipitation over northwestern India and Pakistan. The intensification of the heat low is associated with enhanced southwesterly flow over the Arabian Sea and Persian Gulf that converge over northwestern India and Pakistan. A monsoon trough like condition develops over northwestern India and Pakistan which favors enhanced summer monsoon rainfall.

Moreover, sensitivity simulation experiments are carried out using the ECHAM5 climate model to study the response of rainfall/convection variation over the South Asian monsoon heat low to the large scale mid-latitude circulation and related precipitation over East Asia. It is found that an intensification of the heat low favors enhanced precipitation/convection over northwestern India and Pakistan. The enhanced precipitation/convection over northwestern India and Pakistan can further induce large scale circulation anomalies that resemble the northern summer CGT wavelike pattern extending well into the Asian monsoon region. Accordingly the wavelike response to rainfall increase over the heat low region is associated with anomalous ascent of air above northern China and descent above the South China Sea.

During the summer monsoon of 2010, Pakistan received very heavy rainfall that caused devastating flooding. More than 20 million people are directly affected

and the overall estimates of damage exceeded $US40B. Analysis reveals a blocking high pressure in the upper levels that developed over the western Russia during July 2010. It is found that a co-occurrence of the mid-latitude wave train and the blocking high is associated with a deepening of heat low over Pakistan and adjacent areas of Iran, Afghanistan and Arabian Peninsula. The intensification of the heat low favored the moist southerly flow to intrude deep in to the northern Pakistan where orographic lifting in association with upper level trough fostered convection and hence rainfall.

Finally, an analysis of the IPCC AR4 future climate scenario experiment with doubling CO2 has also been carried out to examine the future CGT and associated rainfall over northwestern India and Pakistan. Analysis reveals a northward shift of the CGT pattern over Eurasia region. The associated sea level pressure show positive anomalies over western parts of the heat low region. The projected monsoon rainfall shows enhanced interannual rainfall variation with increased drought like conditions over northwestern India and Pakistan in future climate.

Chapter 1

Introduction

A large proportion of the world's population residing in the South Asia depends on the summer monsoon mainly through the dependence of agriculture on the timing, duration and strength of the summer monsoon. A strong interannual variability of the summer monsoon affects directly more than 22% of the world population residing in the South Asia region. An example of this strong influence can be seen during the recent summer monsoon of 2010 over Pakistan and adjacent areas that caused devastating flooding in the Indus basin region. More than 20 million people were directly affected from the severe flooding and the overall estimates of damage exceeded $US40B (Webster et al. 2011). Irrigation systems are badly destroyed and planting of subsequent crops delayed or abandoned with agricultural costs exceeding $US500M. The consequences of such type of floods contribute further in raising poverty in the developing countries (Webster and Jian 2011). It is therefore important to understand the factors that could influence the South Asia summer monsoon.

The South Asian summer monsoon undergoes enormous variability ranging from intra-seasonal to interannual and decadal time scales and is influenced by both tropical and extra-tropical forcing (Fig.1.1). Previous studies (e.g., Walker 1924; Rasmusson and Carpenter 1983; Webster and Yang 1992; Goswami 1998; Fasullo and Webster 2002) have mentioned the influence of the El Niño Southern Oscillation (ENSO) on the Asian summer monsoon. The ENSO is associated with above average summer monsoon precipitation during a La Niña and deficits during an El Niño episode (Shukla and Paolina 1983; Kumar et al. 2006). Goswami and Xavier (2005) showed that the ENSO-monsoon co-variability

depends on how the monsoon season is defined. They showed that the tropospheric temperature anomalies over Asia and Indian Ocean are associated with the summer time ENSO. For example the anomalous cold temperatures over much of Asia and warm temperatures over the Indian Ocean are associated with the summer time El Niño events. Such changes in the meridional gradient of tropospheric temperature can affect the monsoon circulation (Webster et al., 1998). In addition to the sea surface temperature (SST) variations over the tropical Pacific Ocean, the monsoon over the South Asian region is also influenced by other factors, such as the Indian Ocean dipole (e.g., Saji et al. 1999; Ashoke et. al. 2000) and SSTs variations over tropical Atlantic Ocean (e.g., Kucharski et. al 2008).

Previous studies (e.g., Krishnan et al. 2009; Ding and Wang 2005, 2007, Kripalani et. al. 1997) have also shown the potential influence of extra-tropical circulation on South Asian summer monoon. However, the relationship between the large scale extra-tropical circulation and the South Asian summer monsoon is not fully established. On intraseasonal to interannual time scales the anomalous mid-latitude circulation over western central and East Asia can induces anomalous cooling in the middle and upper troposphere through cold air advection, which reduces the meridional thermal contrast over the Indian subcontinent. The intrusion of dry extra-tropical wind into northwestern India and Pakistan can decrease the convective instability so that the suppressed convection can in turn weaken the monsoon flow (Krishnan et al. 2009). On the other hand Kripalani et al. (1997) found positive correlations between the enhanced monsoon rainfall over the Indian region and 500 hpa geopotential heights over the west of Pakistan suggesting some common element of low frequency variability is influencing the mid-latitude circulation and Indian summer monsoon.

Branstator (2002) found that the subtropical jet stream over the South Asian region during the winter season acts as a wave guide and found a pattern of variability in which the opposite points on the globe co-vary and named it as

circumglobal teleconnection pattern (CGT). Later on Ding and Wang (2005) found a similar CGT pattern during the summer season. They further found significant correlations between CGT and Indian summer monsoon. They also found that during the positive phase of the mid-latitude wave train anomalous high pressure appears over western central Asia and the northwestern India and Pakistan receive enhanced monsoon rainfall. According to them, one possible mechanism responsible for the enhanced rainfall over northwestern India and Pakistan might be the enhanced wind shear associated with the anomalous high pressure over western central Asia. However, the actual mechanism that links the mid-latitude wave train with monsoon precipitation over northwestern India and Pakistan is not fully established.

In this PhD dissertation a missing link between the mid-latitude circumglobal wave train and summer monsoon over South Asia has been identified. This thesis focuses on intraseasonal to interannual timescales and particularly addresses the following questions:

1. How does the mid-latitude circumglobal wave train influence the summer monsoon precipitation over northwestern India and Pakistan?
2. Does the precipitation/convection variability over the South Asian monsoon heat low produce large scale circulation anomalies in the Asian monsoon region that remotely influence precipitation variability over the East Asia region?
3. What is the role of mid-latitude circulation in the 2010 heavy monsoon rainfall that caused severe flooding over Pakistan and adjacent areas?
4. How does the mid-latitude CGT and associated summer monsoon rainfall over northwestern India and Pakistan change in the future warmer climate?

To answer the above questions, this thesis is divided into four independent chapters (2-5), each of it is designed to be a full paper itself. Therefore some repetitions may inevitably occur in different chapters of the thesis. The references

of all chapters are gathered together into a single reference list at the end of the thesis. The structure of the thesis is as follows:

The second chapter describes the explicit role of the surface heat low in the internal dynamics of mid-latitude and South Asian monsoon circulation. In this chapter the influence of mid-latitude CGT on the summer monsoon over northwestern India and Pakistan has been examined. This chapter has been published in journal of Climate Dynamics (Saeed et al. 2010).

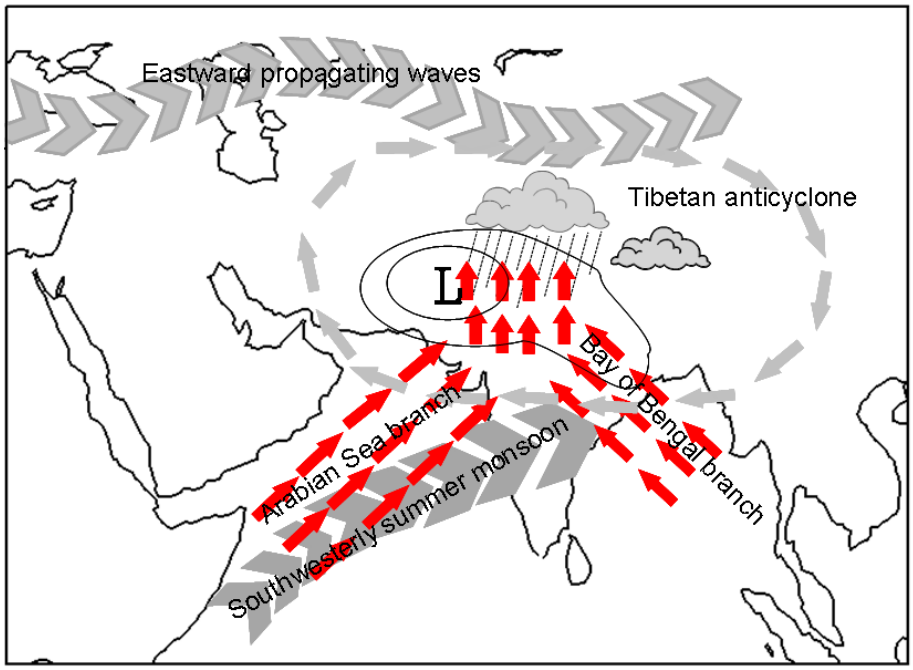

Figure 1.1: Schematic diagram showing the major components associated with the South Asian summer monsoon such as, the surface heat low, the upper level Tibetan anticyclone, low level southwesterly and southeasterly monsoon flow over the Arabian Sea and Bay of Bengal respectively, and the upper level eastward propagating waves in the mid-latitudes.

The heat low over northwestern India and Pakistan shows significant correlation with the mid-latitude circulation over western central and East Asia region (Saeed et al. 2010). This has indicated a positive feedback from the heat low and associated precipitation/convection variability to the mid-latitude circulation and related monsoon precipitation over East Asia region. The third chapter examines the precipitation/convection variability over the monsoon heat low and its

relation to the mid-latitude circulation and related rainfall over East Asia. This chapter has also been published in Geophysical Research Letters (Saeed el al. 2011).

Pakistan received heavy rainfall in July 2010 that caused severe flooding in the Indus River and its tributaries Jhelum, Ravi etc. The circulation pattern prevailed during the heavy rainfall shows resemblance to those shown by Saeed et al 2010. The fourth chapter of this thesis is organized to examine the circulation patterns prevailed during the heavy rainfall event and discuss the possible causes for the abnormal intensification of the rainfall over Pakistan.

Recent studies (e.g., Müller and Roeckner 2008) suggested the future changes in the mid-latitude circulation over distinct regions. Müller and Roeckner (2008) attributed these changes to the changes in the sea surface temperature anomalies over the tropical Pacific Ocean. As discussed above that the summer monsoon rainfall over South Asia is significantly influenced by the mid-latitude circulation on the intraseasonal to interannual time scales. It is therefore important to examine the future changes in the mid-latitude CGT and associated rainfall over northwestern India and Pakistan. The fifth chapter of the thesis analyses the AR4 future climate scenario simulations carried out using the ECHAM5 climate model. This chapter examines the CGT-monsoon relationship in the warmer future climate. The conclusions are given in the last chapter.

Chapter 2

Circumglobal wave train and the summer monsoon over northwestern India and Pakistan: the explicit role of the surface heat low

2.1 Introduction

The seasonal reversal of the surface winds is an indispensable peculiarity of the summer monsoon over South Asia and is profoundly associated with the differential heating between land and sea (Ramage 1971; Webster 1987; Meehl 1994). The intense surface heating during the summer provokes a persistent thermal low pressure over much of southwestern Asia with a core area over northwestern India, Pakistan and the Persian Gulf. This Heat Low (HL hereafter) develops during May and is associated with the low-level westerly monsoon wind regime. The HL circulation is associated with an ascent (decent) below (above) 700-hPa level with convergent easterlies and exports cyclonic vorticity in the middle and upper troposphere (Ramage 1965). The Arabian Sea summer monsoon circulation is also linked with the HL (Hewitt and Jackson 2003; Bansod and Singh 1995).

The surface processes over the South Asia region during the boreal summer are also modified by the upper level tropospheric features of the region. An example is the upper level 200 hPa Tibetan High which plays an essential role in the Asian

monsoon circulation (Hoskins and Wang 2006; He et.al 1987; Yatagai and Yasunari 1995; Park and Schubert 1997). In addition to the large scale circulation change, the Indian monsoon is also markedly influenced by the land sea temperature contrast e.g., due to greater albedo from increased snow cover over Eurasian region (Haln and Shukla 1976; Yasunari et al 1991).

The Indian summer monsoon (ISM) undergoes enormous variability ranging from intraseasonal to interannual and decadal timescales, indicating the influences of tropical and extra-tropical processes (e.g., Shukla 1987; Torrence and Webster 1999, Goswami 1998; Krishnamurthy and Goswami 2000; Goswami and Ajaymohan 2001; Li et al. 2008). On interanual time scale the ISM is modulated by the El Niño/Southern Oscillation (ENSO) (e.g., Walker 1924; Rasmusson and Carpenter 1983; Webster and Yang 1992; Goswami 1998; Fasullo and Webster 2002). Besides its impacts on the large scale circulation, ENSO also exerts influence on the ISM by controlling the length of the rainy season (Goswami and Xavier 2005). However, the ENSO monsoon relationship became feeble in the recent decades (Krishna Kumar et al. 1999; Torrence and Webster 1999; Kinter III et al. 2003) and these deviations in the ENSO monsoon relationship are comprised by the sea surface temperature (SST) over the southern equatorial tropical Atlantic (Kucharski et al. 2008).

Several other studies have also noticed the potential influence of mid-latitude circulation on the ISM rainfall (e.g., Ramaswamy 1962; Raman and Rao 1981; Kripalani et al. 1997; Ding and Wang 2005, 2007). The interannual variability of the summer monsoon over South Asia is also associated with the mid-latitude circulation e.g., Raman and Rao (1981) related the droughts years of ISM with the two blocking ridges in upper levels, one over West Asia and another over East Asia. In another study, Krishnan et al (2009) examined the internal feedbacks arising from monsoon mid-latitude interactions during droughts in the ISM. They suggested that the anchoring of the western central Asian cyclonic anomaly by the stagnant ridge located downstream over East Asia induces anomalous cooling in the middle and upper troposphere through cold air advection, which

reduces the meridional thermal contrast over the subcontinent. Furthermore, the intrusion of dry extra-tropical wind into northwestern India and Pakistan can decrease the convective instability so that the suppressed convection can in turn weaken the monsoon flow (Krishnan et al. 2009). Likewise, the enhanced rainfall over Indian region also exhibits positive correlations with the increased mid-latitude 500 hpa geopotential heights on intraseasonal time scale which reveals that some common element of low frequency variability is influencing the mid-latitude circulation and ISM (Kripalani et al. 1997).

Ding and Wang (2005) identified the mid-latitude circumglobal teleconnection (CGT) pattern (Branstator 2002) also for the northern hemisphere summer. They found significant correlations (~0.5) between CGT and ISM even in the absence of El Niño or La Niña. They further found that the positive phase of the CGT is associated with the enhanced precipitation over northwestern India and Pakistan. They showed that the monsoon activity over this region has a robust connection with the upper level anomalous high over western central Asia. Furthermore, they proposed that the anomalous high over western central Asia might enhance convection over northwestern India and Pakistan and hence the precipitation. However, the actual mechanism of this linkage is still concealed. In particular, it is obscure how the anomalous high over western central Asia modifies the rainfall over northwestern India and Pakistan.

In another study Yadav R. K (2009a, b) proposed that the Rossby wave train over Eurasia may be associated with intensifying the low surface pressure anomaly over the Iranian landmass, which intensifies the monsoon current over the Indian region. In the present study we further investigate this conundrum by exploring the above proposed hypothesis using ERA40 data and high resolution (T106L31) climate model ECHAM5 simulation. Special emphasis is given to the surface HL which forms over Pakistan and adjoining areas of India, Iran and Afghanistan. Since the monsoon precipitation over the South Asia region is strongly modified by the land sea temperature contrast which is closely associated with the sea level pressure contrast (Meehl 1994), thus any mid-latitude system that modulates the

thermal contrast will influence the monsoon intensity (Kripalani et al. 1997; Ding and Sikka 2005). This chapter describes that the upper level anomalous high over western central Asia during the positive phase of the CGT modulates the pressure anomalies in the HL and hence the associated rainfall over northwestern India and Pakistan. Further investigations are carried out to see how the eastward propagation of the mid-latitude wave train influences the surface pressure anomalies and associated rainfall over the Indian domain. The proposed mechanism is further examined by using high resolution climate model simulation of ECHAM5 to see the extent to which model can simulate the proposed mechanism.

The next section describes the data and methods used in this study. In section 2.3, the seasonal mean circulation is presented, section 2.4 gives the relevance of the observed CGT pattern with ISM. Section 2.5 illustrates the connection between the CGT and the surface HL. Section 2.6 describes the role of ENSO in HL-CGT relationship. The model results are presented in the section 2.7. Summary and discussions are given in the last section.

2.2 Data and Methodology

2.2.1 Data

The main analysis has been carried out by using the ERA40 global fields produced by the European Centre for Medium Range Weather Forecast (ECMWF, Uppala et al 2005) from June to September for 44 summer seasons from 1958-2001. In this case, we first analyse the monthly or seasonal mean data. The daily data e.g., 200 hPa geopotential heights, mean sea level pressure (MSLP) and 2m surface air temperature has been used to examine the lead-lag relationship between CGT and HL (discussed below). The observational precipitation and surface air temperature data assembled by the University of Delaware from Global Historical Climate Network (GHCN) with only land coverage has been used (Legates and Willmott 1990a,b). Analysis of the clouds and radiation fields (results not shown)

assembled by the Modern Era Retrospective-Analysis for Research and Application (MERRA) data has been carried out for the period 1979 to 2000 (Bosilovich et al. 2008). The results are also confirmed by using the NCEP/NCAR reanalysis fields (Kalnay et al., 1996).

Further analysis of the ECHAM5 model simulations of AMIP-type run at T106L31 resolution has been carried out for the period 1979-1999 (Roeckner et al. 2006). A detail description of the ECHAM5 model is given by Roeckner et al. (2003). The AMIP-type experiment is performed by using the observed monthly sea surface temperature and sea ice cover (Roeckner et al. 2006). The monthly and daily datasets are detrended and the climatology is removed to eliminate the seasonal variability. Additionally, a 5-day running mean time filter has been applied to the daily data to eliminate the synoptic variability.

2.2.2 EOF and Composite Analysis

Empirical orthogonal function (EOF) analysis has been applied to examine the mid-latitude wave train (Ding and Wang, 2005, 2007) in the northern hemisphere summer. The EOFs are computed using the seasonal (June-September) departures of the 200 hPa meridional wind from its climatological mean (1958-2001) over the region extending from 10° to 60°N and 0° to 120°E. The two leading modes of mid-latitude wave train explain 32% and 11% of the total variance respectively. Following Ding and Wang (2007) we also name the mid-latitude wave train as Eurasian wave train (EWT). By applying a hemispheric EOF analysis (180°W-180°E, 0°-90°N) on the 200 hPa meriodional wind and by comparing the principal components (PCs) of large scale and regional wave train it is found (not shown) that the EWT is a regional segment of the large scale CGT. The analysis therefore focuses on the first leading mode (PC1) of EWT as it reveals a wavelike pattern and explains the higher variance. Following Ding and Wang (2005) a CGT index (CGTI) has been defined as the interannual (intraseasonal) variability of 200 hPa geopotential height averaged over the western-central Asia from 35° to 40°N and 60° to 70°E.

A composite analysis has been carried out based on the positive and negative phases of the EWT. In the following, the cases for which PC1 is above (below) +0.5 (-0.5) standard deviations (Table I) are considered and the composite difference is defined as positive minus negative EWT. The composite patterns with PC1 are analogous to those produced by using CGTI. We used a t-test to find the significance of the composites.

2.2.3 Time-lagged Analysis

A time-lagged relationship is carried out using the singular value decomposition (SVD) analysis to capture the dominant modes between EWT over Eurasia and the MSLP over the Indian domain. The time-lagged SVD analysis (Czaja and Frankignoul 2002) is applied to examine the evolution of mid-latitude ISM coupling mode. This method is similar to the simple SVD analysis except that a time-lag is introduced between the two fields under investigation. In this way we can see the extent to which one system may lead another (Ding and Wang 2007). The SVD analysis has been applied using the 5-day running mean filtered daily 200 hPa geopotential heights over Eurasia (30°W-150°E, 10°-60°N) and MSLP over Indian domain (40°-100°E, 10°-40°N). A total of 41 time lags are calculated from -20 to +20 days.

A Heat Low Index (HLI) is defined as the departure of the summer (June-September) MSLP from its climatological mean (1958-2001) averaged over the area from 25° to 35°N and 55° to 75°E. The HLI realistically depict (discussed in section 3) the surface HL which forms over Pakistan and adjoining areas during the summer season. A lead-lag relationship has been carried out between the CGTI and HLI for the individual seasons which experienced above normal precipitation over northwestern India and Pakistan (Table 1). In this case the unfiltered daily time series has been used to keep the seasonality and precipitation variability. The objective here is to examine the CGT-HL relationship during the extreme precipitation years which cannot be achieved using a filtered time series.

2.3 Mean circulation analysis

This section first addresses the surface HL which develops over much of southwest Asia during the summer season. The northwestern parts of India, Pakistan and adjoining areas of Afghanistan, Iran and Arabian Peninsula display the lowest surface pressure in the northern hemisphere during the boreal summer (Fig. 2.1). This region also encounters high variability in the MSLP during summer. The standard deviations of MSLP are higher over the HL, Himalaya, northwestern China and surrounding regions (not shown). We define the HLI over the area shown in Fig. 2.1. The HLI is characterized by strong year-to-year variability with some lower values in the 1970s and increasing values thereafter (not shown). It is interesting that the pressure anomalies over HL region (25°–35°N, 55°–75°E) in comparison to the pressure anomalies from other parts of South Asia region display significantly higher correlations with mid-latitude circulation over western central Asia as well as the low level monsoon circulation over Arabian Sea and surface precipitation over northwestern India and Pakistan (Fig. 2.2). The correlations either become weak or non significant if we move the HL region to further east of 75°E. The choice of the area chosen to define the HLI is therefore important. Since we found similar patterns for correlations derived either from monthly or seasonal departures, we present here the correlation maps obtained from the monthly departures for the summer season from June to September. A correlation map between the HLI and 200 hPa height anomalies (Fig. 2.2 a) reveals a close association between the HLI and 200 hPa geopotential height anomalies, particular over western central Asia ($r = -0.7$) and East Asia ($r = -0.4$) regions. The negative correlations indicate that the pressure anomalies over the surface in the HL region will decrease (increase) when the height anomalies over western central Asia increase (decrease). Since the correlations are robust over the western central Asia, for brevity we will concentrate more on the height anomalies over western central Asia rather than East Asia.

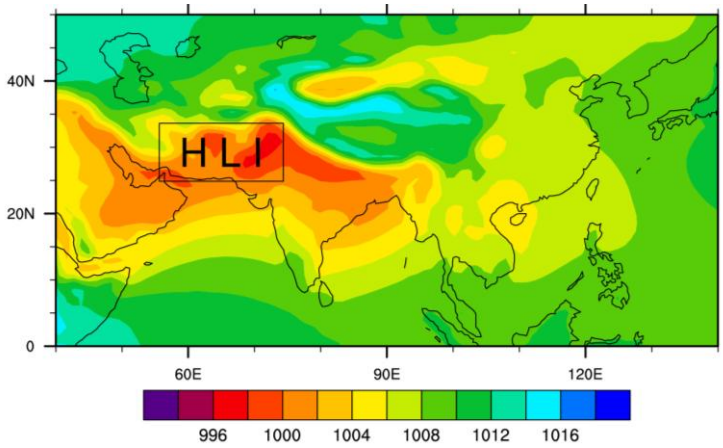

Figure 2.1: Mean sea level pressure (hPa) during the summer season (June to September) for the period 1958-2001 using ERA 40 data. The box represents the area over which the Heat Low Index (HLI) is computed.

The question now arises how the alteration in the height anomalies over western central Asia modulates the pressure anomalies in the HL region and associated precipitation. To address this question, we first correlated the HLI with other monsoon parameters such as 850 hPa zonal and meridional wind and total precipitation, to examine the explicit role of HL in the ISM. The HLI exhibits significant correlations with the observed surface precipitation over northwestern India and Pakistan (Fig. 2.2 b). This indicates a close association between the pressure anomalies over the heat low region and the precipitation over northwestern India and Pakistan. Moreover, the HLI also display significant correlations with 850 hPa zonal and meridional winds over the Arabian Sea (Fig. 2.2 c-d). The intensification of the HL deepens the land-sea pressure contrast (lower pressure over land than over sea), which consequently boosts the southwesterly (Arabian Sea branch) monsoon. Thus anything which can alter the pressure anomalies in the HL region will in turn affect the monsoon circulation and associated precipitation over northwestern India and Pakistan.

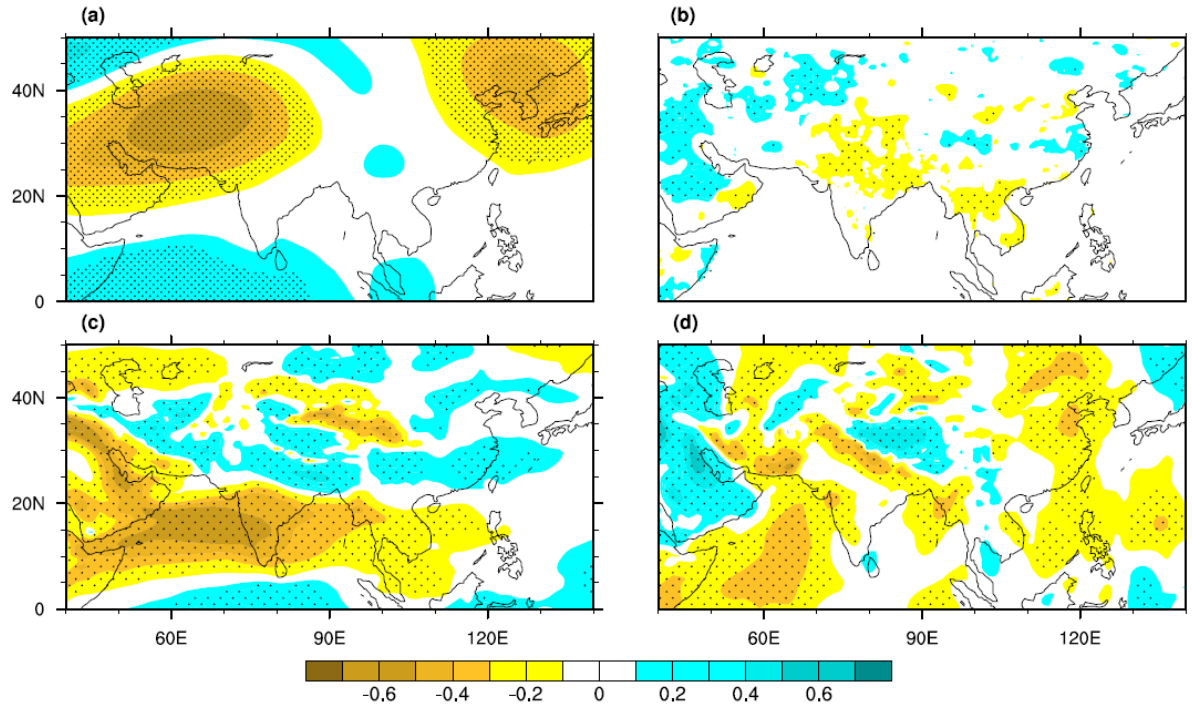

Figure 2.2: Correlation map between HLI and (a)- 200 hPa geopotential height (b)- observed surface precipitation (c)- 850 hPa zonal wind and (d)- 850 hPa meridional wind anomalies. The dotted areas show 95% significance level.

Based on above evidences it is hypothesised that the 200 hPa anomalous high over western central Asia during the positive phase of CGT modulates the pressure anomalies in the HL and associated rainfall over northwestern India and Pakistan. This is underpinned in the following sections.

2.4. Relevance of the observed mid-latitude wave train.

2.4.1 Observed CGT pattern.

Branstator (2002) first noticed that the low frequency disturbances in the vicinity of the subtropical jet stream stretching across South Asia are meridionally trapped and zonally elongated during the winter season. One special phase of this

pattern co-vary with distant regions in mid-latitudes producing a pattern of variability known as the CGT pattern.

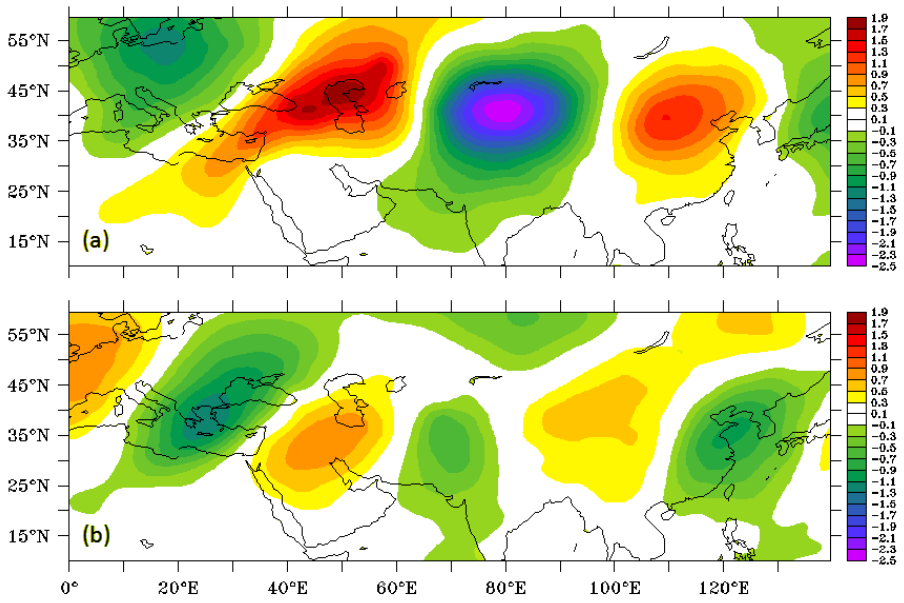

Figure 2.3: The two leading modes of the Eurasian wave train (EWT) explain 29.6% and 10.5% of the total variance. The EOFs are computed using the departures of 200 hPa meridional wind from their seasonal mean for the summer season (June-September).

Later on Ding and Wang (2005) confirmed that a similar teleconnection pattern exists during the summer season. They further proposed a sturdy connection between ISM precipitation and mid-latitude circulation via CGT.

A detailed description of the CGT and EWT during the northern hemisphere summer can be found in Ding and Wang (2005, 2007). Here, it is shown that the same pattern exhibited by ERA40 reanalysis and ECHAM5 model data and further explores its regional manifestation over South Asia. The two leading modes of the EWT (Fig. 2.3) display strong signals over Eurasia. Since the variance explained by the first leading mode is higher than the second mode and it is significantly correlated ($r = 0.9$) with the first mode of hemispheric global CGT (not shown), we therefore focus our analysis on the first leading mode of EWT.

2.4.2 Composite Analysis

The composite difference of the 200 hPa geopotential height and observed surface precipitation using PC1 (Fig. 2.4a) reveals enhanced height anomalies over western-central Asia and East Asia. The composite difference of 200 hPa geopotential height anomalies over western central Asia and East Asia is remarkably analogous to the correlation pattern associated with the HLI (though sign reversed, Fig. 2.2a) underlining the close resemblance of the EWT to the HLI. Further a positive phase of the EWT is also associated with reduced height anomalies over northwestern China and Mongolia. Yatagai and Yasunari (1995) found that the eastward (westward) shift of the upper level Tibetan High is associated with the wet (dry) summer over Taklamakan desert. Krishnan et al. (2000) noticed that the weak ISM is associated with anomalous low pressure over western central Asia around the Caspian Sea region. Since the subtropical jet stream over South Asia acts as a waveguide (Branstator 2002, Ding and Wang 2005), the successive troughs and ridges of the Rossby waves travelling along the jet influence the Tibetan High and hence the ISM circulation (Yadav 2009a, b).
Thus the positive height anomalies over western central Asia (during positive EWT phase) and northwestern China and Mongolia (during negative EWT phase) indicate two centers of actions associated with the enhanced (reduced) ISM precipitation over northern India and Pakistan. The above results are consistent with those presented in the previous studies (e.g., Ding and Wang, 2005, 2007; Yadav 2009a, b).

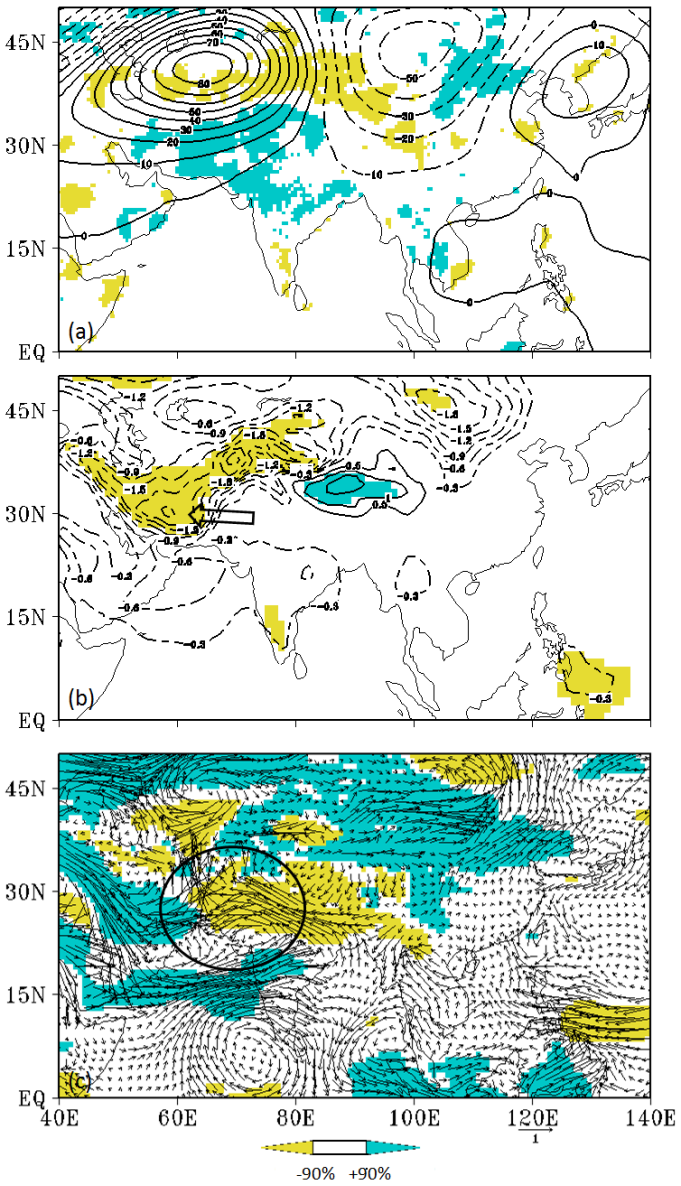

Figure 2.4: Composite difference using PC1 of EWT (a)- 200 hPa geopotential height in gpm (contours) (b)- MSLP in hPa (c)- 850 hPa wind. Shaded areas in (a), (b) and (c) represent 90% confidence level for observed surface precipitation, mean sea level pressure and 850 hPa zonal wind respectively based on the t-test. The cases having PC1 above +0.5 and below -0.5 standard deviation are given in Table I. The negative contours are shown by dashed lines. Contour line intervals in (a)- 10 gpm, and (b)- 0.2 hPa. Wind vectors in (c) are 1 $msec^{-1}$. The arrow in (b) shows westward increasing low pressure anomalies during the positive phase of EWT. The circle in (c) shows the area where moist flow from Arabian Sea and Persian Gulf converge.

Furthermore, it is found that the positive phase of the EWT is also associated with significant decrease in the surface pressure anomalies over the western parts of the HL region (Iran and Afghanistan) and adjoining areas (Fig. 2.4b). The decrease in the pressure anomalies over central parts of Iran (30°–35°N, 50°–60°E) is higher than over the surrounding regions compared to its mean (Fig. 2.1). Composite difference of the 850 hPa wind show cyclonic circulation over northwestern India and Pakistan and an anticyclonic circulation over the southern parts of India, Sri Lanka and adjoining areas of Arabian Sea and Bay of Bengal (Fig. 2.4c). The composite analysis (not shown) further reveals enhanced vertical velocities at 850hPa and 700 hPa over northwestern India and Pakistan during the positive phase of EWT. This indicates a monsoon trough like condition over northwestern India and Pakistan where the moist flow from Arabian Sea and Persian Gulf converges. Fig. 2.4c emanates opposite circulation features over India and Pakistan compared to Fig. 10a, b of Krishnan et al. (2009) which they obtained for the monsoon breaks days. The composite circulation patterns at 850 hPa and 200 hPa during negative phase of EWT (not shown) are also similar to that of monsoon breaks composite. From the above explanation it may be inferred that the EWT modifies the upper level circulation which plays a key role in enhancing (reducing) the monsoon precipitation over northwestern India and Pakistan on interannual time scale.

2.5. Connection between the CGT and the surface HL.

2.5.1. Time- lagged SVD analysis

We have seen that the positive phase of the mid-latitude wave train is associated with enhanced (reduced) 200 hPa height (sea level pressure) anomalies over western central Asia (western parts of the HL region i.e., Iran and Afghanistan). From the composite analysis it is not clear which system may lead another. We therefore investigate the temporal phase relationship between the mid-latitude wave train and the sea level pressure anomalies over Indian domain. For this

purpose the time-lagged SVD analysis has been applied (Czaja and Frankignoul, 2002) between the daily 200 hPa geopotential heights over Eurasia and MSLP over Indian domain to derive the lead-lag pattern. The singular vectors of geopotential heights for the first SVD mode between 200 hPa heights over Eurasia and MSLP over the Indian domain are shown from -20 to +15 days (Fig. 2.5).

A negative sign (e.g., -20 days) denotes the SVD analysis between 200 hPa geopotential heights over Eurasia and MSLP over Indian domain in which the 200 hPa geopotential heights leads the MSLP by 20 days and vice versa for the positive sign. The leading mode of the SVD analysis for each lead-lag condition explains more than 30% of the total squared covariance. The correlation coefficients between the expansion coefficients vary from 0.29 to 0.83 as indicated in Fig. 2.5. The maximum correlation coefficient occurs at 0 lag when the anomalous high resides over western central Asia.

At day -20 (the height leads MSLP by 20 days) a series of high pressures are located over Atlantic Ocean, another over West of Caspian Sea and third high located over East Asia (Fig. 2.5a). The corresponding SLP (Fig. 2.6a) show positive (high) pressure anomalies over much of India, Pakistan and adjoining areas of Iran and Afghanistan and negative (low) pressure anomalies lies over Arabian Peninsula. At day -15 (Fig. 2.5b) the wave train develops as the high pressure in the West of Caspian Sea (East Asia) starts intensifying (weakening). The corresponding SLP anomalies (Fig. 2.6b) over the Indian domain decreases compared to day -20. At day -10 (Fig. 2.5c) the wave train intensifies and moves slight eastward and the high pressure over the Caspian Sea is intensified. The corresponding SLP anomalies (Fig. 2.6c) now converted by the negative (positive) pressure anomalies in the north-west of Indian domain (Himalayan region). Furthermore, the low pressure over the Arabian Peninsula is considerably weaker then at day -15. At day -5 (Fig. 2.5d) the wave train moves eastward with further intensification of the high over western central Asia. The corresponding SLP anomalies (Fig. 2.6d) over the western parts of the HL region are further decreased. The positive (high) pressure anomalies over the Indian domain (which

were present on -20 day) are almost disappeared. Furthermore the negative (low) pressures anomalies over Arabian Peninsula are replaced with positive (high) pressure anomalies.

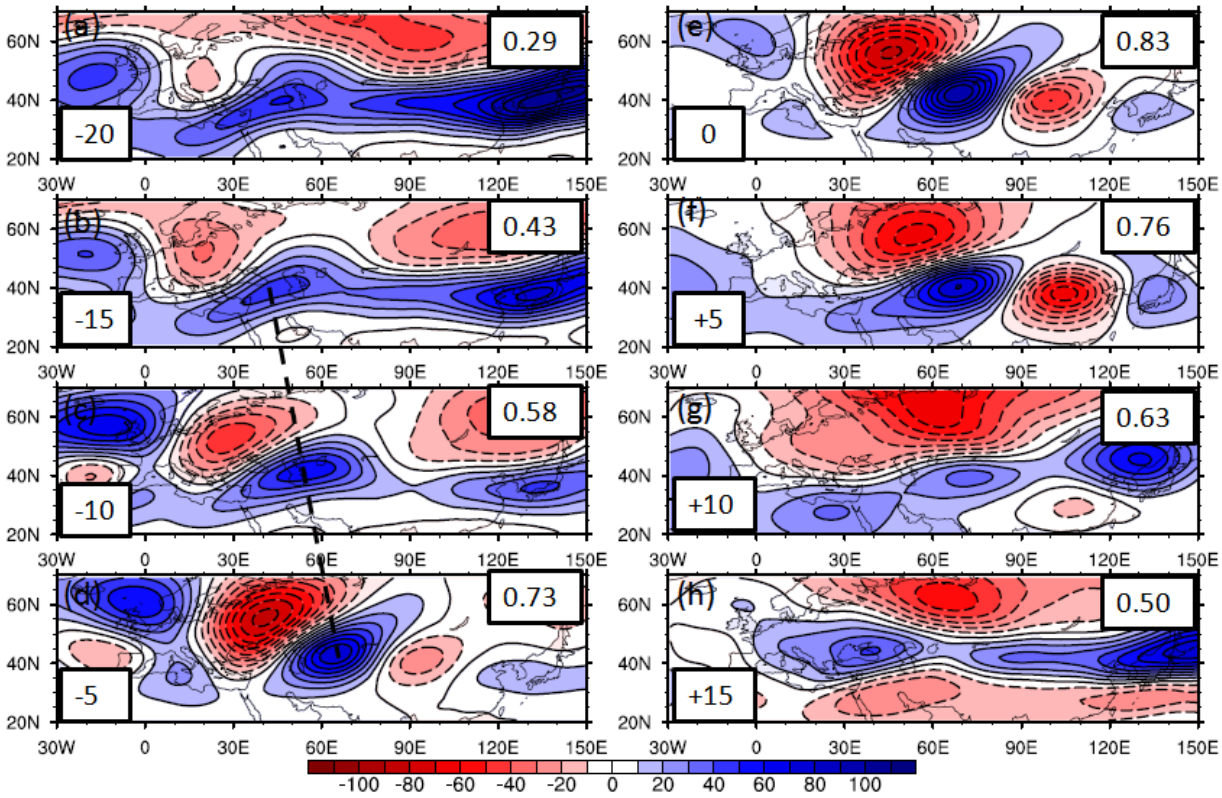

Figure 2.5: Singular vectors of 200 hPa geopotential height over Eurasia for the first SVD mode. The results are shown from -20 to +15 days. Lag days are shown in the lower-left corner of each panel. The negative lag days indicate that the CGT leads MSLP and vice versa for positive days. The correlation coefficients between the expansion coefficients are shown in upper-right corner. The negative contours are shown with dashed lines. The dashed lines joining the centres of high in (b-d) indicate eastward propagation of anomalous high at day -5 compared to day -15.

At day 0 (Fig. 2.5e) the largest upper level height anomalies occurs over western central Asia. The corresponding SLP anomalies (Fig. 2.6e) over the surface are lowest in the western parts of the HL region (over Iran and Afghanistan). Also at day 0 the upper level low pressure over northwestern China also starts intensifying. From day 0 to day +10 the high over western central Asia weakens and at day +15 it almost vanishes (Fig. 2.5f-h). The corresponding pressure

anomalies over the Indian domain (Fig. 2.6f–h) increase and at day +15 a high pressure appears over Arabian Sea and adjoining areas of India and Pakistan.

Table 1: EWT Positive (EWTP) and negative (EWTN) years above +0.5 and below -0.5 standard deviation based on PC1, El Niño and La Niña episodes based on Niño3 SST anomalies and the area averaged summer monsoon precipitation (JJAS) over northwestern India and Pakistan (68°–78E°, 25°–34°N). The blue bold (red light) type letters represent the years when precipitation over northwestern India and Pakistan is above +0.5 and below -0.5 standard deviation. The `*` sign represents the extreme flooding years over northwestern India and Pakistan.

EWTP	**1959***, **1970**, **1973***, **1976***, 1977, **1978***, 1979, **1990**, 1997
EWTN	1962, 1963, 1965, 1966, 1969, 1972, 1974, 1981, 1989, 1998, 1999, 2000, 2001
La Nina	**1964**, **1970**, **1973***, **1975**, 1984, 1985, **1988***, 1998, 1999
El Nino	1963, 1965, 1969, 1972, **1976**, 1982, 1987, 1997

A similar SVD analysis between 200 hPa geopotential heights over Eurasia and 2m surface air temperature over Indian domain further underlines the influence of the wave train on the near surface temperature patterns over Indian domain. It can be seen (Fig. 2.7) that the mid-latitude wave train markedly influence the near surface temperature patterns over the Indian domain. The largest co-variability of positive temperature anomalies over western parts of the HL region (Iran and Afghanistan) occurs from day -5 to day 0 (Fig. 2.7c–d), when the upper level high pressure occurs over western central Asia (Fig. 2.5d–e).

The manifestation of this lead-lag relationship is also seen between the CGTI and HLI (Fig. 2.8) during the above normal precipitation years over northwestern India and Pakistan (Table 1). The CGTI leads HLI by 0–20 days in most of the cases. However, the CGTI also lags HLI by 1–10 days (e.g., during 1970 and 1988). A remarkable difference in the lead-lag relationship can be seen between day -10 and day +10. After days +10 the lag relationship in all cases become non significant. This might be due of the eastward movement of the wave train as discussed earlier.

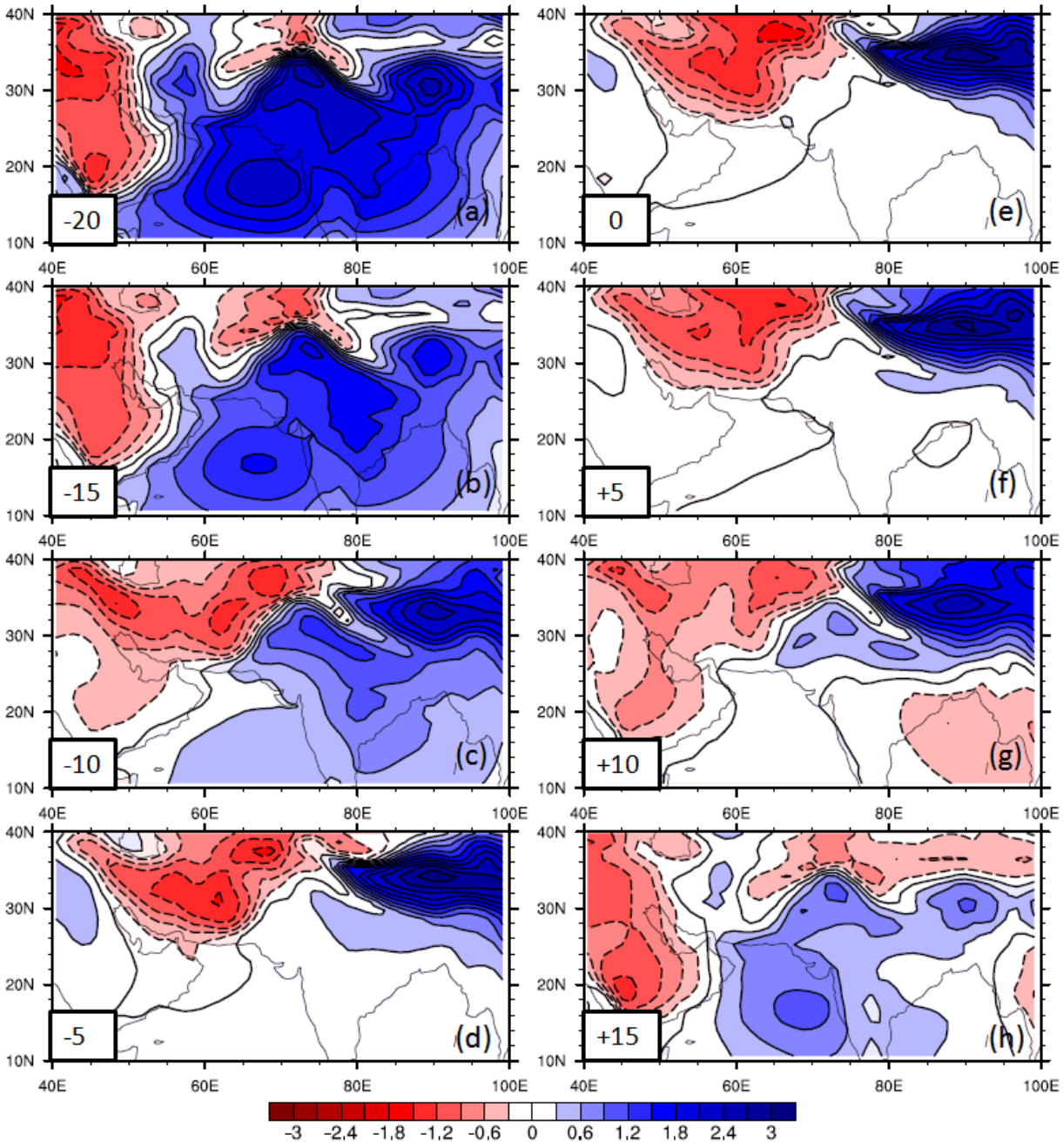

Figure 2.6: Same as Fig. 2.5, except the singular vectors of MSLP for the first SVD mode.

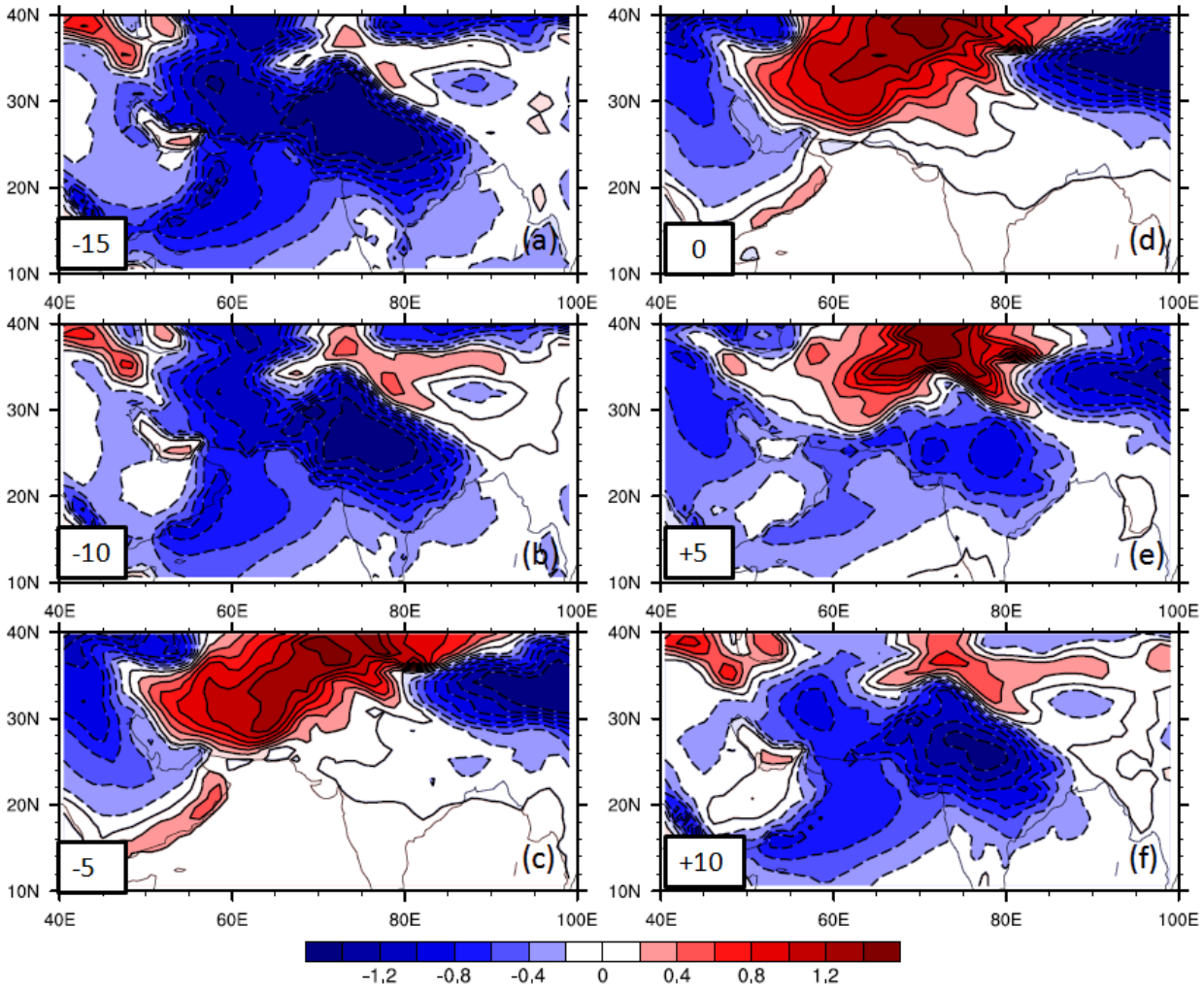

Figure 2.7: Same as Fig. 2.6, except the singular vectors of 2m surface air temperature for the first SVD mode. The results are shown from day -15 to +10. The negative contours are shown by dashed lines.

2.5.2 Influence of the upper level anomalous high on surface HL

We have seen that the pressure anomalies in the HL region are strongly influenced as the mid latitude wave train propagates eastward. Now we will delineate how the HL acts as a bridge connecting the mid-latitude wave train to the summer monsoon and associated precipitation over northwestern India and Pakistan. The anomalous high that develops over western central Asia extends

southward up to 25°N (Fig. 2.4a, Fig. 2.9a). The subsidence associated with the augmented height anomalies above the heat low region (25°-40°N, 55°-75°E) will reduce the surface pressure in the HL by accruing the mean air temperature (warm air is lighter than cold air) in the middle and upper troposphere through adiabatic heating (Fig. 2.9b). The increasing middle tropospheric temperature in turn provokes inversion between the lower and upper (850 hPa – 500 hPa) troposphere above the HL region (not shown). This anomalous inversion limits the vertical motions in the HL region and hence minimizes the middle and low level cloud formation (not shown). Furthermore, the upper level subsidence above the HL region will lessen the high level cloud cover thus favoring more solar radiation to this area (not shown). Consequently, the accruing surface air temperature further decreases the surface air pressure resulting in additional intensification of the HL. The westward accruing surface air temperature in the HL region favors a westward extension in the anomalous core of the low pressure to the west over Iran (Fig. 2.4b). The axis of the HL and associated monsoon trough plays a vital role in determining the rainfall regions over India and Pakistan (Shamshad 1988). The westward intensification of the low pressure with its north-south orientation produces enormous north-south pressure gradient (lower pressure over land and higher over Sea) and associated low level positive vorticity over northwestern India and Pakistan (Fig. 2.4c). This favors a monsoon trough like conditions over northwestern India and Pakistan where the moist southerly flow from Arabian Sea and Persian Gulf converge (Fig. 2.4c). The convective instability and orographic uplifting (Haln and Manabe 1995; Song et al. 2009) further supports the convection and hence the precipitation. Once the monsoon precipitation starts latent heat release will further increase the temperature over northwestern parts of India and Pakistan. The increased heating enhances the positive vorticity over northwestern India and Pakistan resulting in further augmentation of precipitation over this area.

2.6 HL-CGT relationship and ENSO

Several studies (e.g., Walker 1924; Rasmusson and Carpenter 1983; Shukla 1987; Webster and Yang 1992; Torrence and Webster 1999, Krishnamurthy and Goswami 2000; Goswami and Ajaymohan 2001; Goswami 1998; Fasullo and Webster 2002) mentioned the influence of the ENSO on summer monsoon over South Asia.

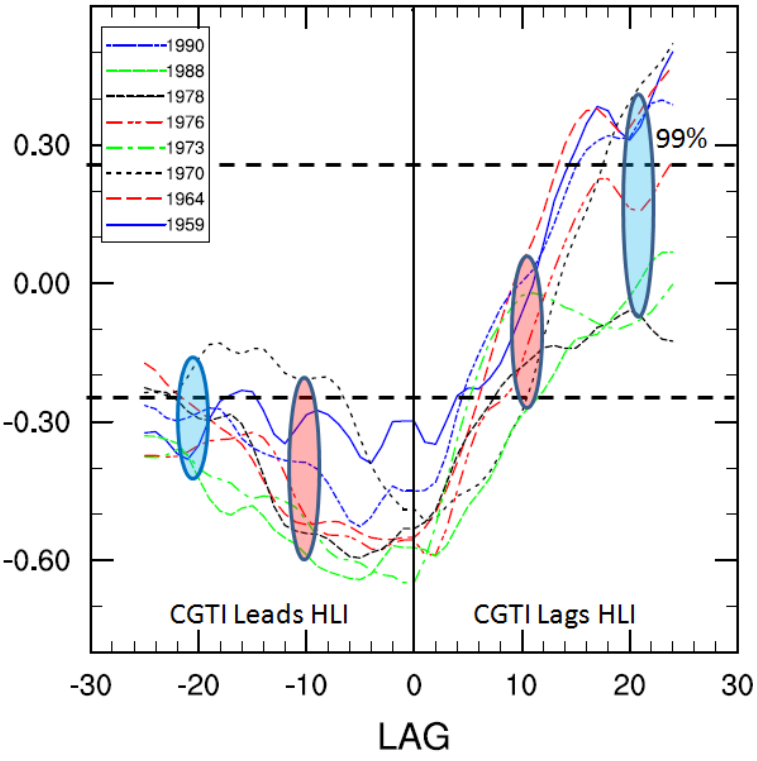

Figure 2.8: Lead lag relationship between CGTI and HLI during the above normal precipitation years over northwestern India and Pakistan (Table 1). The correlations are significant to 99% level if they are greater than 0.25 as indicated by the horizontal dashed lines. The pink (10 days) and sky blue (20 days) circles show correlations at particular lead-lag days.

Others (e.g., Ding and Wang 2005, Yadav 2009a, b) showed that the CGT-ISM relationship is independent of ENSO. Here we examine the HL-CGT relationship during the non-ENSO years and see the individual influences of CGT and ENSO on the monsoon precipitation over northwestern India and Pakistan. We first identified the ENSO episodes based on the Niño3 SST anomalies. A total of 17

ENSO years (8 El Niño and 9 La Niña episodes) are identified (Table I). In the non- ENSO cases these ENSO years are removed from 44-year time series when calculating the one point correlation. The HLI manifests significant correlations with 200 hPa geopotential height, 850 hPa zonal and meridional wind and observed surface precipitation anomalies even in absence of the El Niño and La Niña (Fig. 2.10).

To examine separately the influence of CGT and ENSO on monsoon precipitation over northwestern India and Pakistan, we first computed the area averaged precipitation (68°-78E°, 25°-34°N) over northwestern India and Pakistan (Table I). The rainfall episodes between +0.5 and -0.5 standard deviation are considered as normal precipitation events. It is evident from Table I that about 67% (62 %) of the above (below) normal rainfall cases are associated with the positive (negative) EWT phases and this proportion is 56% (75 %) for ENSO related episodes. Furthermore, there are cases with El Niño (e.g., 1976, 1997) when the monsoon precipitation is either normal or above normal and vice versa for the La Niña episodes (e.g., 1984, 1998, 1999). The same is valid for positive and negative phases of EWT, however it is interesting that none of the positive (negative) EWT cases are associated with below (above) normal rainfall.

Pakistan received severe flooding in its rivers (Indus basin and its tributaries Jhelum, Chenab and Ravi) during the summer monsoon seasons of 1959, 73, 76, 78 and 88. It is interesting that a large frequency of the flooding events (except 1988) is associated with the positive phases of the EWT. Moreover, during the strong 1997 El Niño year there is a positive phase of CGT and the northwestern India and Pakistan received normal rainfall. This adumbrates the important role of CGT in modification of precipitation over northwestern India and Pakistan which needs further investigation. Although CGT and ENSO enforces ISM precipitation, nevertheless, the other players such as Indian Ocean dipole (Saji et al. 1999; Ashok et al. 2001) and the SSTs of tropical and north Atlantic Ocean (Goswami et al. 2006; Kucharski et al. 2008) have also serious impacts on ISM and therefore cannot be ignored.

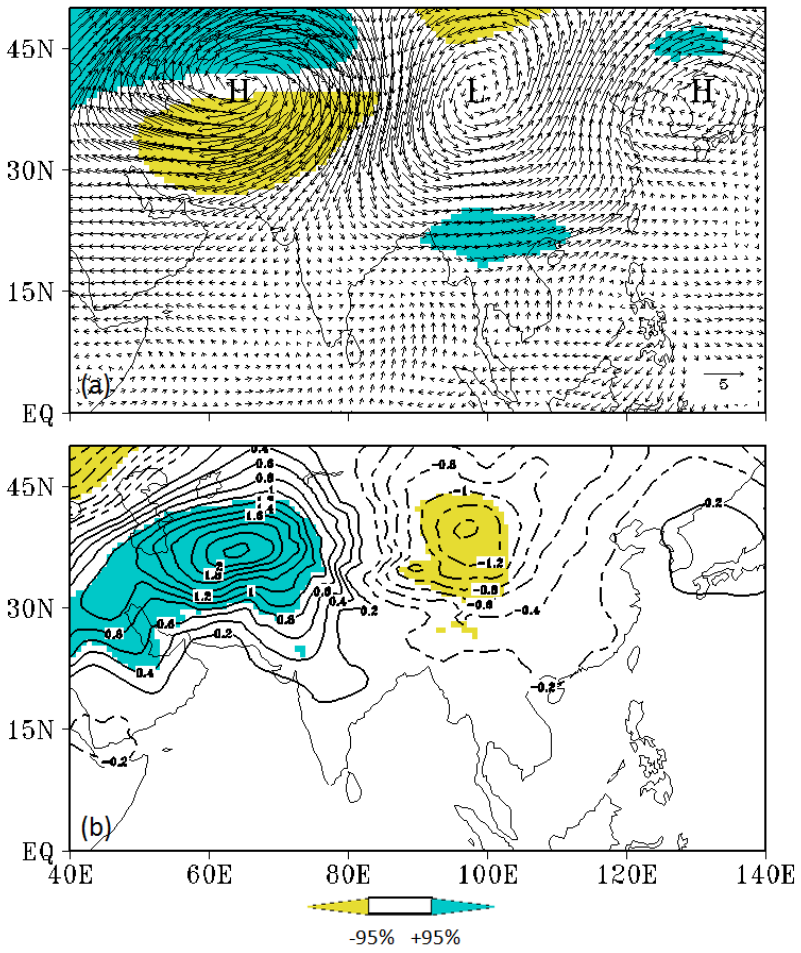

Figure 2.9: Same as Fig. 2.4, except the composite difference of (a)- 200 hPa wind (ms^{-1}) and (b)- 500 hPa mean temperature (°C). The shaded areas shown in (a), (b) indicate 95% significance level for the zonal wind and 500 hPa temperature respectively using the t-test. The negative contours are shown as dashed lines. Contours line intervals in (b) are at 0.2 °C.

2.7 ECHAM5 simulations

On the same lines as for ERA40 data, we examined the proposed mechanism using the high resolution ECHAM5 simulation to see the extent to which this model simulates the proposed HL-CGT relationship. The high resolution T106L31 ECHAM5 AMIP-type simulations are available for the period 1978-1999. Following Roeckner et. al. (2006) we skipped the first year of the simulation and focus our analysis on 21 summer seasons from 1979-1999. Roeckner et. al (2006) found that the ECHAM5 model simulates reasonably well the mean

climate at higher resolutions such as T106L31. We further examined the mean monsoon circulation patterns (not shown) such as the 200 hPa anticyclone over Tibetan Plateau, 850 hPa wind and associated moisture transport and the mean sea level pressure over Indian domain and found reasonable agreements between the model and ERA 40 data.

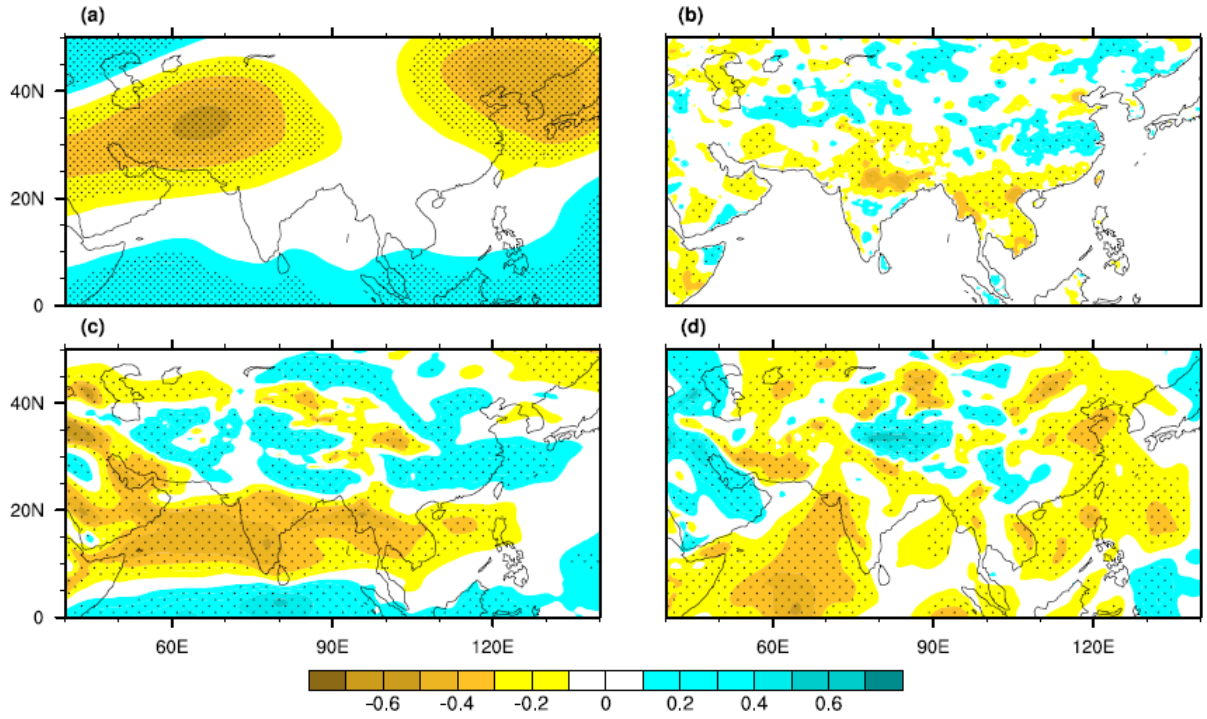

Figure 2.10: Same as Fig. 2.2 except for non-ENSO years. The El Niño and La Niña episodes identified are given in Table 1.

Similar to ERA40 data we computed the HLI using the model data. A one point correlation (Fig. 2.11a) between the HLI and 200hPa geopotential height anomalies reveals significant negative correlation over western central Asia (r = -0.5) and East Asia (r = -0.4) region. The simulated HLI also reveals significant correlations with low level monsoon circulation such as 850 hPa zonal and meridional wind over the Arabian Sea and surface precipitation over the Indian domain (not shown). Because of the difference in the length of the simulated and reanalysis/observed datasets, our objective here is not a one to one comparison between the model and the observations but is to see how well model can simulate the observed HL-CGT relationship. The composite difference of the

simulated 200 hPa geopotential height anomalies (Fig. 2.11b) using CGTI exhibits increased height anomalies over western central and East Asia region. The model simulated anomalous high pressure is shifted slight northeast compared to the ERA40 data (Fig. 2.4a). Moreover, the low pressure over northwestern China is shifted southward and lies over southwestern China and adjoining areas of India. The composite difference of the simulated precipitation show significantly enhanced precipitation over northwestern India and Pakistan (Fig. 2.11b). The composite analysis further reveals enhanced southwesterly monsoon over the Arabian Sea (not shown) as revealed from reanalysis data.

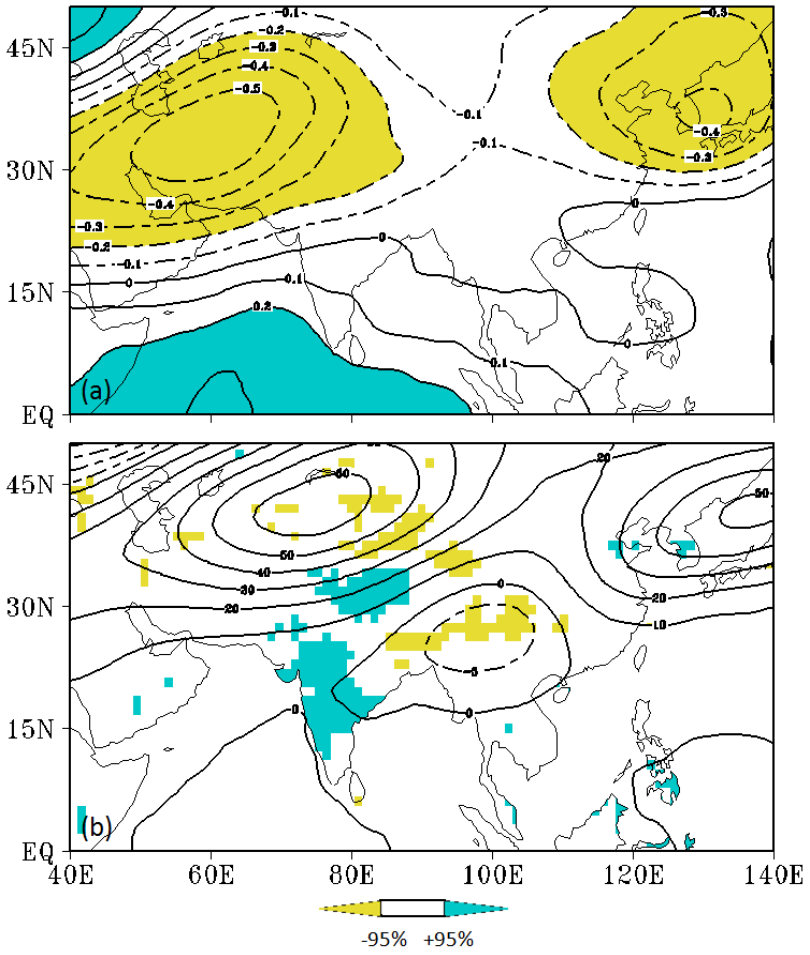

Figure 2.11: Using the ECHAM5 data (a)- correlation map between HLI and 200 hPa geopotentail heights (contour), shaded areas show 95% significance level for correlations, (b)- composite difference of 200 hPa geopotential heights (contours) and surface precipitation (shaded). The shaded areas in (b) show 95% significance level for the surface precipitation.

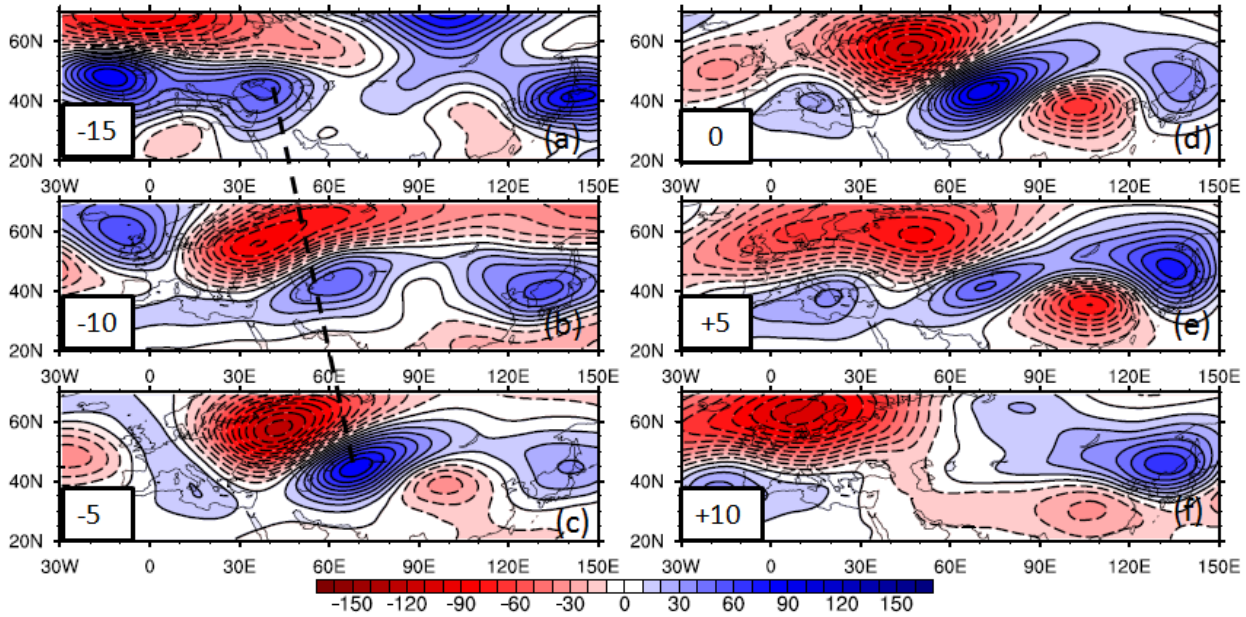

Figure 2.12: Same as Fig. 2.5, except using ECHAM5 data.

To see how model simulates the temporal evolution of the mid-latitude wave train and associated MSLP over the Indian domain, we applied SVD analysis between 200 hPa geopotential heights over Eurasia and MSLP over Indian domain. It is interesting to see that the model simulates reasonably well the eastward propagation of the mid-latitude wave train (Fig. 2.12) and associated changes in the MSLP anomalies over Indian domain (Fig. 2.13). The model results further confirmed that the largest low pressure anomalies over the western parts of the HL occurs in conjunction with upper level anomalous high over western central Asia. Following the previous analysis with reanalysis data, we also computed the lead-lag relationship between CGTI and HLI for the years when simulated precipitation over northwestern India and Pakistan is above one standard deviation. The cases when the area averaged precipitation over northwestern India and Pakistan is above one standard deviation are 1979, 86, 88 and 95. In almost all cases the CGTI leads HLI by 1-20 days (Fig. 2.14). This further supports that the model is able to capture the basic proposed mechanism.

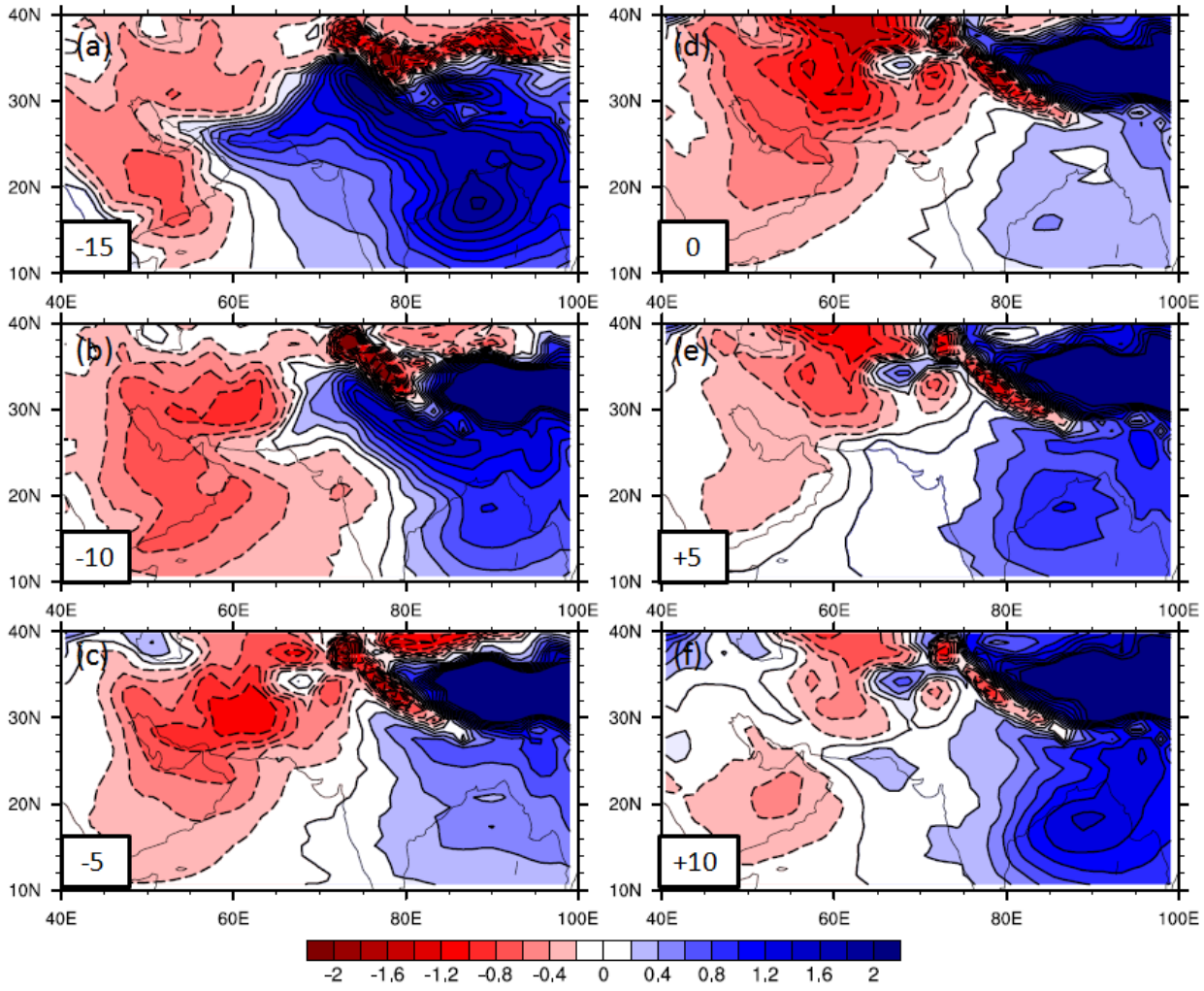

Figure 2.13: Same as Fig. 2.6 except using ECHAM5 data.

2.8 Summary and Discussion

In this chapter the influence of the mid-latitude wave train on the surface HL and associated rainfall over northwestern India and Pakistan has been examined by using the ERA40 data and high resolution (T106L31) climate model ECHAM5 simulations. The HL is a persistent low pressure system during the summer season over Pakistan and adjoining areas of India, Iran and Afghanistan (Fig. 2.1) and is closely associated with the ISM. A HLI is defined to depict the surface HL as the departure of the summer (June-September) MSLP from its climatological mean (1958-2001) averaged over the area from 25° to 35°N and 55° to 75°E. The HLI

displays significantly largest correlations with the upper level mid-latitude circulation over western central Asia as well as the low level monsoon circulation over Arabian Sea and associated precipitation over northwestern India and Pakistan (Fig. 2.2). The HLI also reveals significant correlations with mid-latitude circulation (Fig. 2.10) over western central Asia and East Asia even in the absence of ENSO.

Empirical Orthogonal Function analysis has been applied to examine the mid-latitude wave train (Ding and Wang 2005, 2007) during the summer season. The two leading modes of the Eurasian wave train (EWT) explain 29.6 and 10.5% of the total variance (Fig. 2.3). The composite analysis using PC1 of EWT reveals enhanced precipitation over the northwestern India and Pakistan during the positive phase of EWT (Fig. 2.4a). Further, the positive phase of EWT display enhanced (reduced) 200 hPa height anomalies over western central Asia (northwestern China and Mongolia). Thus the positive height anomalies over western central Asia (during positive EWT phase) and northwestern China and Magnolia (during negative EWT phase) indicate two centers of actions closely associated with the enhanced (reduced) monsoon precipitation over northwestern India and Pakistan. These results are consistent with those of Ding and Wang (2005, 2007).

The composite analysis further reveals significantly reduced SLP anomalies (Fig. 2.4b) over western parts of the HL region (i.e., Iran and Afghanistan) during the positive phase of the EWT. The increased low pressure anomalies over western parts of HL region are associated with low level cyclonic vorticity over northwestern India and Pakistan (Fig. 2.4c). The composite analysis reveals strong convergence of the low level moist southerly flow (from Arabian Sea and Persian Gulf) over northwestern India and Pakistan. Moreover, the composite analysis (not shown) also shows significant increase in the vertical velocities over northwestern India and Pakistan during the positive phase of EWT.

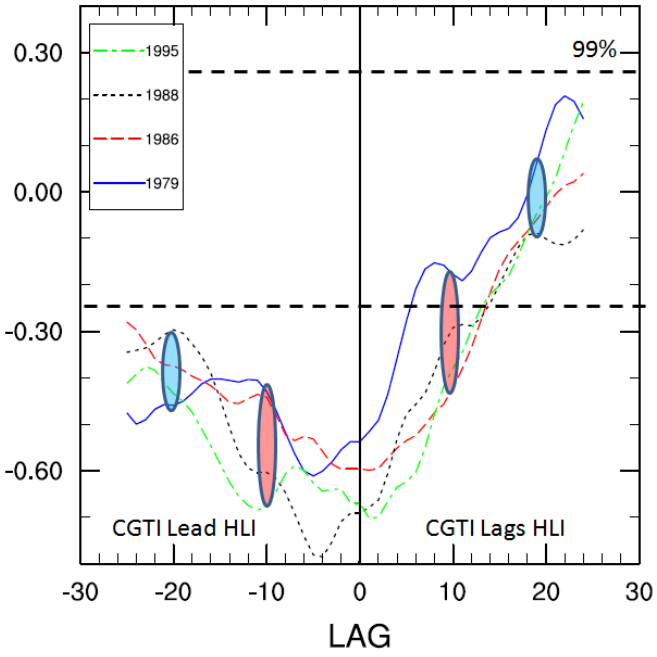

Figure 2.14: Same as Fig. 2.8, except using ECHAM5 data. The cases when simulated precipitaiton exceeds one standard deviation over northwestern India and Pakistan are 1979, 86, 88 and 95.

Although the composite analysis reveals significant association between the mid latitude circulation over western central Asia with the surface HL and associated precipitation over northwestern India and Pakistan, it is not clear which system may lead another. Therefore a time-lagged SVD analysis between the 200 hPa height over Eurasia and the MSLP over the Indian domain has been carried out to see the extent to which the one system may lead another. The time-lagged SVD analysis reveals strong coupling between the two modes. As the mid-latitude wave train propagates eastward (Fig. 2.5) the pressure anomalies over the South Asia region are also influenced (Fig. 2.6). The largest negative pressure anomalies over the western parts of the HL region (i.e., Iran and Afghanistan) occur at 0 lag in conjunction of the upper level anomalous high over western central Asia (Fig. 2.5e, Fig. 2.6e). However, the surface pressure anomalies over the Indian region start increasing as the wave train propagates further eastwards 10-20 days ahead. A similar SVD analysis between the 200 hPa heights over Eurasia and 2m

surface air temperature over Indian region shows noticeable changes in the near surface air temperature anomalies in association with the eastward propagation of the mid-latitude wave train. The largest co-variability of positive temperature anomalies over western parts of HL occurs when the anomalous high resides over western central Asia (Fig. 2.5d-e, Fig. 2.7c-d). The manifestation of this lead-lag relationship is also seen (Fig. 2.8) between the CGTI and HLI for the individual above normal precipitation season over northwestern India and Pakistan (Table 1). In most of the cases the CGTI lead the HLI. It is interesting that the large frequency of above normal (flooding) episodes over northwestern India and Pakistan are associated with the positive phase of CGT, however further investigations are needed to reach a definite conclusion

In summary Fig. 2.15 shows a schematic diagram that illustrates how the 200 hPa anomalous high over western central Asia during the positive phase of wave train modifies the pressure anomalies in the HL and hence the associated monsoon circulation and precipitation over northwestern India and Pakistan. The southern flank of the anomalous high extends southward up to 25°N (Fig. 2.4a, Fig. 2.9a). The subsidence associated with enhanced 200 hPa height anomalies above the HL region reduces the surface pressure in the HL (1)- by raising the temperature of the middle and upper tropospheric air (warmer air is lighter than the colder air) through adiabatic heating (Fig. 2.9b), (2)- by creating anomalous inversion between lower and upper troposphere (not shown). The anomalous inversion restricts the middle and low level cloud formation aloft the HL region (not shown). Furthermore, the upper level anomalous subsidence above the HL also reduces the high cloud cover thus favoring more solar radiation to this area (not shown).

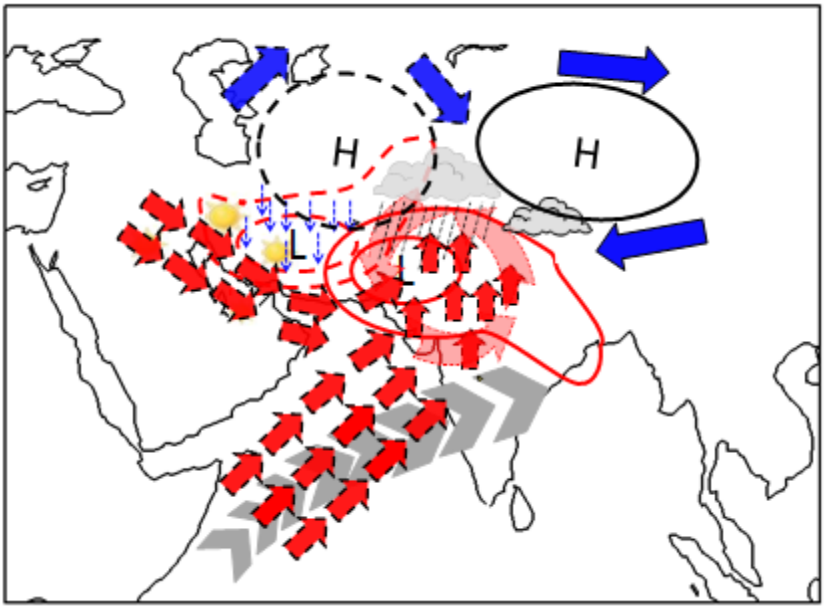

Figure 2.15: Schematic diagram illustrate how the anomalous high over western central Asia modulated the pressure anomalies in the heat low region and associated monsoon precipitation over northwestern India and Pakistan. The solid black and solid red circles show the mean position of upper level Tibetan high and surface Heat Low (HL). The dashed black and dashed red circles indicate the position of upper level 200 hPa anomalous high over western central Asian and the associated westward appearance of the anomalous core of the low pressure during the positive phase of CGT. The bold solid blue arrows indicate the upper level circulation associated with 200 hPa Tibetan high and anomalous high over western central Asia. The subsidence associated with the enhanced height anomalies aloft the HL is shown by the light blue dashed arrows. The mean southwesterly flow is shown by the light grey arrows over the Arabian Sea. The red arrows over Arabian Sea and Persian Gulf indicate the enhanced low level moist southerly flow that converges and favors the monsoon trough like conditions over northwestern India and Pakistan (see the text for further explanation).

Consequently, the accruing surface air temperature further decreases the surface air pressure resulting in additional intensification of the HL. The westward accruing surface air temperature favors a westward extension of the anomalous core of the low pressure over Iran. The westward extension of the intensified low pressure with its north-south orientation produces enormous north-south pressure gradient (lower pressure over the land than over the sea) and a positive vorticity over northwestern India and Pakistan. This enables the moist southerly

flow from the Arabian Sea at lower levels to intrude deep into northwestern India and Pakistan. A monsoon trough like conditions develops over northwestern India and Pakistan where moist flow from the Arabian Sea and the Persian Gulf converge. The convergence is additionally supported by the orographic lifting (Haln and Manabe 1995; Song et al. 2009) which further fosters the convection and hence the precipitation over this area. The high resolution climate model ECHAM5 simulation also underlines the proposed mechanism. The correlation and composite patterns associated with HLI and CGTI are reasonably simulated by the model. The model also simulates reasonably well the eastward propagation of the mid-latitude wave train and associated surface pressure changes over Indian domain.

From the above discussion it is inferred that the surface HL plays a momentous role in connecting the mid-latitude wave train and the ISM precipitation over northwestern India and Pakistan. Since the HL divulges significant correlation with the upper level geopotential height anomalies over East Asia, it is abstruse currently if there is any feedback from HL to the CGT and the associated precipitation over East Asia region. A lag relationship of CGTI with HLI further supports the previous hypothesis of Ding and Wang (2005, 2007) about the positive feedback from ISM to CGT. Since ECHAM5 model reasonably simulates the above proposed mechanism the next chapter further explores this conundrum by using sensitivity model experiments.

Chapter 3

Precipitation variability over the South Asian monsoon heat low and associated teleconnections

3.1 Introduction

The Asian summer monsoon system can broadly be divided into two subsystems, the Indian summer monsoon (ISM) and the East Asian summer monsoon (EASM) system, which are to a greater extent independent of each other and, at the same time, interact with each other (Kripalani and Singh, 1993; Wang and Fan 1999; Wang et al. 2001; Ding and Chan 2005). On interannual time scales, the monsoon rainfall over India and northern China (southern Japan) are known to co-vary in phase (out of phase) indicating a common element of large-scale low-frequency variability (e.g., Kripalani and Singh, 1993; Kripalani and Kulkarni, 1997, 2001; Krishnan and Sugi, 2001). While it is known that El Niño/Southern Oscillation (ENSO) is an important contributor to the interannual variations of monsoon rainfall over the two regions (e.g., Walker 1924; Webster and Yang 1992; Wang et al., 2000; Fasullo and Webster 2002; Hu et al., 2005), a substantial portion of monsoonal variability, particularly over South Asia, also arises from the strong internal dynamics and convectively coupled processes of the monsoon system (e.g., Palmer and Anderson, 1994; Sperber and Palmer, 1996; Sugi et al. 1997; Goswami 1998; Krishnan et al., 2009).

Observations suggest that the interannual variability of the EASM rainfall is related to the west North Pacific summer monsoon heat source, as well as the convection over the ISM domain (Wang et al., 2001). Studies have reported two upper level barotropic anticyclonic anomalies during the excess ISM years, one located over the western central Asia and another over East Asia (e.g., Krishnan and Sugi, 2001; Wang et al., 2001). Ding and Wang (2005) found a circumglobal wave train in the northern hemispheric during boreal summer and pointed out that the CGT pattern can favor co-varying patterns of rainfall anomalies over South and East Asia. In fact the recent summer monsoon of 2010 is a good example to illustrate the out-of-phase rainfall and circulation variability between the two regions. Figure 3S1 shows that the anomalous rainfall enhancement over Northwest-Central India and Pakistan is associated with convergence of winds from the Arabian Sea and Bay-of-Bengal; whereas a large-scale anticyclonic anomaly can be seen over the Northwest Pacific. In a previous study, Saeed et al. (2010) noted that the eastward propagation of mid-latitude wave train associated with the CGT modulates the surface pressure variations over the monsoon heat-low (HL) region (25°-35°N, 55°-75°E), and thereby favors enhanced southwesterly monsoonal flow and increased rainfall over northwestern India and Pakistan (NWIP). They found significant lead-lag correlations between the HL and the upper level circulation over western central Asia and also over East Asia. Despite the aforementioned studies, it is not yet adequately clear as to what extent the variability of rainfall / convection over the monsoon HL region can actually influence the large-scale circulation response and rainfall anomalies over East Asia. This chapter addresses the above question by conducting numerical simulation experiments using a high-resolution atmospheric GCM.

3.2 Methods

In this chapter the high resolution (T106L31) ECHAM5 climate model has been used. A detailed description of ECHAM5 is given by Roeckner et al. (2003). At high resolution, such as the one used here, ECHAM5 simulates reasonably well

the mean climate (Roeckner et al., 2006) and the HL–CGT relationship (Saeed et al., 2010). Similar to Roeckner et al. (2006), we have conducted a control AMIP-type run of the ECHAM5 at T106L31 resolution to verify the mean summer monsoon circulation pattern over Asia. It is found that the model simulates fairly well the salient features of the boreal summer mean monsoon circulation e.g., the South Asian monsoon trough, the surface HL over northwest India and adjacent area, the southwest monsoon cross-equatorial flow, the Mascarene High, the upper-tropospheric Tropical Easterly Jet and the Tibetan anticyclone (Fig. 3S2). Also the overall distribution of the summer monsoon rainfall over the Indian region is quite robust, as the model simulates reasonably well the precipitation maxima along the west coast and over Bay of Bengal (10°-20°N) and a small portion of rain shadowing area near western Ghatts (Fig. 3S2).

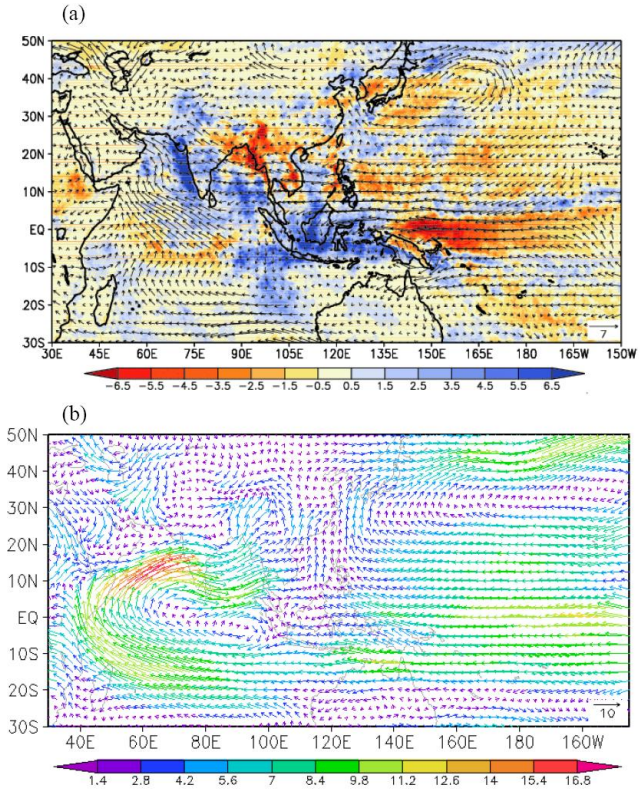

Figure 3S1: (a)- The rainfall and 850 hPa wind anomaly for JJAS 2010. (b)- mean 850 hPa wind ($msec^{-1}$) during the summer monsoon (JJAS) 2010. The rainfall data is from TRMM 3B42 dataset. The winds are from NCEP reanalysis.

In addition to the control experiment, two sensitivity simulations have been carried out to examine the influence of convection variability over the monsoon HL region on the large-scale response. The strategy adopted for generating the convection variations over the monsoon HL region is by modifying the surface albedo. As pointed out by Meehl (1994), the lower land albedos are associated with warmer land temperatures, greater land-sea temperature contrast, and a stronger Asian summer monsoon. This approach has been adopted in our study to vary the convection over the monsoon HL region. The first experiment is the intensified heat low (IHL) run in which the convection over the surface HL is enhanced by reducing the surface albedo from 0.3 to 0.05 over the HL region (55°-75°E, 25°-35°N). The second experiment corresponds to the shallow heat low (SHL) run in which the convection over the HL is suppressed by increasing the surface albedo from 0.3 to 0.55 over the HL region. In each case the model is forced with observed sea ice and sea surface temperatures for the period from 01st January 1978 to 31st December 1999. The first year of each simulation is skipped and the analysis focuses on the remaining 21 summer seasons. Each summer season spans 122 days from 1st June to 31st September. Daily data are pre-processed with a 3-day running mean time filtering in order to eliminate synoptic variability. For simplicity the difference (IHL minus SHL) between the two experiments is referred to as IMSHL.

In an accompanying set of experiments, the influence of convection variations over the East Asian monsoon region on the large-scale circulation response has been assessed. For this purpose, two additional simulations covering the same period as above has been carried out, however, we first increased (decreased) the convection over the East Asia region (100°-120°E, 25°-35°N) by decreasing (increasing) the surface albedo. These two experiments are abbreviated as EAIL (EASL). The difference (EAIL minus EASL experiment) is referred as EAIMS. A t-test has been applied to assess the significance of the simulated response.

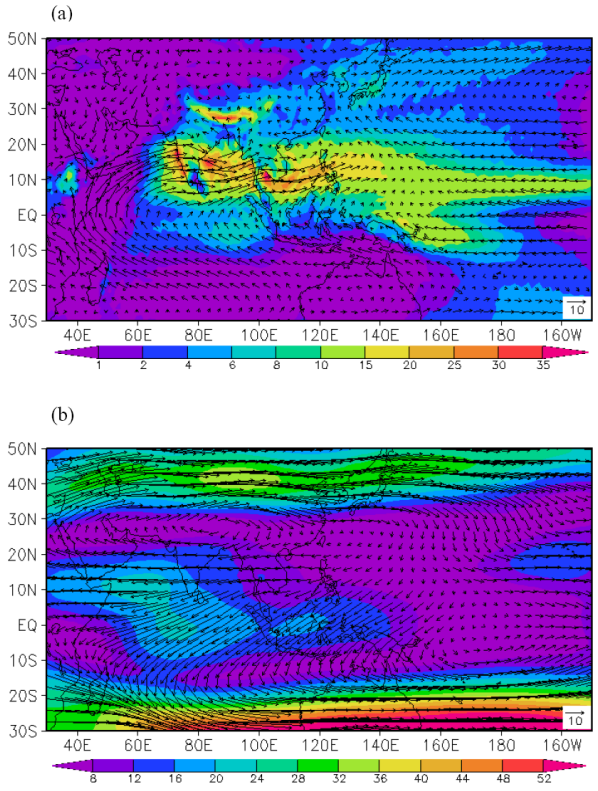

Figure 3S2: The JJAS climatological mean simulation from ECHAM5 model (a) Rainfall (shaded) and 850 hPa winds (b) 200 hPa winds. Shaded area in (b) shows wind magnitude. The unit of rainfall is mm and wind is $msec^{-1}$.

3.3 Results and discussions

3.3.1 Analysis of IMSHL

In the Asian monsoon region, the intensification of the HL is associated with significantly decreased pressure anomalies over the Arabian Sea and adjoining areas of Saudi Arabia and West Asia (Fig. 3.1a). High-pressure anomalies over the South China Sea and the northwestern Pacific can also be noted in Fig. 3.1a. The low level 850 hPa wind flow (Fig. 3.1b) shows convergence of the flows from the Arabian Sea and the Bay of Bengal occurring over the NWIP and adjoining areas, with accompanying rainfall anomalies over the region. It is also interesting to note that the large-scale structure of the wind anomalies in Fig. 3.1b shows

anomalous divergence over the South China Sea. The upper-tropospheric wind anomalies in Fig. 3.1c are nearly out-of-phase with the low-level circulation response. Furthermore, it can be noticed that the enhanced rainfall over the HL and adjacent areas is characterized by a wave like response in the upper levels similar to CGT (Fig. 3.1b-c, 3.2a, 3.2c). Studies have examined the influence of large-scale circulation anomalies on the precipitation variability over northern China (e.g., Wang et al., 2001). The strong convergence of the low level moist southerly flow favors enhanced precipitation and upper level divergence over northern China (Fig. 3.1b-c). On the other hand, the suppressed rainfall over the South China Sea is associated with anomalous low level divergence over the region (Fig. 3.1b). The map of vertical velocity anomalies at 500 hPa for the IHL experiment reveals anomalous ascent over the HL region and also over northern China (30°-45°N, 100°-120°E) as seen from Fig. 3.2a-c. However when rainfall over the HL region is suppressed, the large-scale teleconnection is absent over the East Asia monsoon region (Fig. 3.2b, 3.2d). In other words, the large-scale circulation response to decrease of precipitation over the HL region is not simply a mirror image of the response to increased precipitation over the HL region. Furthermore, it must be pointed out that the rainfall over the HL region show larger variability in case of the IHL (standard deviation 1.53 mm day^{-1}) as compared to the SHL (standard deviation 0.79 mm day^{-1}) (Fig. 3.3a-b). Thus the likelihood of the occurrence of heavy rainfall over NWIP increases in case of IHL.

The ISM displays positive correlations with rainfall over northern China suggesting co-occurrence of floods and droughts over both regions (Kripalani and Kulkarni 2001). To further examine this relationship, we also carried out a lead-lag correlation analysis between the sea level pressure over HL and precipitation over northern China (35°-42°N, 100°-120°E). For this purpose we first computed the intense HL years. The years when the sea level pressure anomalies over the HL region (Saeed et al. 2010) are below 0.5 standard deviations are considered as intense HL years. Out of 21 years only 7 years are indentified as intense HL years. We found that the sea level pressure over the HL region leads precipitation over northern China by several days with maximum

correlation occurring between 10-20 leading days (Fig. 3.3c). Though statistically significant the correlations are small. It is realized that the East Asian monsoon variability is influenced by number of other factors like convection and circulation changes over the north of Philippines (Nitta, 1986, 1987), northwest Pacific heat source (e.g., Wang et al. 2001), El Nino Southern Oscillation (e.g., Huang and Wu 1989; Zhang et al. 1999; Wang et al. 2000; Wang et al. 2001), the tropical Indian Ocean sea surface temperature (e.g., Li et al. 2008), the north Atlantic Oscillation (e.g., Sung et al. 2006), etc. However, we tested the significance of the correlation value for HL leading the precipitation up to 20 days by evaluating a nonparametric estimate for the likelihood of a nonrandom occurrence of the result using a bootstrap method (e.g., Zanchettin et al., 2008). In this lead-lag range, the correlation values test as significant above the 95% confidence against a random occurrence, thereby suggesting a linkage of the detected signal to the true features of the process. Basically, the circulation response over the East Asian monsoon region can be interpreted as large-scale quasi-stationary waves induced by convection changes over the monsoon HL region.

It is known that the summertime upper-tropospheric westerlies extending over West-Central Asia and the northern flanks of the Indo-Pakistan region can act as a waveguide and allow generation of stationary wave patterns (see Ambrizzi et al. 1995; Terao, 1999; Enomoto et al. 2003; Ding and Wang 2005; Krishnan et al. 2009). Terao (1999) showed that eastward propagating waves along the westerly jets in the upper troposphere are more strongly trapped in the westerly jet than the westward propagating ones. Therefore, convectively generated wave motions over the heat-low region have the potential to extend downstream up to the Far East in the form of large-scale quasi-stationary circulation anomalies. It is seen from the present results that the HL and associated precipitation/convection variability can also modulate the EASM rainfall variability

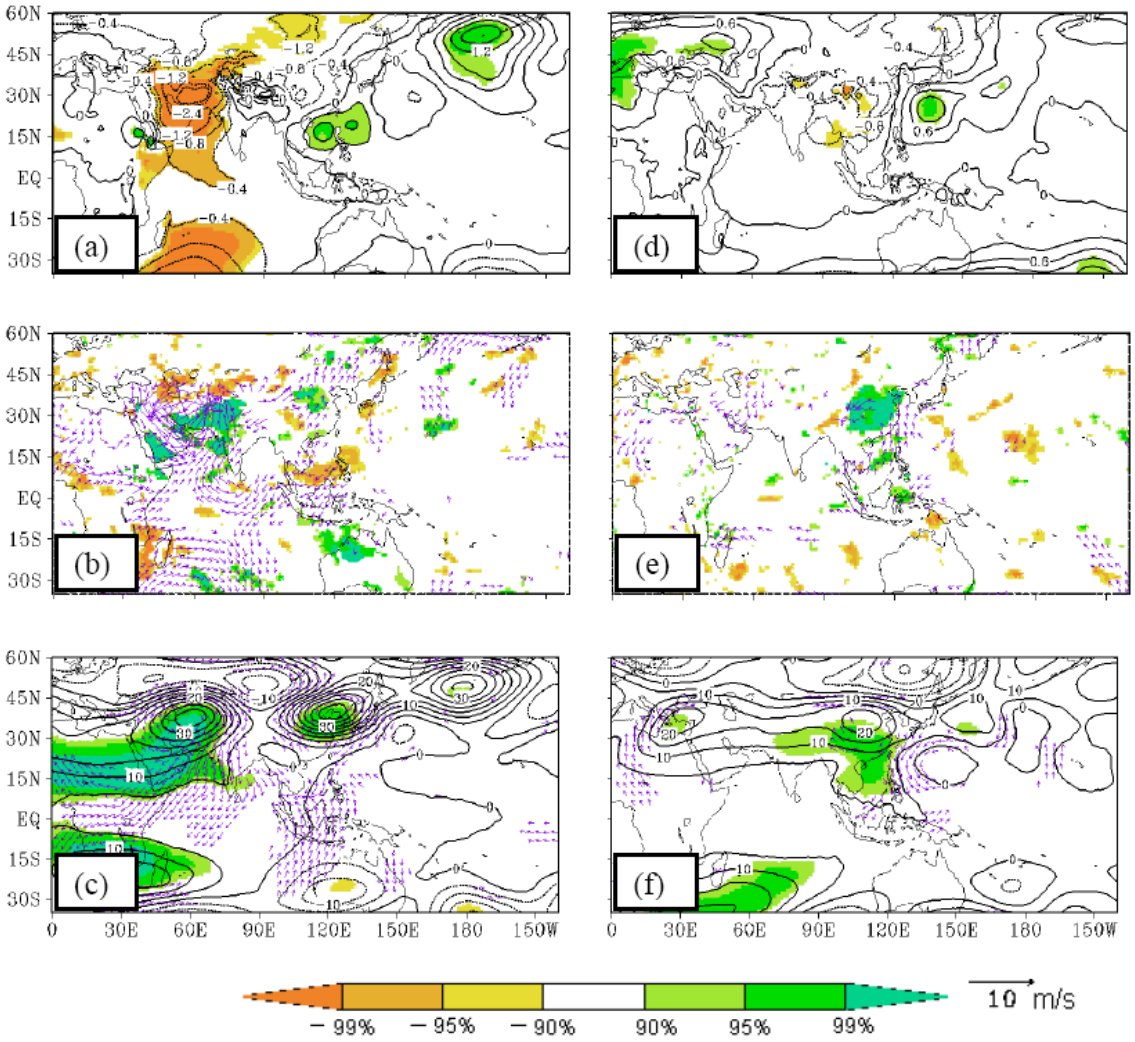

Figure 3.1: Mean difference of 21 summer seasons (June-September) from 1979-1999 between the intensified and shallow heat low experiment (IMSHL) (a) sea level pressure (hPa) (b) 850 hPa wind (vectors) and surface precipitation (shaded) (c) 200 hPa geopotential height (contours) and wind (vectors). The shaded areas in (a, b, c) indicate differences that are significant at 90% confidence level based on t-test for mean sea level pressure, surface precipitation and 200 hPa geopotential height respectively. The wind vectors associated to differences below 95% confidence level are omitted in (b, c). Negative contours in (a, c) are shown by dashed line. Panels (d-e) are similar to (a-c) except for EAIME experiment.

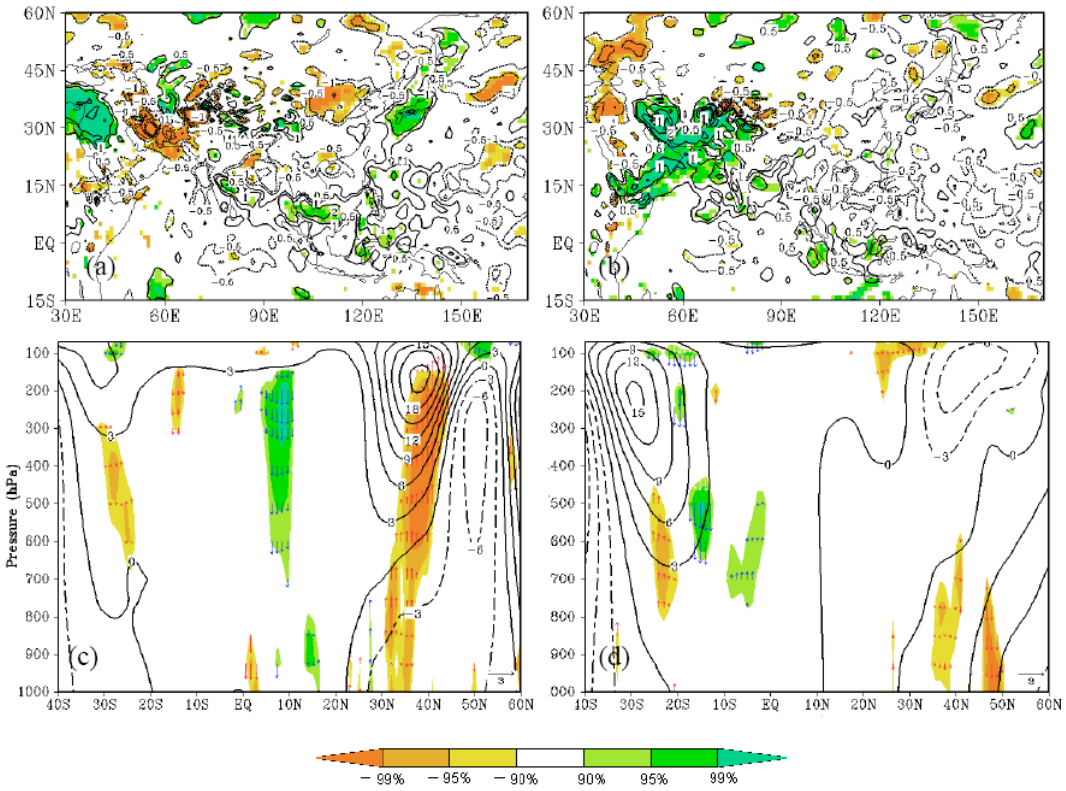

Figure 3.2: Mean differences of vertical velocity at 500 hPa (a) IHL minus Control experiment (b) SHL minus Control experiment. The difference in the height-latitude cross-section of vertical velocity (shaded) and geopotential height (contours) averaged between 100°-120°E (c) IHL minus Control experiment (d) SHL minus Control experiment. The difference is computed for 21 summer seasons (June-September) from 1979-1999 using monthly data. The shaded areas in (a-d) indicate differences that are significant at 90% confidence level for vertical velocity based on t-test. The vectors in (c, d) indicate ascent (descent) if pointing upward (downward). The blue (red) vectors show significant increase (decrease) in ascent or descent. The wind vectors associated to differences below 90% confidence level are omitted in (c, d). The negative contours in (a-d) are shown by dashed lines.

3.3.2 Analysis of EAIMS.

The EAIMS reveals (Fig. 3.1d-f) remarkable differences in lower and upper level circulation and pressure patterns as compared to those simulated in the IMSHL (Fig. 3.1a-c). In this case, the anomalous response shows an east-west sea level

pressure dipole with low pressure anomalies over land and high over the northwestern Pacific Ocean (Fig. 3.1d)

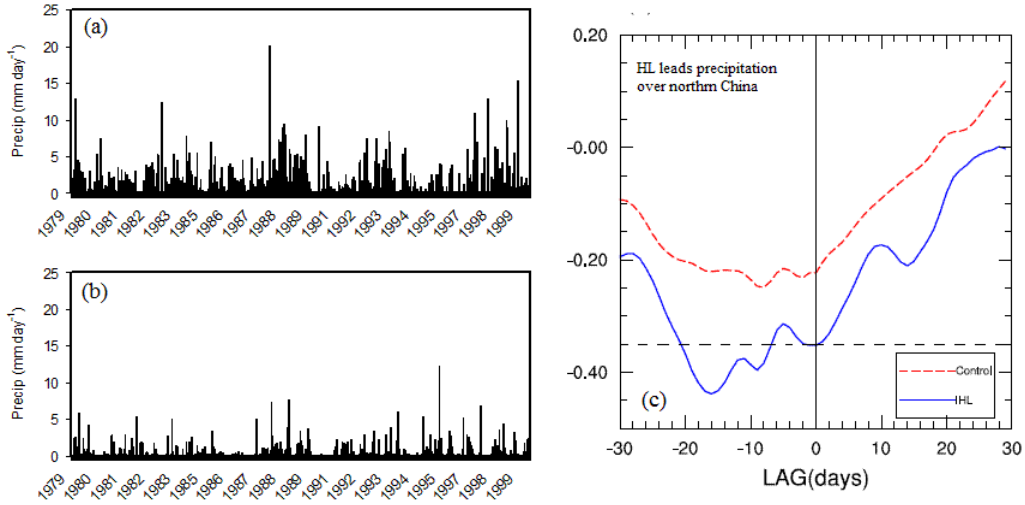

Figure 3.3: Area averaged daily rainfall over the HL region (a) IHL, (b) SHL. The lead-lag correlations between the sea level pressure over HL region and rainfall over northern China (35°-42°N, 100°-120°E) is shown in (c). The solid and dashed line in (c) represents the correlations during the intense HL years and the Control experiment respectively. Out of 21 year 7 years are identified as IHL years. The horizontal dashed line in (c) represents the 95% confidence level for correlations using the t-test.

The associated low level cyclonic (anticyclonic) circulation over land (ocean) favors enhanced moisture convergence and hence precipitation over the northern China (Fig. 3.1e). In contrast to the IMSHL which shows suppressed rainfall over the South China Sea and adjacent areas (Fig. 3.1b), the EAIMS reveals enhanced rainfall starting from South China Sea to northern China. Moreover, the decreased rainfall over the northwestern Pacific Ocean due to the anticyclonic circulation extends eastward in case of the EAIMS which can influence the downstream regions of North Pacific and the US region as noticed by several previous studies (e.g., Lau and Weng; 2002; Lau et al. 2004a). Furthermore, the large scale circulation response seen in the case of IMSHL over the Asian monsoon region (Fig. 3.1c) is absent in EAIMS experiment (Fig. 3.1f),

suggesting the importance of the rainfall/convection variations over the South Asian monsoon heat low on the .downstream circulation response over East Asia.

3.4 Summary and Conclusions

In this chapter the rainfall variability over the South Asian monsoon HL and its response to the large scale circulation and related summer rainfall over East Asia has been examined. For this purpose we imposed modifications to the South Asian monsoon HL by using the climate model ECHAM5 and performed high resolution (T106L31) simulations to investigate the related feedbacks to the Asian monsoon climate. Results suggest that the rainfall/convection variability over South Asian monsoon HL region can influence the EASM rainfall variability through the tropical and extra-tropical components of large-scale teleconnections. The intensification of the HL favors enhanced convection and rainfall above HL region. The enhanced rainfall/convection above HL is further associated with a wave like response in the upper level similar to the CGT pattern extending well into the Asian monsoon region. At lower levels, the strong convergence above HL favors significantly enhanced cross equatorial flow across the India-Africa region and anomalous divergence above the South China Sea. The existence of this teleconnection is further supported by small but statistically significant lead-lag correlations between the heat low and precipitation over northern China. Conversely, a suppressed convection and rainfall above HL region do not display significant circulation anomalies above East Asia region.

Chapter 4

Circumglobal teleconnections and heavy rainfall of July 2010 over Pakistan

4.1 Introduction

Pakistan lies at the northwestern edge of the South Asian monsoon region and has a long latitudinal extent from 24˚N to 37˚N. The climate of the country varies widely due to heterogeneous land surface physiography and floods have been considered as a major natural calamity. Pakistan has a long history of flooding from the Indus River and its tributaries Jhelum, Chenab, Ravi and Sutlej e.g., floods of 1928, 29, 57, 59, 73, 76, 88, 92, 2001, which caused tremendous damages to the life and property (www.pakmet.com.pk).

Due to its unique geographical location both tropical and mid-latitude circulations influence the climate over Pakistan. Previous studies (e.g., Ding and Wang 2005, 2007; Saeed et al., 2010) have shown that the mid-latitude circulation can influence the monsoon precipitation over northwestern India and Pakistan. The monsoon precipitation over northwestern India and Pakistan is often characterized by frequent mesoscale convective developments that can lead to heavy precipitation if sufficient moisture is available. These heavy rainfall episodes contribute significantly to the mean seasonal rainfall over the region. Ding and Wang (2007) found that the active/ break monsoon phases over northwestern India and Pakistan appears to be associated with the mid-latitude wave train. They suggested that the vertical shear associated with the enhanced

easterly might be a responsible mechanism for the northward shift in the convective activity. In addition to the vertical shear the mid-latitude wave train also modulates the surface pressure anomalies over the heat low region (southern Pakistan and adjacent areas of Iran, Afghanistan and Arabian Peninsula) which favors enhanced southwesterly monsoon and associated monsoon rainfall over northwestern India and Pakistan (Saeed et. al. 2010). Syed et al. (2010) found that a warm temperature anomaly over the north Hindu Kush-Himalaya region appears a few days before the active monsoon phase starts over northern Pakistan and adjacent areas. They suspected that the warm temperature anomalies might be associated with the mid-latitude wave train (Ding and Wang, 2007) or the internal variation of the Tibetan High (Popovic and Plumb, 2001).

During the summer monsoon of 2010, very heavy rainfall occurred in the last week of July that caused severe flooding in the Indus River and its tributaries (Fig. 4.1). This was the worst flood in the past 100 years and caused severe damage to the infrastructure and agricultural crops that act as a back bone in the economy of the country. More than 20 million people were affected and the overall estimates of damage exceed $US40B (http://www.pakistanfloods.pk). A week after the Pakistan flood, the northeastern parts of China received heavy rainfall in the early half of August. It is now known that the precipitation/convection variability over the South Asian monsoon heat low can induce large scale circulation anomalies that influence the precipitation variability over northern China (Saeed et al. 2011).

Webster et al. (2011) showed that the heavy rainfall over Pakistan during July 2010 was highly predictable. They used 15–day ensemble of the European Center for Medium Range Weather Forecast and concluded that the high risk of flood in Pakistan could have been seen if the extended quantitative precipitation forecast had been available in Pakistan. Beside the aforementioned deficiencies in Pakistan it is important to understand the underlying causes that were responsible for the abnormal intensification of the circulation that led the heavy rainfall over Pakistan. The present study therefore aimed to examine the circulation patterns

associated the heavy rainfall event to understand the underlying physical mechanism associated with the heavy rainfall over Pakistan.

The next section will describe the data used in this study. An overview of the mean climatology of July is given in the section 4.3. The anomalous circulation associated with the heavy rainfall is discussed in section 4.4. Summary and conclusions are presented in the last section.

4.2 Data and Methods

The major data set used in this study is the NCEP/NCAR reanalysis (Kalney et al. 1996). Both monthly and daily data sets are used. For precipitation over Pakistan during July 2010, we used observed meteorological station data from 73 meteorological stations in Pakistan. A triangular mesh type interpolation has been applied to interpolate the meteorological station data over Pakistan. We computed thirty years (1970-2000) July climatology for different variables such as geopotential heights, temperature and wind circulation at 200 hPa, vertical velocity at 500 hPa, low level wind circulation at 850 hPa, surface temperature and mean sea level pressure to examine the mean circulation over Eurasian region during the month of July. A t-test has been applied to access the difference between the July 2010 event and its climatology.

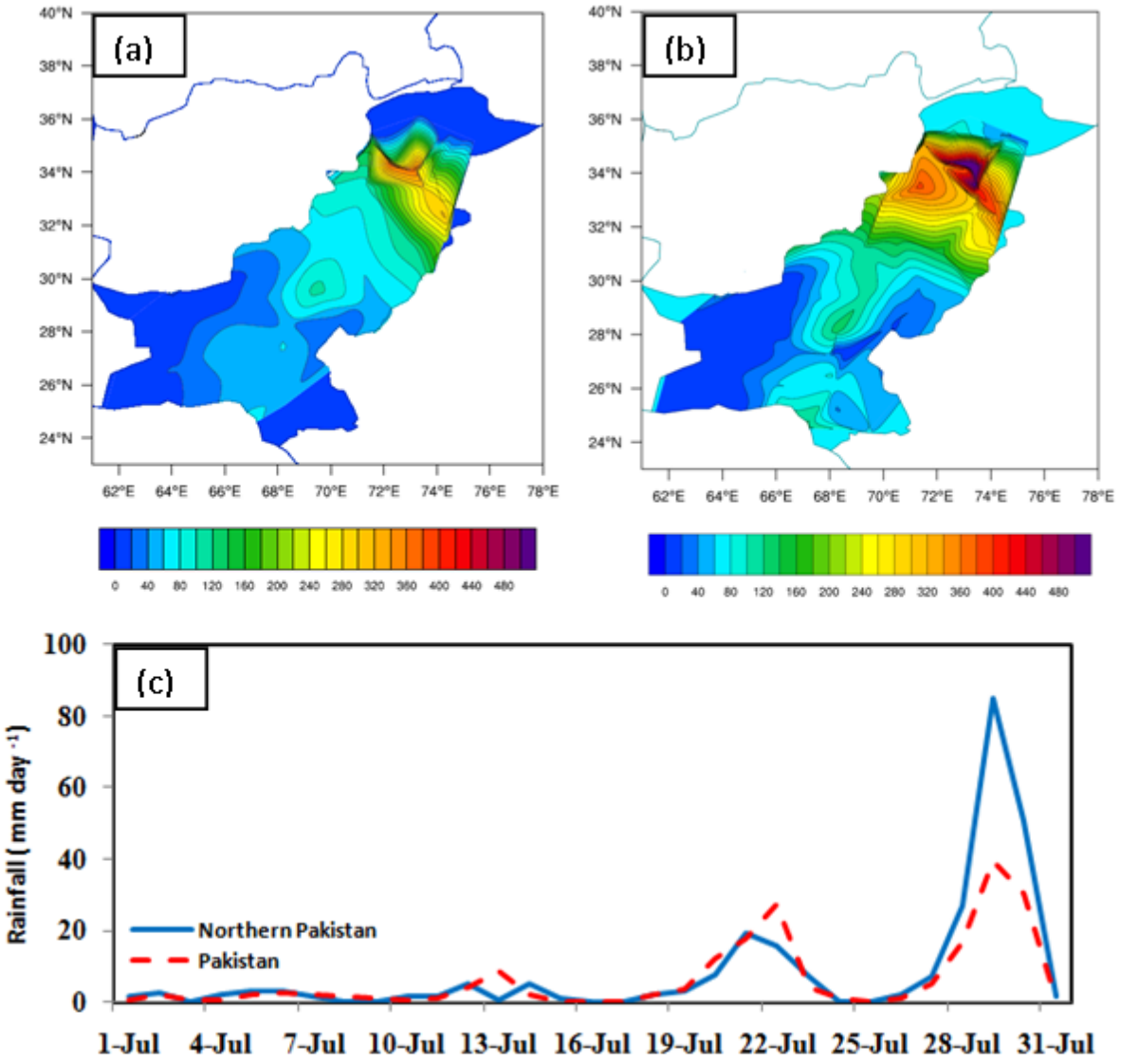

Figure 4.1: Observed precipitation (mm day^{-1}) over Pakistan using meteorological station data (a)- 30 years (1971-2000) climatology of July (b)- July 2010 (c) time series mean daily rainfall over northern Pakistan (solid) and Pakistan (dashed) during July 2010. Triangular mesh grid type interpolation is carried out to interpolate the precipitation data from 73 meteorological stations inside Pakistan.

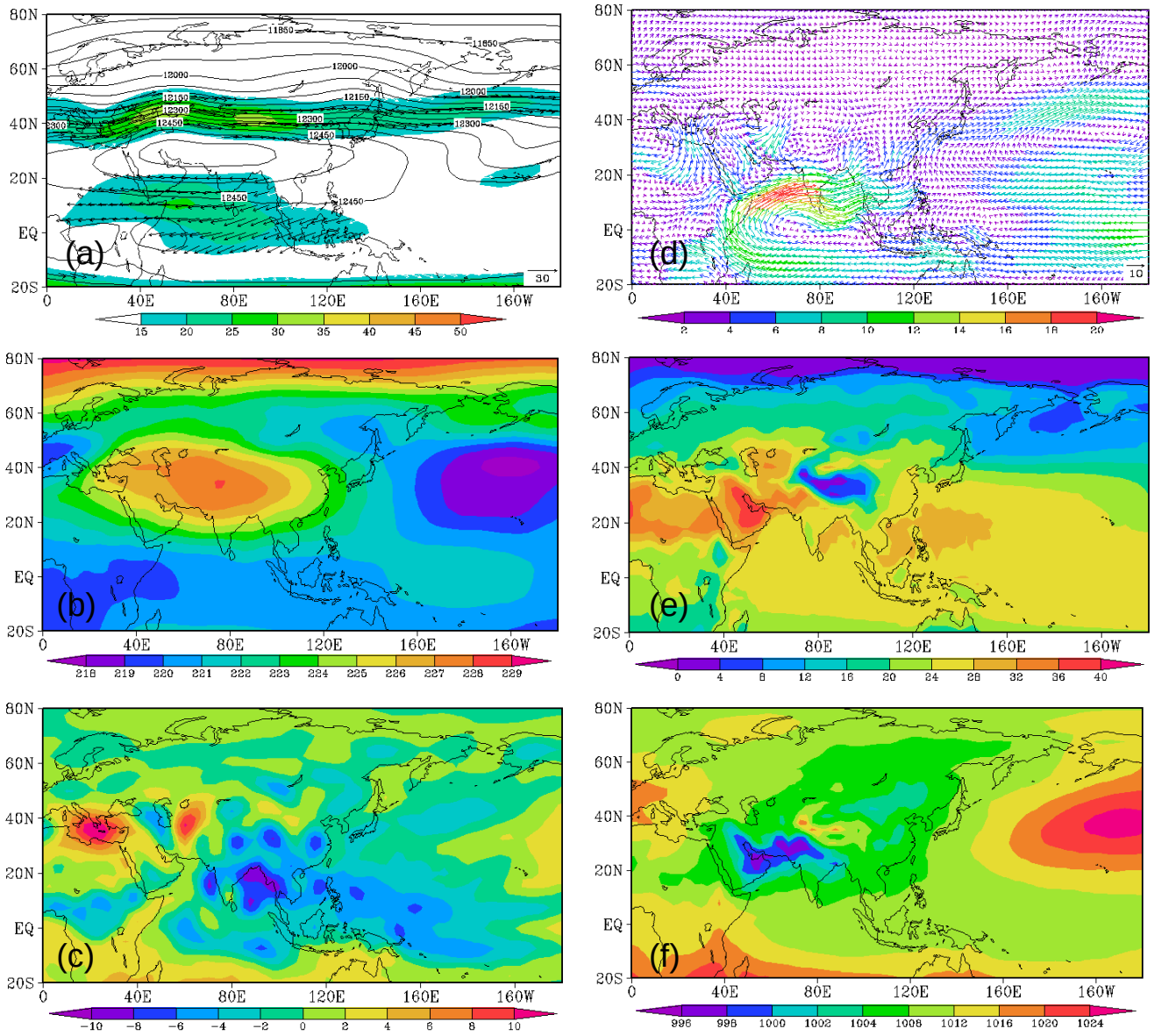

Figure 4.2: 30-years (1971-2000) mean climatology of July using NCEP reanalysis data (a)- 200 hPa heights (contours) and wind (vectors ,shaded) (b)- 200 hPa temperature (c)- 500 hPa vertical velocity (hPa sec^{-1}) (d)- 850 hPa wind ($msec^{-1}$) (e)- surface temperature (°C) (f)- sea level pressure (hPa).

4.3 Mean circulation during July

The month of July is generally considered as one of the peak monsoon months over northern Pakistan and adjacent areas. The observed climatologically during July reveals enhanced rainfall (~ 80-300 mm) over northern parts and adjacent areas (32°-36°N) compared to the dry southern parts (Fig. 4.1a). The associated upper level circulation at 200 hPa reveals well known Tibetan high pressure with maximum heights ~ 12550 gpm and the subtropical jet with maximum wind speed ~ 30-35 ms^{-1} (Fig. 4.2a).

Several studies (e.g., Flohn, 1957; Krishnamurti, 1973; Haln and Manaba, 1995; Yani and Wu, 2006; Liu et al., 2007) have noticed that the Tibetan Plateau acts as an elevated heat source (Fig. 4.2b) that maintains the upper-tropospheric anticyclonic circulation during the boreal summer. The major convection in July occurs over the head of Bay of Bengal (Fig. 4.2c). Rodewell and Hoskin (1996) noticed that the convection over Bay of Bengal during the summer monsoon is associated with a Rossby wave like response to the west and subsidence over the eastern parts of Caspian region and over Mediterranean region. At lower level the wind circulation at 850 hPa shows southwesterly flow over Arabian Sea with maximum speed ~18-20 ms^{-1} (Fig. 4.2d).

The dry arid parts in southern Pakistan and adjacent Arabian Peninsula receive higher surface temperature in the northern hemisphere during July (Fig. 4.2e). In association with the high surface temperatures this region also receives the lowest mean sea level pressure in the northern hemisphere during the boreal summer. The mean sea level pressure during July shows low pressure (~1000 hPa) over southwestern Pakistan and adjacent areas of Arabian Peninsula and a high pressure (~1024 hPa) over Pacific Ocean around 35°N, 165°W (Fig. 4.2d).

4.4 Anomalous circulation during July 2010

Much of the northern parts of Pakistan and adjacent areas received heavy rainfall during July 2010 (Fig. 4.1b). Two very active rain spells occurred over Pakistan in the second half of July. The rain spell occurred in the last week from 27-30th July, 2010, over northern Pakistan caused devastating flooding in the Indus basin region (Fig. 4.1c). At the same time the mid-latitude circulation shows abnormal intensification over the Eurasia region (Fig. 4.4a-b).

To examine the circulation associated with the heavy rainfall over Pakistan we first analyse the 200 hPa geopotential height during July 2010. In the first week of July a blocking high pressure starts developing over the western Russia (Fig. 4.3a). From day 06 to 10, the blocking high intensifies and shifts little eastward (Fig. 4.3b). From day 11 to 15, the blocking high further intensifies and a wave like pattern with successive lows and highs can be seen in the mid-latitude (Fig. 4.3c). From day 16 to 20, the blocking high shifts little eastward (Fig. 4.3d). The wavelike pattern disappears over the Asian monsoon region, however to the west of the blocking high a wave like pattern with successive low and high can be seen. From day 21 to 25 this wavelike pattern propagates eastward (shown by the vertical dashed line in Fig. 4.3d-f).

The eastward propagation of the mid-latitude wave train influenced the blocking high. To the east of the blocking high a wavelike pattern also appears over the Asian monsoon region (Fig. 4.3e). From day 26 to 31, a well developed wave train in the mid-latitude can be seen that extends from the North Atlantic to Asian monsoon region (Fig. 4.3f). The eastward propagation of the wave train influenced the shape and orientation of the blocking high. The blocking high has changed its shape and orientation from east-west (Fig. 4.3c-e) to north-south direction (Fig. 4.3f).

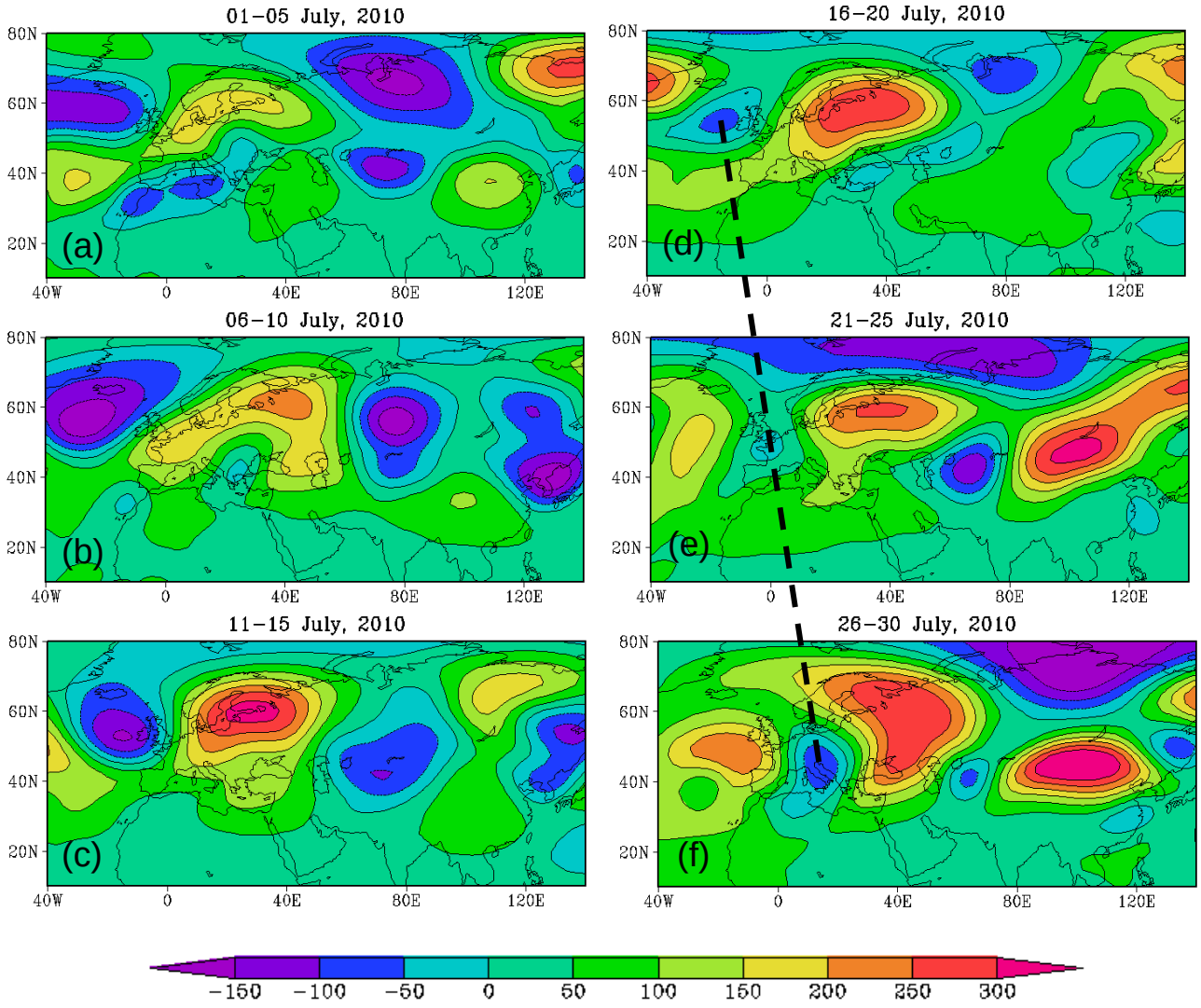

Figure 4.3: (a–f) 200 hPa geopotential heights anomalies during July 2010 show the development of the persistent blocking high over western Russia and eastward propagation of mid-latitude wave train. The anomalies are computed from 30-years (1971–2000) July mean climatology. The vertical dashed line (d–f) shows the mid-latitude wave train propagates eastward and influences the blocking high over western Russia that appeared during the early half of July.

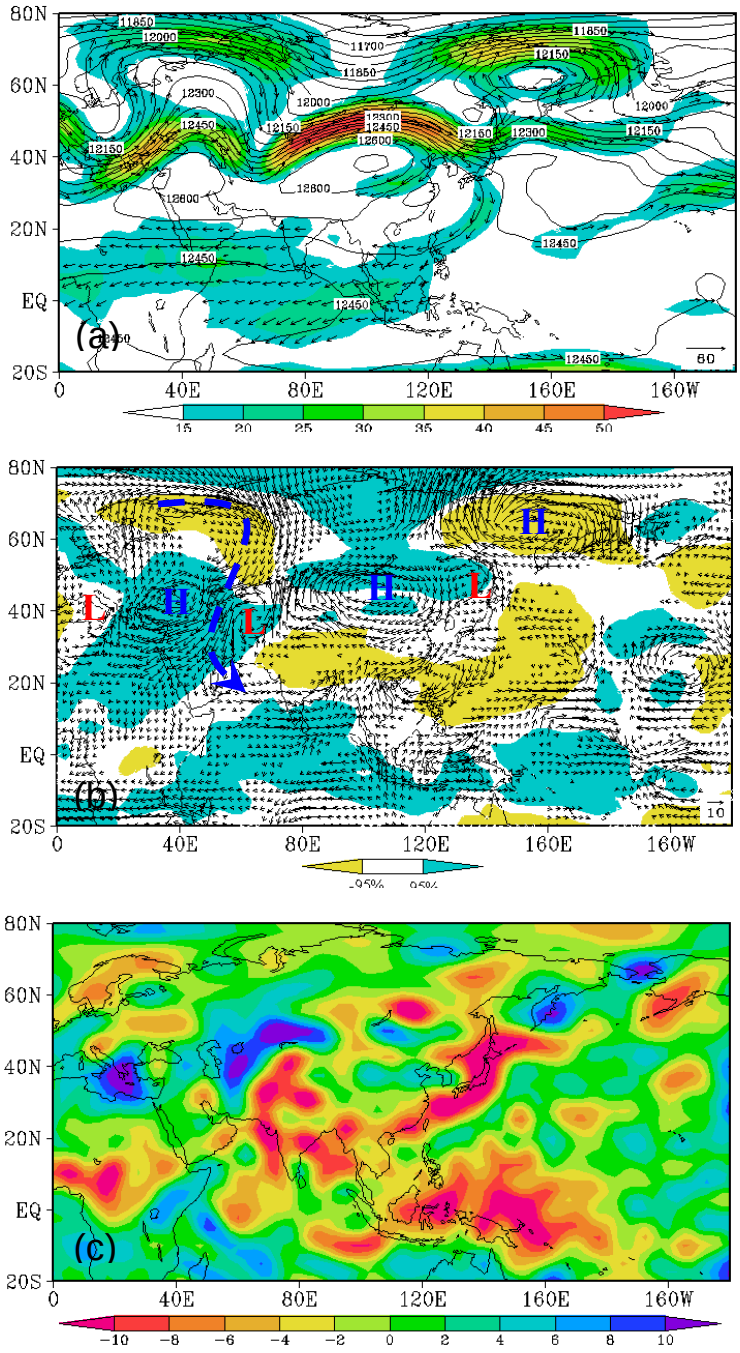

Figure 4.4: (a)- 200 hPa geopotential heights (contours) and wind (vectors) during July 27-30, 2010. Shading shows wind magnitude (b)- 200hPa temperature anomalies (shaded) and wind (vectors) during 27-30 July 2010. (c)- 500 hPa vertical velocity (hPa sec^{-1}). The shaded areas in (b) show differences that are significant at 95% confidence level for 200 hPa temperatures. The wind vectors associated to differences below 95% confidence level are omitted in (b). The blue dashed arrow in (b) shows the extratropical cold air drawn to the southern latitudes.

Saeed et al. (2010) showed that the eastward propagation of the mid-latitude wave train can influence the pressure anomalies over the heat low region and associated monsoon rainfall over northwestern India and Pakistan. The sea level pressure shows positive anomalies over much of India in the early half of July 2010 (Fig. 4.5a-c). In co-occurrence with the upper level wave train the sea level pressure display negative pressure anomalies and hence the deepening of the low pressure over northern Pakistan and adjacent areas, the Arabian Sea and adjoining Arabian peninsula and Persian Gulf and Iran (Fig. 4.5e-f). With some exceptions this behavior of sea level pressure over the Indian region in association of mid-latitude wave train is similar to that shown in Figs. 2.5 and 2.6 of chapter 2.

The east-west oriented blocking high (Fig. 4.3c-f) shifts little eastward and takes north-south orientation as discussed above (Fig. 4.3f). The north-south oriented blocking high in association with the wave train favors the extratropical cold air further southward towards the Asian monsoon region (Fig. 4.4a, b). As a result the jet stream moved further south than its normal position with its trough approaching northern Pakistan and hence dividing the Tibetan anticyclone in to two parts (Fig. 4.4a). The eastward propagating wave train in association with enhanced Tibetan High and sinking cold extratropical air produced warmer surface temperature anomalies that favored further deepening of the low pressure over northern Pakistan and adjacent areas, Arabian Sea and adjoining areas Arabian Peninsula (Fig. 4.5d-f). The associated low level 850 hPa winds reveal enhanced monsoon flow over the Arabian Sea and Bay of Bengal (Fig. 4.6e-f). The low level monsoon flow over the Arabian Sea and adjacent areas during the last week of July (Fig. 4.6e-f) resembles to that shown in Fig. 4.4c of Chapter 2. The deepening of the surface low favored enhanced moist southerly flow from the Arabian Sea and the Bay of Bengal to intrude deep in to northern Pakistan and adjacent areas. The enhanced upper level trough above northwestern Pakistan (Fig. 4.4a) in association with orographic lifting favored strong convection (Fig. 4.4c) and associated rainfall over northern Pakistan and adjacent areas.

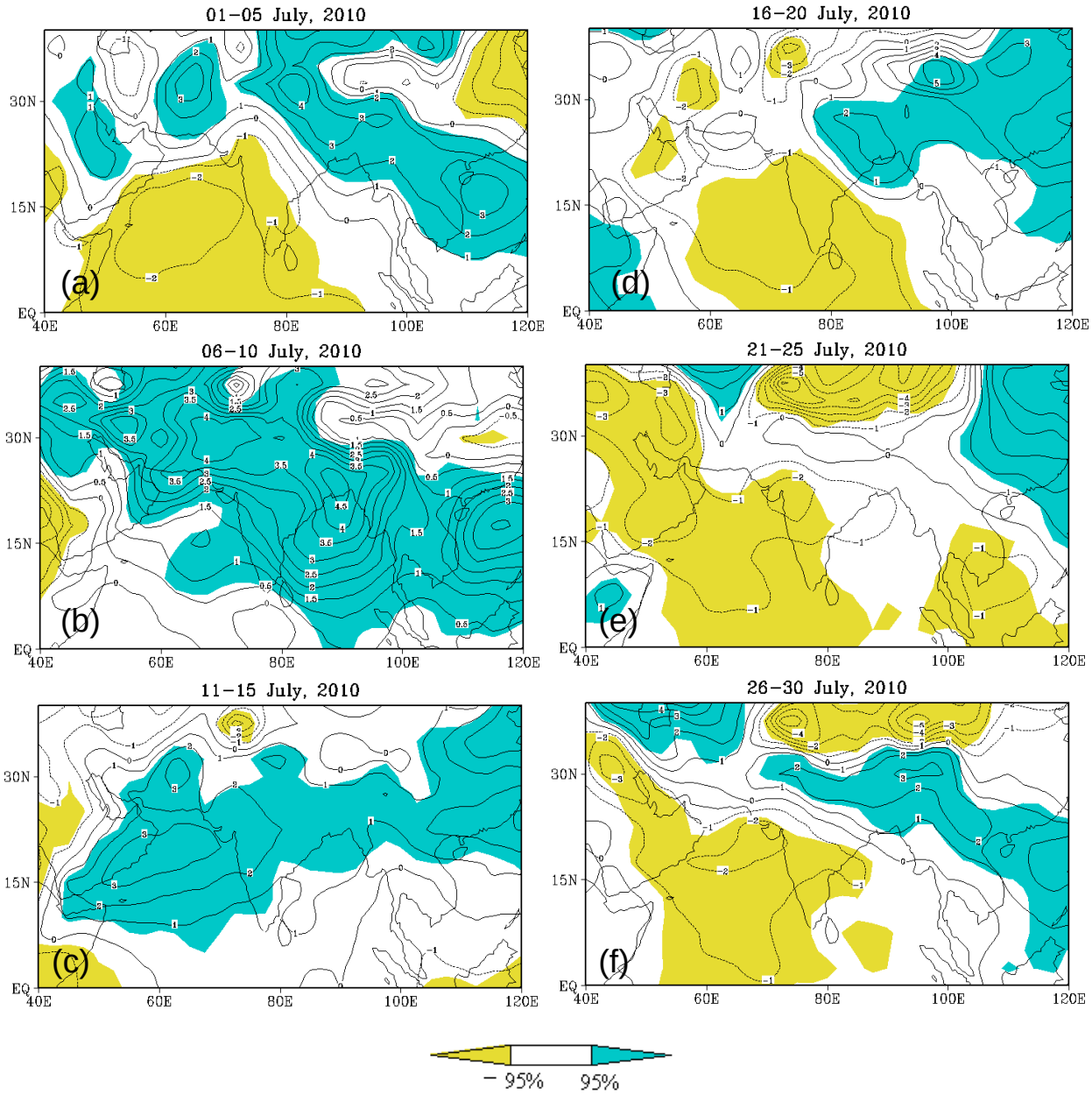

Figure 4.5: (a–f) Mean sea level pressure anomalies during July 2010. The anomalies are computed from 30-years (1971–2000) July mean climatology. The shaded areas show anomalies that are significant to 95% confidence level. The negative contours are shown by dashed lines.

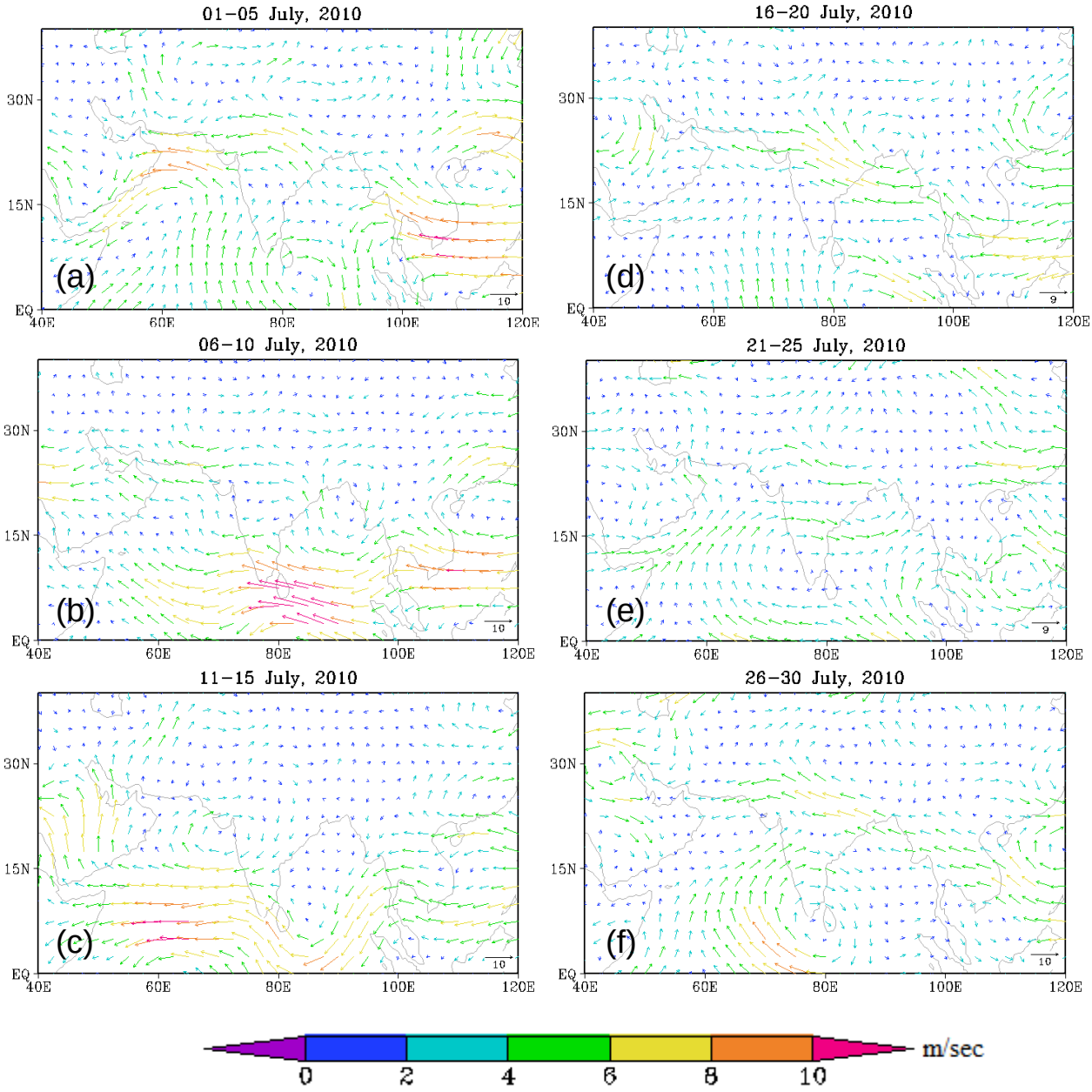

Figure 4.6: (a–f) 850 hPa wind anomalies during July 2010. The anomalies are computed from 30-years (1971–2000) July mean climatology.

By comparing Fig. 4.1c and Fig. 4.3, it can be seen that the development of the precipitation over Pakistan during July 2010 is associated with a co-occurrence of eastward propagating mid-latitude wave train and blocking high. The co-occurrence of a well developed wave train and the blocking high is further associated with the maximum precipitation over northern Pakistan that occurred in the last week of July 2010.

4.5 Summary and discussion

Pakistan has received history's worst flooding during 2010 summer monsoon that caused severe damage to infrastructure and agricultural crops. More than 20 million people were directly affected and the total damage costs nearly 40B US$. Webster et al. (2011) showed that the heavy rainfall over northern Pakistan was highly predictable using high resolution numerical models used in ECMWF. However, what has caused the abnormal rainfall over Pakistan has not been identified and discussed so far. In this chapter the circulation patterns associated with the 2010 heavy rainfall over Pakistan has been examined to understand the underlying physical mechanism.

A blocking high pressure in the upper levels is developed over the western Russia during July 2010. Analysis reveals a wave like pattern similar to the CGT in the mid-latitudes that influence the blocking high and hence the precipitation over northern Pakistan and adjacent areas. The eastward propagation of the mid-latitude wave train seems influencing the blocking high. The east-west oriented blocking high shifted eastward and took a north-south orientation. The north-south oriented blocking high in association with the wave train favored the extratropical cold air to intrude southward into the Asian monsoon region. As a result the jet stream moved further south than its normal position with its trough approaching northern Pakistan and hence dividing the Tibetan anticyclone in to two parts. The eastward propagating wave train in association with enhanced Tibetan High and sinking cold extratropical air produced warmer surface temperature anomalies that favored further deepening of the low pressure over northern Pakistan and adjacent areas, Arabian Sea and adjoining areas Arabian Peninsula. The deepening of the surface low favored enhanced moist southerly flow from Arabian Sea and Bay of Bengal to intrude deep in to northern Pakistan and adjacent areas. The enhanced upper level trough above northwestern Pakistan in association with orographic lifting fostered strong convection and associated precipitation over northern Pakistan and adjacent areas.

It is however not clear that what has caused the upper level blocking over western Russia. The sea surface temperature (SST) anomalies over the tropical Pacific showed El Niño like conditions during the early half of 2010 and a developing La Niña thereafter. Historically La Niña is associated with above normal summer monsoon rainfall over the Indian region. Moreover, the observed SSTs anomalies during 2010 show warm SST anomalies in the eastern Indian Ocean and the North Atlantic Ocean. Further investigations are therefore needed to understand the causes of the blocking high and associated abnormal intensification of mid-latitude circulation. Finally, assuming the potential influence of ENSO onto the mid-latitude part of the monsoon region, but also shown the high level of ENSO predictability (Latif et al. 1998), we suspect potential predictability also for the floods over NWIP. On even shorter timescale Webster et al. (2011) have shown a predictive skill of the Pakistan floods. They have applied the ECMWF NWP forecast system and could predict the extreme flood at least one week ahead. How much the skill can be extended to seasonal timescales is an open issue.

Chapter 5

Future circumglobal teleconnections and summer monsoon over northwestern India and Pakistan

5.1 Introduction

A large proportion of the world's population depends on the Asian summer monsoon precipitation which is broadly divided into the South Asian and the East Asian summer monsoon subsystems. Several studies based on climate model simulations reveal possible changes in the South Asian summer monsoon due to the future increase in greenhouse gases. Some studies (e.g., Lal and Singh 2001; Zhao and Kellogg 1988, Lal et al. 1994, 1995) have reported that the South Asian summer monsoon will be weaker or there is no significant precipitation change in future, however others (e.g., Kripalani et al. 2007; Meehl and Arblaster 2003; Ashrit et al. 2003; May 2002, 2004; Hu et al. 2000a,b; Kitoh et al. 1997; Bhaskaran et al. 1995; Meehl and Washington 1993) showed increase in both the seasonal and mean precipitation and interannual variability.

The interannual variability of the summer monsoon over South Asia is influenced by both tropical and extratropical components, such as El Niño Southern Oscillation (ENSO) (e.g., Shukla 1987; Torrence and Webster 1999; Krishnamurthy and Goswami 2000; Goswami and Ajaymohan 2001; Li et al. 2008), circumglobal wave train (CGT) and North Atlantic Oscillation (Syed et al. 2011; Saeed et al. 2010; Ding and Wang 2005, 2007). Most of the modeling

studies (e.g., Meehl and Arblaster 2003; Hu et al. 2000a,b; Kitoh et al., 1997; Bhaskaran et al. 1995; Meehl and Washington 1993) projected an increase in the interannual variability associated with the increase in mean monsoon precipitation. By using the coupled MPI ECHAM4 climate model Hu et al. (2000b) showed a projected increase in the interannual variability of ISM rainfall after 2030. They related the increasing rainfall variability to the tropical Pacific SST. Meehl and Arblaster (2003) further found that the increased variability in the evaporation and precipitation in the Pacific due to increased SST influences the South Asian monsoon variability through the Walker circulation. However, the ENSO monsoon relationship became weak in the recent decades and shows remarkable decadal fluctuations (Krishna Kumar et al. 1999a; Torrence and Webster 1999; Kinter III et al. 2003). By using a multimodel technique of 19 models used in IPCC AR4, Kripalani et al. (2007) also showed a weakening of the ENSO monsoon relationship in the future warmer climate. They showed a significant increase in the mean monsoon precipitation of 8% and a possible extension of the mean monsoon period. They attributed the projected increase in the monsoon precipitation to the projected intensification of the heat low over northwest India, the trough of low pressure over Indo-Gangetic plains, and land-ocean pressure gradient during the establishment phase of the monsoon.

Syed et al. (2011) showed that the CGT and summer North Atlantic Oscillation are the two dominant modes in the extra-tropics that influence the interannual variability of South Asian summer monsoon. Saeed et al. (2010) found that the mid-latitude wave train influences the heat low which in turn favors enhanced monsoon circulation over the Arabian Sea and associated precipitation over northwestern India and Pakistan. In another study Saeed et al. (2011) found that the precipitation/convection variability over the heat low can induce large scale circulation anomalies similar to CGT wavelike pattern that remotely influence the precipitation over the East Asian region. The objective of the present study is to examine the CGT and associated monsoon rainfall over northwestern India and Pakistan in the warmer future climate. Previous studies (e.g., Saeed et al. 2011; Saeed et al. 2010; Roeckner et al. 2006) have shown that the ECHAM5 climate

model reasonably simulates the mean monsoon climate and HL-CGT relationship. Here, ECHAM5/MPIOM climate model simulations are analysed to examine the CGT and associated rainfall over northwestern India and Pakistan in future climate. There are several scenarios available under IPCC AR4 simulations, here, the analysis focuses on the transient runs under the 1% per year CO_2 increase until reaching double concentrations and held constant thereafter. The next section will describe the data used in this study. Results and discussions are presented in section 5.3. Summary and conclusions are given in the last section.

5.2 Data and Methodology

5.2.1 Data

The IPCC AR4 climate simulations carried out using the coupled climate model of ECHAM5/MPIOM (Jungclaus et al. 2006) are analysed in this Chapter. ECHAM5/MPIOM simulates reasonably well the mean monsoon circulation, the annual cycle and the interannual variability (Kriplani et al. 2007). There are several scenarios under which the projections are available. Following Kripalani et al. (2007), the analysis here focuses on the transient runs with a 1% per year increase in CO_2 until reaching double concentrations and held constant thereafter. This experiment is abbreviated as EnhCO2E hereafter. Here, the peak monsoon months of July and August are analysed. We first constructed a 30-years climatology based on the 20th century run (for simplicity 20CRExp hereafter) from 1971-2000. We analysed the last 30-years of the EnhCO2E when the CO2 is held constant and compared the circulation patterns and associated teleconnections to those obtained with 20CRExp simulations. A t-test has been applied to identify the significant differences between the two experiments.

5.2.2 EOF and composite analysis

We applied empirical orthogonal function (EOF) analysis to examine the CGT pattern in the northern hemisphere summer. The EOFs are computed using the seasonal (July–August) departures of the 200 hPa meridional wind from its climatological mean (1971–2000) over the region extending from 0 to 90°N and 0 to 140°E. We carried out a composite analysis based on the first principal component of the EOF analysis (PC1). In the following, we consider the cases for which PC1 is above +0.5 (below -0.5) standard deviation and the composite difference is defined as positive minus negative PC1. Similar to the current climate simulations we also carried out EOF analysis to examine future CGT and associated rainfall over northwestern India and Pakistan. We further examined the interannual variability of monsoon rainfall over northwestern India and Pakistan. The years when area averaged (25°-34°N, 68°-78°E) rainfall is above +1 Std dev (below -1 Std dev) are considered as wet (dry) monsoon years over northwestern India and Pakistan.

5.3 Results and Discussion

Previous studies (Ding and Wang 2005, 2007; Saeed et al 2010; Syed et al. 2011) have shown that the CGT influences the summer monsoon precipitation over South Asia region. Saeed et al (2010) found that the CGT can influence the sea level pressure anomalies over the heat low region which in turn favors enhanced southwesterly monsoon flow over the Arabian Sea and associated precipitation over northwestern India and Pakistan. Here, we first analyse the 200 hPa meridional wind during summer monsoon season (July-August) to examine the CGT pattern in the current and future climate. In the current climate simulations the 200 hPa meridional wind reveals a CGT wavelike pattern over the Eurasia region and extending up to the northwestern Pacific Ocean (Fig. 5.1a). The projected changes in the meridional wind reveal a northward shift of CGT over Eurasia and the North Pacific region (Fig. 5.1c). The projection also reveals increased sea surface temperature (SST) anomalies over the tropical Pacific, the

northwestern Pacific and the northwestern Atlantic Ocean (Fig. 5.1d). The northward shift in the projected CGT over the North Pacific and Eurasia regions may be associated with changes in the mid-latitude zonal flow structure associated with storm tracks (Bengtsson et al. 2008) and the strength and position of the Aleutian low (Müller and Roecknor 2008), the later is associated with changes in tropical Pacific mean SST.

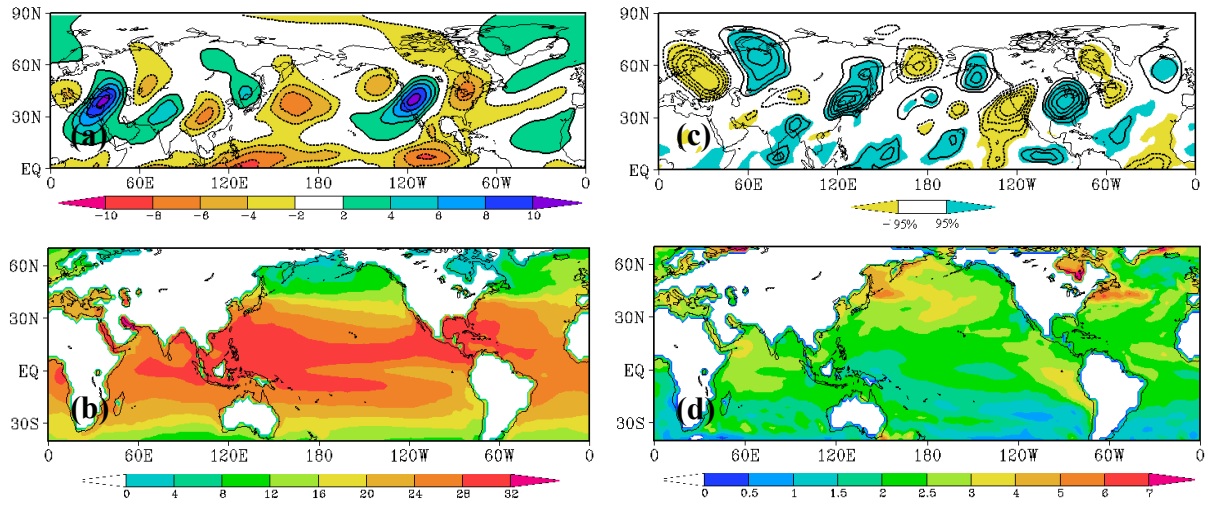

Figure 5.1: (left) 30-years (1971-2000) mean simulated climatology of (a) 200 hPa meridional wind and (b) sea surface temperature (SST). (right) simulated future change in (c) 200 hPa meridional wind and (d) SST. Shaded areas in (c) show changes in the meridional wind that are significant to 95% confidence level. The contours in (c) are shown at 0.5 m sec^{-1}.

Empirical Orthogonal Function (EOF) analysis has been carried out to further examine the CGT pattern and associated rainfall over northwestern India and Pakistan. The EOFs are computed using the 200 hPa meridional wind anomalies for both the current and future climate simulations. In the current climate simulation the leading EOF mode explains 29.8% of the total variance. The leading EOF mode reveals a CGT wavelike pattern extending well in to the Asian monsoon region (Fig. 5.2a).

The simulated precipitation composites using first principal component of EOF show positive anomalies over northwestern parts of India and Pakistan (Fig. 5.2b). These results resembles to the previous studies (e.g., Ding and Wang 2005; Saeed

et al. 2010), in which CGT is associated with enhanced rainfall over northwestern India and Pakistan. In the future climate simulations the leading EOF mode explains 24.5% of the total variance. Compared to the current climate simulation (Fig. 5.2a), the leading EOF in future climate reveals a northward shift in the CGT wavelike pattern over the Eurasia region (Fig. 5.2c). This shift in the CGT patter is similar to that shown in Fig. 5.1c. The simulated precipitation composites using PC1 of leading EOF show small but not significant negative precipitation anomalies over northwestern parts of India and Pakistan (Fig. 5.2d). From this it is hypothesised that a northward shift in the future CGT during the peak monsoon months of July-August may be associated with reduced monsoon precipitation over northwestern India and Pakistan.

As shown in Fig. 5.3d , the future sea level pressure show positive anomalies over the western parts (25°-30°N, 55°-70°E) of the heat low region. Saeed et al. (2010) found significant correlations between the pressure anomalies over this region and monsoon circulation over Arabian Sea. They found that the intensification of the heat low is associated with enhanced southwesterly monsoon flow over Arabian Sea and vice versa. The projected decrease in the southwesterly monsoon flow over the Arabian Sea may be associated with the projected suppression of the heat low activity over western parts of heat low region. The suppression of the heat low reduces the southwesterlies monsoon flow entering into land from Arabian Sea, hence creating conditions favorable for currents from Bay of Bengal to intrude deep into western India and Pakistan (Saeed et al. 2009). The projected suppression of heat low activity over western parts (as discussed above) during summer monsoon season (JA) may favor enhanced moist flow from Bay of Bengal as suggested by Saeed et al. (2009) and may result in the increased precipitation over the Indian region. This is also evident from Fig. 5.3e which shows reduced (enhanced) monsoon flow over the Arabian Sea (Bay of Bengal).

This hypothesis has been further examined by investigating the future changes in the precipitation and associated circulation over the South Asia during the summer (July-August) monsoon season. The current climate simulations reveals

the well known heat low over northwestern India and Pakistan, the low level southwesterly monsoon flow over the Arabian Sea and the spatial pattern of monsoon rainfall over the Indian subcontinent (Fig. 5.3a-c). The future projection show small but significant increase (decrease) in the sea level pressure over the western parts of the heat low (monsoon trough region), significant decrease (increase) in the monsoon currents over the Arabian Sea (Bay of Bengal) and significantly enhanced monsoon precipitation over Indian Ocean and adjacent areas of Indian subcontinent (Fig. 5.3d-f).

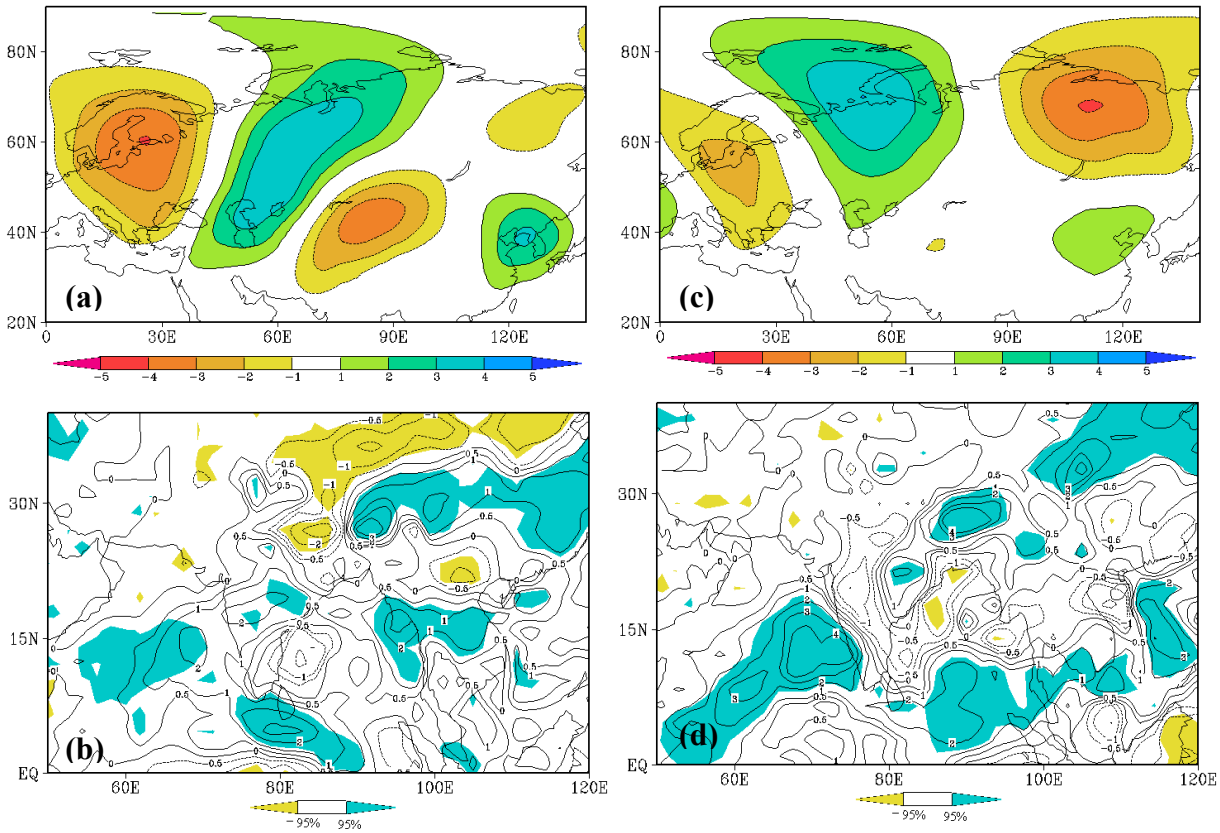

Figure 5.2: The leading mode of the EOF analysis using 200 hPa meridional wind anomalies for (a) 20CRExp and (c) EnhCO2E. The leading EOF modes explain 29.8% and 24.5% of total variance respectively. Precipitation composites difference using the first principal component of the leading EOFs for (b) 20CRExp and (d) EnhCO2E. The composite difference is simply the positive minus negative PC1 above 0.5 (below -0.5) standard deviations. Shaded areas in (c, d) show precipitation changes significant to 95% level. The contours in (c, d) are shown at 0.5 mm day^{-1}.

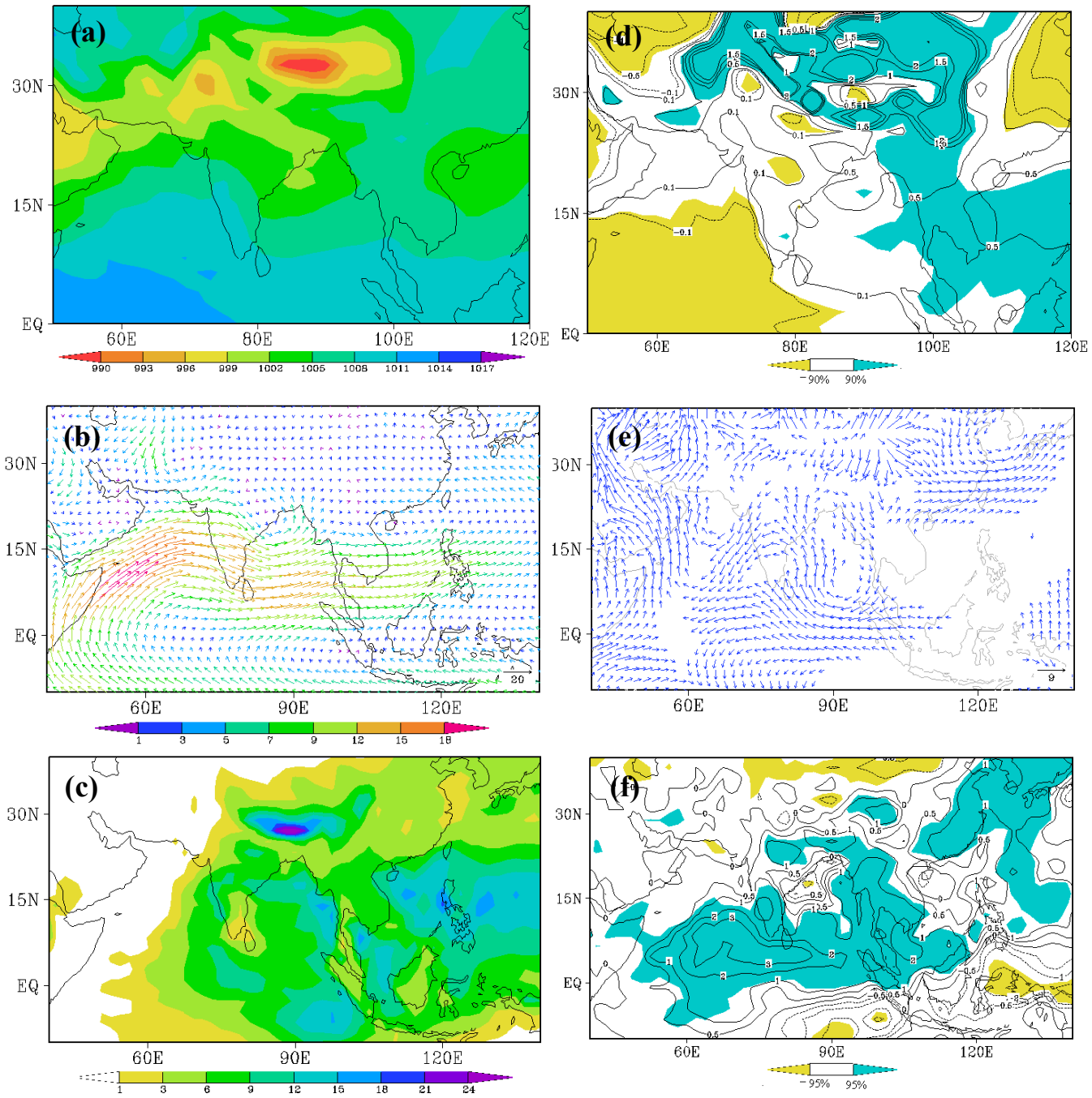

Figure 5.3: (left) 30-years (1971-2000) mean simulated summer monsoon (July-August) climatology of (a) mean sea level pressure, (b) 850 hPa wind and (c) precipitation. (right) Projected changes in (d) mean sea level pressure, (e) 850 hPa wind and (f) precipitation. Shaded areas in (d, f) show changes in sea level pressure and precipitation that are significant to 95% and 90% level. The wind vectors insignificant to 95% significance level are omitted in (d). The units of precipitation, wind and pressure are mm day^{-1} , m sec^{-1} and hPa respectively.

Saeed et al. (2010) further showed that the sea level pressure over the heat low region is influenced by the mid-latitude wave train. We will now examine the co-variability of the sea level pressure over the heat low and mid-latitude CGT in future climate. The projected changes in the mean sea level pressure during July-August reveal positive anomalies over the western parts of the heat low region (i.e., Iran and Afghanistan) (Fig. 5.3d). The associated CGT shows a northward shift over the Eurasia region (Fig. 5.1c, 5.2c).

The monsoon precipitation over northwestern India and Pakistan is often characterized by frequent mesoscale convective developments that can contribute significantly to the seasonal mean precipitation if sufficient moisture is available from the Arabian Sea. A significant decrease in the future southerwesterly monsoon flow over the Arabian Sea can therefore influence the seasonal mean precipitation over northwestern India and Pakistan.

As discussed earlier the interannual variability of the summer monsoon over South Asia is influenced by the CGT and the future projection shows a northward shift in the CGT pattern. Will this northward shift in the CGT pattern influence the interannual variability of summer monsoon over northwestern India and Pakistan? We therefore examine the projected interannual variability of the summer monsoon over northwestern India and Pakistan. Fig. 5.4a, b shows the standard deviation (Std dev) maps of the monsoon rainfall over the Indian domain for 20CRExp and EnhCO2E, respectively. It can be seen that the Std dev values are larger (1-1.5 mm day^{-1} over the west coast of India and 0.5 -1.0 mm day^{-1}) over northwestern India and Pakistan region in the future climate simulation. Moreover, the Std dev values are also larger over Indian landmasses and Indian Ocean compared to 20CRExp. The projection further reveals increased interannual rainfall variability over the northwestern India and Pakistan (25°-34°N, 68°-78°E) in future climate (Fig. 5.4c, d). The intensity of dry seasons appears increasing in the future climate. The wet seasons show no change as the two simulations show an equal number of wet seasons.

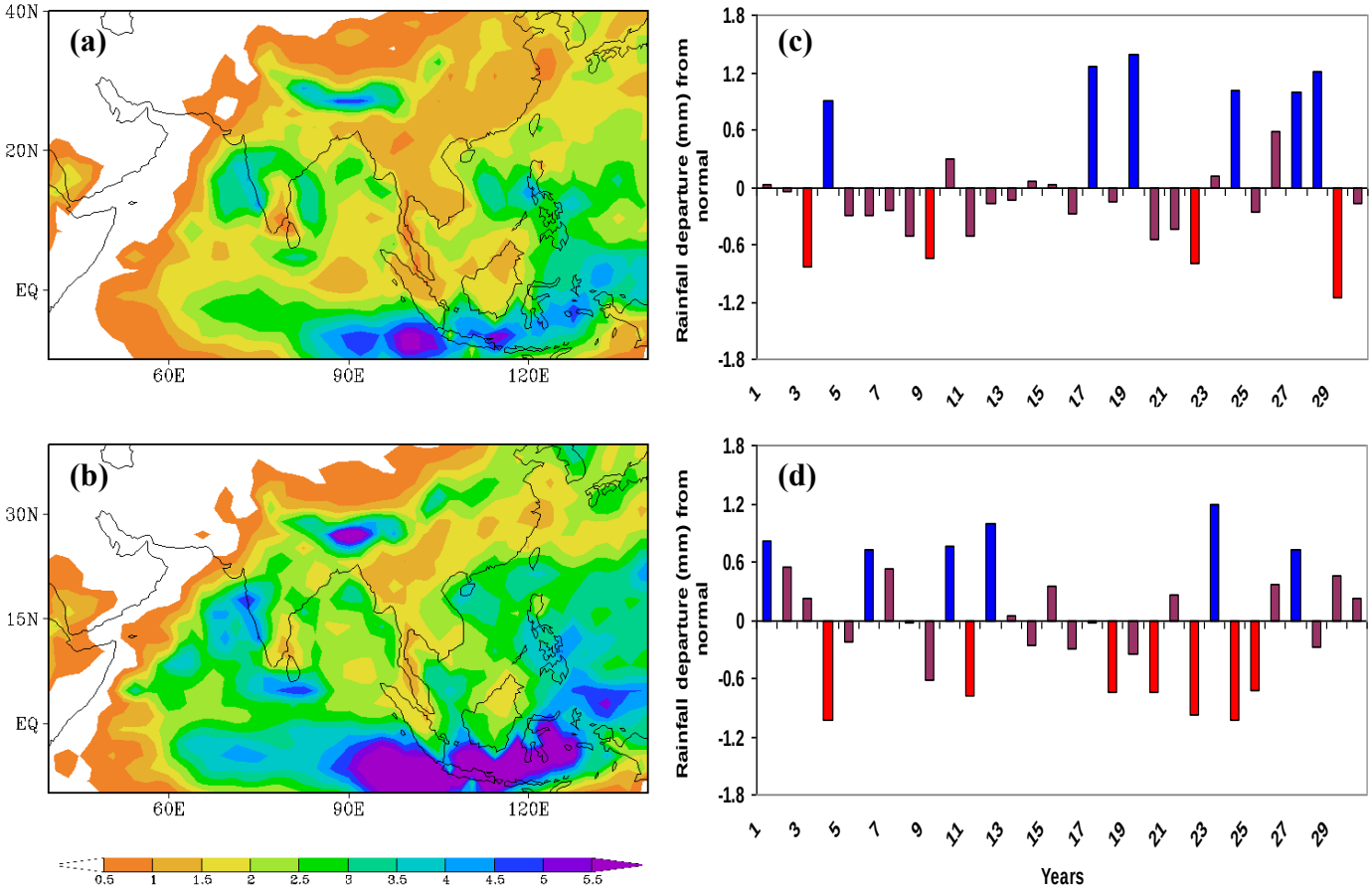

Figure 5.4: (left) Std dev maps of the July–August summer monsoon rainfall (mm day–1) for (a) 20CRExp and (b) EnhCO2E. (right) Time series of the interannual variability of the summer monsoon (JA) rainfall over northwestern India–Pakistan region (25°–34°N, 68°–78°E) for (c) 20CRExp and (d) EnhCO2E. The rainfall variations in (c) and (d) are expressed as the departure of area averaged rainfall from its normal. The blue (red) bars in (c, d) represent the rainfall above (below) +1 (–1) Std dev. For 20CRExp the years 4, 17, 17, 24, 27, 28 (3, 9, 22, 29) corresponds to the wet (dry) summer monsoon. For EnhCO2E the years 1, 6, 10, 12, 23, 27 (4, 11, 18, 20, 22, 24, 25) corresponds to wet (dry) summer monsoon.

5.4 Summary and conclusions

In this chapter an analysis of the IPCC AR4 coupled climate model ECHAM5/MPIOM simulations has been carried out to examine the future CGT and associated summer monsoon rainfall variability over northwestern India and

Pakistan. The future projection under the 1% per year CO_2 increase scenario has been analysed to examine the projected changes in the CGT and associated summer monsoon (July–August) rainfall over this region.

Analysis reveals a northward shift in the CGT over the Eurasia region during the peak summer monsoon months of July–August. The associated sea level pressure shows positive (negative) pressure anomalies over the western parts of heat low (monsoon trough region). The associated low level circulation at 850 hPa reveals reduced (enhanced) southwesterly (southeasterly) monsoon circulation over the Arabian Sea (Bay of Bengal). The projections further show enhanced monsoon precipitation over the Indian Ocean and adjacent areas of Indian subcontinent.

Saeed et al. (2010) found significant correlations between the pressure anomalies over the western parts of the heat low region (Iran and Afghanistan) and southwesterly monsoon over the Arabian Sea. They showed that the intensification of the heat low over this region is associated with the enhanced southwesterly monsoon flow over the Arabian Sea and vice versa. The projected reduced southwesterly monsoon over the Arabian Sea may therefore be associated with the suppressed heat low activity over this region. The suppression of the heat low reduces the westerlies entering into land from Arabian Sea, hence creating conditions favorable for currents from Bay of Bengal to intrude deep into western India and Pakistan (Saeed et al. 2009). This hypothesis is further supported by the projected positive sea level pressure anomalies over the heat low region and associated reduced (enhanced) monsoon flow over the Arabian Sea (Bay of Bengal).

Analysis of the projected interannual variability of the summer monsoon rainfall has been carried out to examine the future wet and dry seasons over northwestern India and Pakistan. Analysis reveals increased number of dry monsoon seasons over northwestern India and Pakistan in the future climate. It is hypothesised that the projected increase in the dry monsoon over northwestern India and Pakistan during July–August may be associated with the northward

shift in the mid-latitude wave train which influences the interanuual variability of summer monsoon over northwestern India and Pakistan (Syed et al. 2011; Saeed et al. 2010, Ding and Wang 2005).

Here, the mean state of future CGT during summer season (July-August) has been analysed, it is not clear to what extent the future CGT can contribute to extreme monsoon rainfall on intraseasonal time scales, such as the July 2010 rainfall over northwestern India and Pakistan. The above analysis however, suggest a tendency towards less mean rainfall as the CGT is shifted northward and less affective to the heat low. A decrease in the seasonal mean summer monsoon rainfall in future may directly influence the growth of agicultural crops. In order to avoid the economic losses associated with the agriculture in the dry monsoon seasons, it is important to construct more water reservoirs to store the excess water in the wet seasons. The above results are based on single model simulations and the model uncertainties are also not taken into account. Further investigations are therefore needed in this regard.

Chapter 6

Summary and Outlook

6.1 Summary

In this thesis the large scale mid-latitude circulation and its associated influence on the South Asian summer monsoon rainfall has been studied. Special emphasis is given to the large scale mid-latitude circumglobal wave train (CGT) and associated summer monsoon rainfall over northwestern India and Pakistan. This chapter summarizes the major conclusions and answers to the questions raised in the first chapter.

Ding and Wang (2005) found significant correlations between mid-latitude CGT and Indian summer monsoon on interannaul time scale. They showed that during the positive phase of CGT anomalous high pressure forms over western central Asia which is associated with enhanced monsoon rainfall over northwestern India and Pakistan. However, it was not clear that how CGT influences the summer monsoon rainfall over northwestern India and Pakistan. By using ERA40 reanalysis and ECHAM5 climate model simulations it is found that:

1. *The eastward propagation of the mid-latitude wave train can influence the pressure anomalies over the western part of the surface heat low (HL) that forms over northwestern India, Pakistan and adjacent areas of Iran and Afghanistan. The intensification of the heat low is associated with enhanced southwesterly monsoon flow over the Arabian Sea and Persian Gulf that converge over northwestern India and Pakistan. A monsoon trough like condition appears over northwestern India and Pakistan that*

favors enhanced convections and associated precipitation over northwestern India and Pakistan.

A heat low index (HLI) is defined to depict the surface heat low that forms over northwestern India, Pakistan and adjacent areas (Saeed et al. 2010). The HLI display significant correlations with low level monsoon circulation over the Arabian Sea and upper level mid-latitude circulation over western central and East Asia region. On intraseasonal to interannual time scales observation (Kripalani and Singh, 1993; Kripalani and Kulkarni, 1997, 2001; Krishnan and Sugi, 2001) shows positive correlation between the summer monsoon over India and northern China, suggesting co-occurrence of flood and droughts over both regions. To what extent the rainfall/convection variability over the South Asian monsoon heat low can influence the large scale circulation anomalies and associated rainfall over East Asia region is not clear. For this purpose sensitivity simulation experiments using ECHAM5 climate model are carried out to examine the response of the rainfall/convection variability over South Asia monsoon heat low to the large scale mid-latitude circulation and associated rainfall over East Asia. It is found that:

2. *An intensification of the heat low favors enhanced precipitation/convection over northwestern India-Pakistan. The enhanced precipitation/convection over northwestern India-Pakistan can induce large-scale circulation anomalies that resemble the northern summer CGT wave-like pattern extending well into the Asian monsoon region. Accordingly the wave-like response to rainfall increase over the heat low region is associated with anomalous ascent over northern China and descent over the South China Sea. On the other hand, suppressed convection and rainfall over the heat low region do not reveal any significant large-scale circulation anomalies.*

Pakistan has received heavy rainfall during the summer monsoon of 2010 resulting in severe flooding that affected more than 20 million people and the overall estimates of damage exceed $US40B. Saeed et al (2010) found a

tendency of the CGT to lead the HL and associated rainfall over northwestern India and Pakistan. They further found that a large proportion of above normal precipitation (flooding) episodes over northwestern India and Pakistan is associated with the positive phase of CGT. Analysis of the 2010 flood over Pakistan has been carried out to examine the underlying physical mechanisms that are responsible for the heavy rainfall. It has been found that:

3. *A co-occurrence of mid-latitude wave train and blocking high is associated with heavy rainfall over northern Pakistan and adjacent areas. The eastward propagating mid-latitude wave train seems influencing the upper level blocking high pressure that formed over the western Russia during the month of July. The east-west oriented blocking high is shifted little eastward and took a north-south orientation. The north-south oriented blocking high in association with the wave train favored the cold extra-tropical air to further southward into the Asian monsoon region. As a result the jet stream moved further south than its normal position with its trough approaching northern Pakistan and hence dividing the Tibetan anticyclone in to two parts. The co-occurrence of the wave train and blocking high is further associated with the deepening of the low pressure over northern Pakistan and adjacent areas, the Arabian Sea and adjoining areas of Arabian Peninsula. Consequently, an intensification in the surface low pressure favored the moist southerly flow to intrude deep over northern Pakistan where orographic lifting in association with upper level trough fostered convection and hence precipitation.*

As discussed above, the interannual variability of the summer monsoon over South Asia is strongly influenced by the mid-latitude circulation (Syed et al. 2011; Saeed et al. 2010; Ding and Wang 2005, 2007). Müller and Roeckner (2008) examined the changes in the future mid-latitude circulation in distinct regions in the northern hemisphere. They attributed these changes to increase of the tropical SST in the Pacific Ocean. It is therefore important to examine the future mid-latitude CGT and associated rainfall over northwestern India

and Pakistan. For this purpose an analysis of 1% increase CO2 climate scenario under IPCC AR4 has been carried out using ECHAM5/MPIOM coupled climate model simulations. The analysis reveals:

4. *A northward shift in the mid-latitude wave train during the peak summer monsoon months of July-August. The associated sea level pressure show positive anomalies over western parts of the heat low region. The low level monsoon circulation also shows decreased (increased) southwesterly (southeasterly) flow over the Arabian Sea (Bay of Bengal). The projections further reveal enhanced interannual variability of summer monsoon rainfall over northwestern India and Pakistan. The projected intensity of dry monsoon seasons increases over northwestern India and Pakistan suggesting more intense drought like conditions over northwestern India and Pakistan in future climate. This may be associated with the northward shift of the wave train over Eurasia region.*

The conclusions of chapter 5 are based on the coupled ECHAM5/MPIOM climate model simulations. Previous studies (Saeed et al. 2010; Saeed et al. 2011) have shown the capability of ECHAM5 climate model in simulation of HL-CGT relationship and associated precipitation and circulation over the Asian monsoon region. Although the above studies addressed challenging questions in the mid-latitude monsoon internal dynamics, however, these studies also raised several other questions that need to be addressed. The next section will give an overview of these questions.

6.2 Outlook

Saeed et al (2010) showed a tendency of CGT to lead the heat low and associated rainfall over northwestern India and Pakistan on intraseasonal to interannual time scales. Moreover, it is shown in chapter 4 that the co-occurance of CGT and blocking high is associated with enhanced 2010 summer monsoon rainfall over Pakistan and adjacent areas. However, the causes of the intensification of the mid-latitude circulation are yet not known. The observed warm sea surface temperature (SST) anomalies during 2010 show SST anomalies in the tropical west Pacific and eastern Indian Ocean associated with the strong La Niña conditions. Also warm SST anomalies were seen in the North Atlantic Ocean. One hypothesis is that the La Niña in the tropical Pacific may be associated with this abnormal intensification of the mid-latitude circulation that led to the heavy rainfall over Pakistan. It is not clear whether the blocking over western Russia and wave train appeared by chance or are there other reasons for this co-occurrence? Observations also show a westward shift in the subtropical high pressure over the North Pacific. Whether the westward shift in the subtropical high over the North Pacific influenced the large scale summer monsoon circulation during 2010 is also not clear. This issue may be further examined by using model sensitivity experiments with varying SST forcing over tropical Pacific, tropical Indian and Atlantic Ocean. A week later the Pakistan flood the northeastern parts of China received heavy rainfall that caused severe flash flooding. In the 3rd chapter (Saeed et al. 2011) it is shown that rainfall/convection variability over South Asian monsoon heat low can favor rainfall anomalies over northeastern China. It will be further interesting to examine this hypothesis using the observed historical flood episodes over northwestern India and Pakistan.

Chapter 5 show enhanced interannual summer monsoon rainfall variability over northwestern India and Pakistan. The projection show increased intensity of drought like conditions over northwestern India and Pakistan. This may be associated with the changes in the mid-latitude circulations under warmer future climate. Agriculture is the major source of the economy and is highly dependent

on the South Asian summer monsoon rainfall. A strong interannual/intraseasonal variability of the summer monsoon can affect the agricultural growth and hence the economy of the region. Therefore it is important to further investigate this issue using high resolution climate model simulations.

Acknowledgements

First of all, I would like to thank my supervisor Wolfgang A. Müller for his kind supervision which enabled me to complete this PhD thesis. Throughout my stay in MPI, he was always available all the time for discussing striking problems related to my PhD research work. I am also thankful to my co-advisor Stefan Hagemann and Panel Chair Daniela Jacob for their worthy suggestions and discussions that helped me a lot to keep on track my PhD research. Special thanks are also due to Martin Claußen for reading this thesis as the first referee.

This PhD study is financed by the International Max Planck Research School on Earth System Modeling (IMPRS), Hamburg, Germany. I am very much thankful to the International Max Planck Research School on Earth System Modelling (IMPRS), especially, Antje Weitz and Cornelia Kampamann for their kind support throughout my stay in MPI. Whenever I visited them I found them smiling and ready for solving my problems (if any). They really made my work and life much easier during my PhD studies.

I am also thankful to Qammar-uz-Zaman Chaudhry, Arif Mahmood and Ghulam Rasul from Pakistan Meteorological Department for their support. Being a member of Pakistan Meteorological Department, I focused my research on the understanding of the summer monsoon over Pakistan and adjacent areas of northwestern India. The present findings further improve our understandings regarding the summer monsoon over northwestern India and Pakistan and its association with extra-tropical circulation. However, several other questions are raised in this thesis which needs further investigation.

I also wish to thank my friend Fahad Saeed for a wonderful time with him, my colleagues of IMPRS School, Robert, Bikash, Andreas, Tobias, Tanje and many others, my office mates Davide and Max and the staff member of MPI for their kind cooperation and support during my stay in MPI.

I have no words to express my sincere thanks to my mother for her unconditional support, prayers and endless sacrifices throughout her life. This was a dream of my late father whose memories are always with me at every stage of my life. I am also thankful to my siblings for their moral support. Finally, I thank my beloved wife Shazia and my sweet daughters Narin and Nawal for being with me. Shazia always encouraged and supported me especially during my PhD research.

Bibliography

Ambrizzi, T., B. J. Hoskins, and H.-H Hsu (1995), Rossby wave propagation and teleconnection patterns in the austral winter. *J. Atmos. Sci., 52, 3661-3672.*

Ashok, K., Z. Guan, and T. Yamagata (2001), Impact of the Indian Ocean dipole on the relationship between the Indian monsoon rainfall and ENSO. *Geophys. Res. Lett.,* 28, 4499-4502.

Ashrit R. G., H. Douville, and K. R. Kumar(2003), Response of the Indian monsoon and ENSO-monsoon teleconnection to enhanced greenhouse effect in the CNRM coupled model. *J. Meteorol. Soc. Japan,* 81, 779–803.

Bansod, S. D., and S. V. Singh (1995), Pre-Monsoon surface pressure and summer monsoon rainfall over India. *Theor. Appl. Climatol.* 51, 59-66.

Bengtsson, L., K.I. Hodge, N. Keenlyside (2008), Will extratropical storms intensify in a warmer climate? *J. Climate, 22, 2276-2301,* doi. 10.1175/2008JCLI2678.1

Bhaskaran B., J.F.B. Mitchell, J. R. Lavery, M. Lal (1995), Climatic response of the Indian subcontinent to double CO2 concentrations. *Int J Climatol, 15, 873-892.*

Bosilovich, M., J. Chen, F. R. Robertson and R. F. Adler (2008), Evaluation of global precipitation in Reanalysis. *J. Appl. Meteor and Climatol.* 47, 2279-2299.

Branstator, G. (2002), Circumglobal teleconnecctions, the jet stream waveguide, and North Atlantic Oscillation. *J. Climate,* 15, 1893-1910.

Czaja, A., and C. Frankignoul (2002) Observed impact of Atlantic SST anomalies on the North Atlantic Oscillation. *J. Climate,* 15, 606-623.

Ding, Q., and B. Wang (2005), Circumglobal teleconnection in northern hemisphere summer. *J. Climate,* 18, 3482–3505.

Ding, Q., and B. Wang (2007), Intraseasonal teleconnection between the summer Eurasian wave train and Indian Monsoon. *J. Climate,* 20, 3551–3767.

Ding, Y.-H., and D. R. Sikka (2005), Synoptic system and weather in the Asian monsoon. *The Asian Monsoon, B. Wang, Ed., Springer Praxis,* 131–201.

Ding, Y., and J. C. L. Chan (2005), The east Asian summer monsoon: and overview, *Meteorol. Atmos. Phys.,* 89, 117–142, DOI 10.1007/s00703-005-0125-z.

Enomoto, T., B. J. Hoskins, and Y. Matsuda (2003), The formation mechanism of the Bonin high in August. *Quart. J. Roy. Meteor. Soc., 129, 157–178.*

Fasullo, J., and P. J. Webster (2002), Hydrological signatures relating the Asian summer monsoon and ENSO. *J. Climate,* 15, 3082–3095.

Flohn, H. (1957), Large-scale aspects of the summer monsoon in South and East Asia, *J. Meteor. Soc. Japan, 75, 180–186.*

Goswami, B. N. (1998), Interannual variations of Indian summer monsoon in a GCM: External conditions versus internal feedbacks. *J. Climate,* 11, 501–522.

Goswami, B. N., and R. S. Ajayamohan (2001), Intraseasonal oscillations and interannual variability of the Indian summer monsoon. *J. Climate,* 14, 1180–1198.

Goswami, B. N., and P. K. Xavier (2005), ENSO control on the South Asian monsoon through the length of the rainy season. *Geophy. Res. Lett.,* 32, L18717, DOI:10.1029/2005 GL023216.

Goswami, B. N., M. S, Madhusoodanan, C. P. Neema, and D. Senguta (2006), A physical mechanism for North Atlantic SST influence on the Indian summer monsoon. *Geophy. Res. Letter,* 33, L02706, DOI:10.1029/2005 Gl024803.

Haln, D. G., and S. Manabe (1995), The role of mountains in the South Asian Monsoon Climate. *J. Atmos. Sci.* 32, 1515-1541.

Haln, D. G., and J. Shukla (1976), An apperent relationship between Euroasian snow cover and Indian monsoon rainfall. *J. Atmos. Sci.,* 33, 2461-2462.

Hewitt, C. N., and A. Jackson (2003), Hand Book of the Atmospheric Science: Principles and Applications, *Blackwell Publication,* PP 81.

Hoskins B. J., and B. Wang (2006), Large-scale atmospheric dynamics. *The Asian Monsoon, B. Wang, Ed. Springer-Praxis,* 357-415.

Hu Z-Z., L. Bengtsson, and K. Arpe (2000a), Impact of the global warming on the Asian winter monsoon in a coupled GCM. *J. Geophys. Res.,* 105, 4607–4624.

Hu Z.-Z, M. Latif, E. Roeckner, and L. Bengtsson (2000b), Intensified Asian summer monsoon and its variability in a coupled model forced by increasing greenhouse gas concentrations. *Geophys. Res. Lett.,* 27, 2681–2684.

Huang R. H., and Y. Wu (1989), The influence of ENSO on the summer climate change in China and its mechanism. *Adv. Atmos. Sci.*, 6, 21-32.

Hu, Z.-Z., R. Wu, J. L. Kinter III, and S. Yang (2005), Connection of summer rainfall variations in South and East Asia: role of El Nino-Southern Oscillation, *Int. J. Climatol.,* 25, 1279-1289.

Jungclaus, J.H., M. Botzet, H. Haak, N. Keenlyside, J.-J. Luo, M. Latif, J. Marotzke, U. Mikolajewicz, and E.Roeckner (2006), Ocean circulation and tropical variabilit

y in the coupled model ECHAM5/MPI-OM. J. Climate, 19, 3952-3972.

Kalnay E, et al. (1996), The NCEP/NCAR 40-year reanalysis project, *Bull. Amer. Meteor. Soc.,* 77: 437-470.

Kaplan, A., M. Cane, Y. Kushnir, A. Clement, B. Blumenthal, and B. Rajagopalan (1998), Analyses of Global Sea Surface Temperature 1856– 1991, *J. Geophys. Res.,* 103, 18,567–18,589.

Kinter III, J. L., K. Miyakoda, S. Yang (2002), Reccent change in the connection from the Asian monsoon to ENSO. *J. Climate,* 15, 1203-1215.

Kripalani, R. H., and S.V. Singh (1993), Large scale aspects of India-China summer monsoon rainfall, *Adv. Atmos. Sci., 10, 72-84.*

Kripalani, R. H., A. Kulkarni, and S.V. Singh (1997), Association of the Indian summer monsoon with the northern hemisphere mid-latitude circulation, *Int. J. Climatol.,* 17, 1055-1067.

Kripalani, R. H., and A. Kulkarni (1997a), Rainfall variability over South-east Asia- connections with Indian monsoon and ENSO extremes: new perspectives, *Int. J. Climatol.,* 17, 1155-1168.

Kripalani, R. H., A. Kulkarni (2001), Monsoon rainfall variations and teleconnections over South and East Asia, *Int. J. Climatol.,* 21, 603-616.

Kripalani RH, J.H. Oh, A. Kulkarni, S.S. Sabade, H.S. Chaudhari (2007), South Asian summer monsoon precipitation variability: Coupled climate model simulations and projections under IPCC AR4. *Theor. Appl. Climatol.*, 90, 133-159.

Krishnan, R., V. Kumar, M. Sugi, and J. Yoshimura (2009), Internal feedbacks from monsoon-mid-latitude interactions during droughts in Indian summer monsoon. *J. Atmos. Sci.,* 66, 553-578.

Krishnan, R., C. Zhang, and M. Sugi (2000), Dynamics of breaks in Indian monsoon. *J. Atmos. Sci.,* 57, 1354-1372.

Krishnan, R., and M. Sugi (2001), Baiu rainfall variability and associated monsoon teleconnections, *J. Meteor. Soc. Japan,* 79, 851-860.

Krishna Kumar, K., B. Rajagopalan, M. A. Cane (1999), On the weakening relationship between the Indian monsoon and ENSO. *Science,* 264, 2156-2159.

Krishnamurthy, V., and B. N. Goswami (2000), Indian monsoon ENSO relationship on interdecadal timescale. *J. Climate,* 13, 579-595.

Krishnamurti T.N. (1973), Tibetan high and upper tropospheric tropical circulation during northern summer, *Bull Amer. Meteor. Soc.,* 54, 1234-1249.

Kitoch A, Yukimo S, Noda A, Motoi T (1997), Simulated changes in the Asian monsoon at times of increased atmospheric CO2. *J. Meteor. Soc Japan*, 75, 1019-1031.

Kumar, K.K., Rajagopatan B, Hoerling M, Bates G, M. Cane (2006), Unraveling the mystery of Indian monsoon failure during El Niño. *Science,* 314 (5796), 115–119.

Kucharski, F., A. Bracco, J. H. Yahoo, and F. Molten (2008), Atlantic forced component of the Indian monsoon interannual variability. *Geophys. Res. Lett.,* 35, L04706, doi: 10.1029/2007GL033037.

Lal, M., and S.K. Singh (2001), Global warming and monsoon climate. *Mausam,* 52, 245–262.

Lal M., U. Cubasch, R. Voss, J. Waszkewitz (1995), Effect of transient increase in greenhouse and sulphate aerosols on monsoon climate. *Curr. Sci.,* 69, 752-763.

Lal, M., U. Cubasch, B.D. Santer (1994), Effect of global warming on Indian monsoon simulated with coupled ocean-atmosphere general circulation model. *Curr. Sci.,* 66. 430-438.

Latif, M., D. Anderson, T. Barnett, M. Cane, R. Kleeman, A. Leetmaa, J. O'Brien, A. Rosati and E. Schneider (1998), A review of the predictability and prediction of ENSO. *J. Geophys. Res.*, 103, C7, 14,375-14,393.

Lau, K. –M., and H. –Y. Weng (2002), Recurrent teleconnection patterns linking summer time precipitation variability over east Asia and North America, *J. Meteor. Soc. Japan,* 80, 1309-1324.

Lau, K. –M., K. –M. Kim, and J. –Y. Lee (2004a), Interannual variability, global teleconnection and potential predictability associated with Asian summer monsoon. *East Asian Monsoon, C.P. Change, Ed. World Scientific, 564 pp.*

Legates, D. R., and C. J. Willmott (1990a), Mean seasonal and spatial variability global surface air temperature. *Theor. Appl. Climatol.,* 41, 11-21.

Legates, D. R., and C. J. Willmott (1990b), Mean seasonal and spatial variability in guage-corrected, global precipitation. *Int. J. Climatol.,* 10, 111-127.

Li, S., J. Perlwitz, X. Quan, and M. P. Hoerling (2008), Modelling the influence of North Atlantic multidecadal warmth on the Indian summer rainfall, *Geophys. Res. Lett.,* **35**, L05804, doi:10.1029/2007GL032901.

Li, S., J. Lu, G. Huang, K. Hu (2008), Tropical Indian Ocean Basin Warming and East Asian Summer Monsoon: A Multiple AGCM Study, *J. Climate*, 21, 6080–6088, DOI. 10.1175/2008JCLI2433.1

Liu, Y., B.J. Hoskins, and M. Blackburn (2007), Impact of Tibetan orography and heating on the summer flow over Asia, *J. Meteor. Soc. Japan,* 85B, 1–19.

May, W (2004), Potential future changes in the Indian summer monsoon due to greenhouse warming: analysis of mechanisms in a global time-slice experiment. *Clim. Dyn.*, 22, 389–414.

May, W (2002), Simulated changes of the Indian summer monsoon under enhanced greenhouse gas conditions in a global time-slice experiment. *Geophys. Res. Lett.*, 29, doi 10.1029/2001GL013808.

Meehl, G. A., and J.M. Arblaster (2003), Mechanisms for projected future changes in south Asian monsoon precipitation. *Clim. Dyn.*, 21, 659–675.

Meehl, G.A., and W.M. Washington (1993), South Asian summer monsoon variability in a model with doubled atmospheric carbondioxide concentration. *Science*, 260, 1101–1104.

Meehl, G. A. (1994), Influence of land surface in the Asian summer monsoon: External conditions versus internal feedbacks. *J. Climate,* 7, 1033–1049.

Müller, W. A. and E. Roeckner (2006): ENSO Impact on Mid-latitude Circulation Patterns in Future Climate Projections. *Geophys. Res. Lett.* , 33, DOI L05711 10.1029/2005GL025032.

Nitta, T. (1986), Long-term variations of cloud amounts in the western Pacific region. *J. Meteor.Soc.Japan,* 64, 373–390.

Nitta, T. (1987), Convective activities in the tropical western Pacific and their impact on the Northern Hemisphere summer circulation. *J. Meteor:Soc:Japan,* 65, 373-390.

Palmer T. N., and D. L. T. Anderson (1994), The prospects for seasonal forecasting, a review paper. *Quart. J. Roy. Meteor. Soc.*, 120, 755–793.

Park, C. K., and S. D. Schubert (1997), On the nature of the 1994 East Asia summer drought. *J. Climate,* 10, 1056-1070.

Popovic, J. M., and R. A. Plumb (2001), Eddy shedding from the upper tropospheric Asian monsoon anticyclone, *J . Atmos. Sci.,* 58, 93-104.

Raman, C. R. V., and Y. P. Rao (1981), Blocking highs over Asia and monsoon droughts over India. *Nature,* 289, 271-273.

Ramage, C. S. (1965), The summer atmospheric circulation over the Arabian Sea. *J. Atmos. Sci,* 23, 144-150.

Ramage, C. S. (1971), Monsoon Meteorology, *International Geophysics Series, 15, Acd Press, Scan Diego, California,* pp.296.

Ramaswamy, C. (1962) Breaks in the Indian summer monsoon as a phenomenon of interaction between the easterly and subtropical westerly jet streams. *Tellus,* 14A, 337-349.

Rasmusson, E. M., and T. H. Carpenter (1983), The relationship between the eastern Pacific sea surface temperature and rainfall over India and Sri Lanka. *Mon. Weather Rev.,* 111, 517-528.

Roeckner, E., et al. (2003), The atmospheric general circulation model ECHAM5. Part I: Model description, *Max Planck Institute for Meteorology, Rep.* 349, 127 pp.

Roeckner, E., et al. (2006), Sensitivity of simulated climate to horizontal and vertical resolution in the ECHAM5 atmosphere model, *J. Climate – Special Section*, 19, 3771-3791.

Rodwell, M. J., and B. J. Hoskin (1996), Monsoon and dynamics of deserts, *Q. J. R. Meteorol. Soc.* 122, 1385–1404.

Saeed, S., W. A. Müller, S. Hagemann, D. Jacob, M. Mujumdar, and R. Krishnan (2011), Precipitation variability over the South Asian monsoon heat low and associated teleconnections, *Geophys. Res. Lett.*, 38, L08702, doi:10.1029/2011GL046984.

Saeed. S., W. A. Muller, S. Hagemann, D. Jacob (2010), Circumglobal wave train and summer monsoon over northwestern India and Pakistan; the explicit role of the surface heat low, *Clim. Dyn.,* DOI 10.1007/s00382-010-0888-x.

Saeed F, Hagemann S, and Jacob D (2009), Impact of irrigation on the South Asian summer monsoon *Geophys. Res. Lett.*, 36, L20711, doi:10.1029/2009GL040625.

Saha, S. K., S. Halder, K. K. Kumar and B.N. Goswami (2009), Pre-onset land surface processes and 'internal' interannual variabilities of the Indian summer monsoon. *Clim. Dyn.* 36, 2077-2089, DOI: 10.1007/s00382-010-0886-z.

Saji, N. H., B. N. Goswami, P. N. Vinayachandran, and T. Yamagata (1999), A dipole made in the tropical Indian Ocean. *Nature*, 401, 360-363.

Song, J.-H., H.-R, Kang, Y.-H, Byuan, and S-Y., Hong (2009), Effects of the Tibetan plateau on the Asian summer monsoon; a numerical case study using a regional climate model. *Int. J. Climatol.* DOI: 10. 10002/joe.

Shamshad, K.M. (1988), The Meteorology of Pakistan, *Royal Book Company Publishers.* pp 313 ISBN 10: 9694070821.

Shukla, J. and D. A. Paolina (1983), The southern oscillation and long range forecasting of the summer monsoon rainfall over India, *Mon. Weather Rev.,* 111, 1830-1837.

Shukla, J. (1987), Interannual variability of monsoons. *Monsoons, J. S. Fein and P. L. Stephens, Eds., Wiley and Sons,* 399-464.

Sperber, K.R., and T.N. Palmer (1996), Interannual tropical rainfall variability in general circulation model simulations associated with the atmospheric model inter-comparison project. *J. Climate*, 9, 2727-2750.

Sugi, M., and R. Kawamura, and N. Sato (1997), A study of SST-forced variability and potential predictability of seasonal mean fields using the JMA global model. *J. Meteor. Soc. Japan*, 75, 717-736.

Sung, M.-K., W.-T. Kwon, H.-J. Baek, K.-O. Boo, G.-H. Lim, and J.-S. Kug (2006), A possible impact of the North Atlantic Oscillation on the east Asian summer monsoon precipitation, *Geophys. Res. Lett.*, 33, L21713, doi:10.1029/2006GL027253.

Syed, F. S., J.H. Yoo, H. Körnich, F. Kucharski (2011), Extratropical influences on the inter-annual variability of South-Asian monsoon, *Clim. Dyn.* DOI: 10.1007/s00382-011-1059-4

Syed, F. S., J.H. Yoo, H. Körnich, F. Kucharski (2010), Are intraseasonal summer

rainfall events micro monsoon onsets over the western edge of the South Asian monsoon, *Atmos. Res.,* 98, 341-346.

Terao, T. (1999), The zonal wavelength of the quasi-stationary Rossby waves trapped in the westerly jet. *J. Meteor. Soc. Japan*, 77, 687-699.

Torrence, C., and P. J. Webster (1999), Interdecadal changes in the ENSO-Monsoon system. *J. Climate,* 12, 2679- 2690.

Uppala, et. al. (2005), The ERA-40 re-analysis. *Quart. J. R. Meteorol. Soc.,* 131, 2961-3012.DOI:10.1256/qj.04.176

Walker, G. T. (1924), Correlations in seasonal variations of weather. *Mem. 24, Indian Meteorol. Dep., New Delhi*, pp. 275-332.

Wang, B., R. Wu, and K.-M. Lau (2001), Interannual variability of Asian summer monsoon: contrasts between the Indian and the western North Pacific-East Asian Monsoons, *J. Climate,* 14, 4073-4090.

Wang, B., R. Wu, and X. Fu (2000), Pacific-East Asian teleconnection: How does ENSO affect East Asian climate? *J. Climate*, 13, 1517-1536.

Wang, B., and Z. Fan (1999), Choice of south Asian summer monsoon indices, *Bull. Amer. Meteor. Soc.,* 80, 629-638.

Wang, Y., B. Wang, and J. H. Oh (2001), Impact of the preceding El Niño on the East Asian summer atmosphere circulation. *J. Meteorol. Soc. Japan*, 79 (1B), 575-588.

Webster, P. J. (1987), The elementary monsoon. *Monsoons, J.S. Fein and P. L. Stephens, Eds., John Wiley and Sons,* 3-32.

Webster, P. J., and S. Yang (1992), Monsoon and ENSO: Selectively interactive systems. *Quart. J. R. Meteor. Soc.,* 118, 877–926.

Webster, P. J., V. O. Magan˜a, T. N. Palmer, J. Shukla, R. A. Tomas, M. Yanai, and T. Yasunari (1998), Monsoons: Processes, predictability and the prospects for prediction, *J. Geophys. Res.,* 103, 14,451–14,510.

Webseter, P. J., V. E. Toma and H-M. Kim (2011), Were the 2010 Pakistan floods predictable? *Geophys. Res. Lett.,* 38, L04806, doi.10.1029/2010GL046346.

Webster, P. J., and J. Jian (2011), Probability, uncertainty and prediction: A pathway towards the alleviation of poverty in the developing world, *Philos. Trans. R. Soc., in press.*

Yani, M., and G.X. Wu (2006), Effects of Tibetan Plateau. *The Asian –Monsoon, B. Wang, Ed. Springer-Praxis,* 513-549.

Yasunari, T., A. Kitoh, and T. Tokioka (1991), Local and remote responses to excessive snow mass over Euroasia appearing in the northern spring and summer climate-A study with the MRI-GCM. *J. Metoer. Soc. Japan.* 69, 473-487.

Yatagi, A., and T. Yasunari (1995), Internanual variations of summer precipitation in the arid/semi-arid regions in China and Mongolia: Their regionality and relation to Asian monsoon. *J. Meteor. Soc. Japan,* 73, 909-923.

Yadav, R. K. (2009a), Role of equatorial central Pacific and northwest of North Atlantic 2-meter surface temperature in modulating Indian summer monsoon variability. *Clim. Dyn.,* 32, 549-563.

Yadav, R. K. (2009b) Change*s* in the large-scale features associated with the Indian summer monsoon in the recent decades. *Int. J. Climatol.* 29, 117-133.

Zanchettin, D., A. Rubino, P. Traverso, and M. Tomasino (2008), Impact of variations in solar activity on hydrological decadal patterns in northern Italy, *J. Geophys. Res.*, 113, D12102, doi:10.1029/2007JD009157.

Zhang R. H., A. Sumi, and M. Kimoto (1999), A diagnostic study of the impact of El Niño on the precipitation in China. *Adv. Atmos. Sci.*, 16, 229–241.

Zhao, Z.C., and W.M. Kellogg (1998), Sensitivity of soil moisture to doubling of carbon dioxide in climate model experiments. Part II: The Asian monsoon region, *J. Climate*, 1, 367–378.



ISSN 1614-1199